Theses and Dissertations

Spring 2019

Development of Models for Road-Rail Intermodal Freight Network Under Uncertainty

Md Majbah Uddin

Recommended Citation

DEVELOPMENT OF MODELS FOR ROAD-RAIL INTERMODAL FREIGHT NETWORK
UNDER UNCERTAINTY

by

Md Majbah Uddin

Bachelor of Science
Bangladesh University of Engineering and Technology, 2012

Master of Science
University of South Carolina, 2015

Master of Applied Statistics
University of South Carolina, 2018

_____

Submitted in Partial Fulfillment of the Requirements

For the Degree of Doctor of Philosophy in

Civil Engineering

College of Engineering and Computing

University of South Carolina

2019

Accepted by:

Nathan N. Huynh, Major Professor

Robert L. Mullen, Committee Member

Yuche Chen, Committee Member

Pelin Pekgun, Committee Member

Cheryl L. Addy, Vice Provost and Dean of the Graduate School

DEDICATION

To my Mother (Farida Begum) and Father (Md Gias Uddin)

ACKNOWLEDGEMENTS

ABSTRACT

Freight activities are directly related to a country's Gross Domestic Product and economic viability. In recent years, the U.S. transportation system supports a growing volume of freight, and it is anticipated that this trend will continue in the coming years. To support the projected increase in freight volume, an efficient, reliable, and low-cost freight logistics system is necessary to keep the U.S. competitive in the global market. In addition, intermodal transport is becoming an increasingly attractive alternative to shippers, and this trend is likely to continue as state and federal agencies are considering policies to induce a freight modal shift from road to intermodal to alleviate highway congestion and emissions. However, the U.S. intermodal freight transport network is vulnerable to various disruptions. A disruptive event can be a natural disaster or a man-made disaster. A number of such disasters have occurred recently that severely impacted the freight transport network. To this end, this dissertation presents four studies where mathematical models are developed for the road-rail intermodal freight transport considering the network uncertainties.

The first study proposes a methodology for freight traffic assignment in large-scale road-rail intermodal networks. To obtain the user-equilibrium freight flows, gradient projection (GP) algorithm is proposed. The developed methodology is tested on the U.S. intermodal network using the 2007 freight demands for truck, rail, and road-rail intermodal from the Freight Analysis Framework, version 3, (FAF3). The results indicate that the proposed methodology's projected flow pattern is similar to the FAF3

assignment. The second study formulates a stochastic model for the aforementioned freight traffic assignment problem under uncertainty. To solve this challenging problem, an algorithmic framework, involving the sample average approximation and GP algorithm, is proposed. The experiments consider four types of natural disasters that have different risks and impacts on the transportation network: earthquake, hurricane, tornado, and flood. The results demonstrate the feasibility of the model and algorithmic framework to obtain freight flows for a realistic-sized network in reasonable time.

The third study presents a model for the routing of multicommodity freight in an intermodal network under disruptions. A stochastic mixed integer program is formulated, which minimizes not only operational costs of different modes and transfer costs at terminals but also penalty costs associated with unsatisfied demands. The routes generated by the model are found to be more robust than those typically used by freight carriers.

Lastly, the fourth study develops a model to reliably route freight in a road-rail intermodal network. Specifically, the model seeks to provide the optimal route via road segments, rail segments, and intermodal terminals for freight when the network is subject to capacity uncertainties. The proposed methodology is demonstrated using a real-world intermodal network in the Gulf Coast, Southeastern, and Mid-Atlantic regions of the U.S.

TABLE OF CONTENTS

LIST OF TABLES

LIST OF FIGURES

CHAPTER 1

INTRODUCTION

Freight transportation is a vital component of the U.S. economy. Its chief role is to move raw materials and products in an efficient manner (Hall, 2003). The U.S. has the largest freight transportation system in the world (Research and Innovative Technology Administration, 2010). In 2015, it moved a daily average of about 49.3 million tons of freight valued at more than $52.5 billion and the freight tonnage is projected to increase at about 1.4 percent per year between 2015 and 2045 (Bureau of Transportation Statistics, 2017). The majority of the freight shipments were transported by truck and rail (70% and 16%, respectively, in terms of tonnage). The average distance for freight shipment transported by truck was 216 miles and by rail was 811 miles in 2012 (Bureau of Transportation Statistics, 2018); this shows the long-haul nature of the rail mode.

Intermodal transport is a special type of multimodal transport where freight is transported from an origin to a destination in a container (Huynh et al., 2017). Consequently, there is no need for handling of the goods when changing modes. Intermodal transport is becoming an increasingly attractive alternative to shippers in recent years. It is anticipated that this increasing intermodal trend is likely to continue as state and federal agencies are considering policies to induce a freight modal shift from road to intermodal. Moreover, greater use of intermodal can yield significant social benefits such as enhanced highway safety, reduction in need for building highways, etc. (Brown and Hatch, 2002).

Given that the majority of freight is transported via truck mode, freight transportation has significant impact on road traffic safety (Uddin and Ahmed, 2018; Uddin and Huynh, 2017, 2018), pavement performance (Rahman et al., 2017; Rahman and Gassman, 2018), and environment (Winebrake et al., 2008a, 2008b). In the near future, the projected increase in freight volume will stress both public and private infrastructures (Strocko et al., 2013), which in turn will negatively impact the above-mentioned areas. Intermodal freight could help alleviate the increased truck transportation-related issues.

Transportation infrastructures, particularly those supporting intermodal freight, are vulnerable to natural disasters and man-made disasters. These disruptions can drastically degrade the capacity of a transportation mode and consequently have adverse impacts on intermodal freight transport and freight supply chain. For these reasons, adequate redundancy in the freight transport network is needed to prevent significant service losses in the event of a disruption (Uddin and Huynh, 2019; Uddin et al., 2019).

An efficient, reliable, and low-cost freight logistics system is necessary to keep the U.S. competitive in the global market. To this end, this dissertation develops mathematical models for freight assignment and routing in road-rail intermodal transportation, with the consideration of network uncertainties arising from disasters or disruptions.

1.1 RESEARCH PROJECT I – INTERMODAL FREIGHT ASSIGNMENT

This study develops a methodology for freight traffic assignment in large-scale road-rail intermodal networks. To obtain the user-equilibrium freight flows, a path-based

traffic assignment algorithm, gradient projection (GP), is proposed. The developed methodology is tested on the U.S. intermodal network using the 2007 freight demands for truck, rail, and road-rail intermodal from the Freight Analysis Framework, version 3, (FAF3). The results indicate that the proposed methodology's projected flow pattern is similar to the FAF3 assignment. The proposed methodology could be used by transportation planners and decision makers to forecast freight flows and to evaluate strategic network expansion options.

1.2 RESEARCH PROJECT II – INTERMODAL FREIGHT ASSIGNMENT UNDER UNCERTAINTY

This study presents a methodology for freight traffic assignment in a large-scale road-rail intermodal network under uncertainty. A stochastic model is formulated to obtain the user-equilibrium freight flows. To solve this challenging problem, an algorithmic framework, involving the sample average approximation (SAA) and GP algorithm, is proposed. The developed methodology is tested on the U.S. intermodal network with freight flow data from the FAF3. The experiments considered four types of natural disasters that have different risks and impacts on the transportation network: earthquake, hurricane, tornado, and flood. The results demonstrate the feasibility of the model and algorithmic framework to obtain freight flows for a realistic-sized network in reasonable time. It is found that for all disaster scenarios the freight ton-miles are higher compared to the base case without uncertainty.

1.3 RESEARCH PROJECT III – INTERMODAL FREIGHT ROUTING UNDER DISRUPTIONS

This study presents a mathematical model for the routing of multicommodity freight in an intermodal network under disruptions. A stochastic mixed integer program is formulated, which minimizes not only operational costs of different modes and transfer costs at terminals but also penalty costs associated with unsatisfied demands. The SAA algorithm is used to solve this challenging problem. The developed model is applied to an actual intermodal network in the Gulf Coast, Southeastern and Mid-Atlantic regions of the U.S., to demonstrate its applicability, with explicit consideration of disruptions at links, nodes, and terminals. The model results indicate that under disruptions, goods in the study region should be shipped via road-rail intermodal due to the built-in redundancy of the freight transport network. Additionally, the routes generated by the model are found to be more robust than those typically used by freight carriers.

1.4 RESEARCH PROJECT IV – RELIABLE ROUTING OF INTERMODAL FREIGHT UNDER UNCERTAINTY

To address freight service disruption, this study develops a model to reliably route freight in a road-rail intermodal network. Specifically, the model seeks to provide the optimal route via road segments, rail segments, and intermodal terminals for freight when the network is subject to capacity uncertainties. A major contribution of this work is that a framework is provided to allow decision makers to determine the amount of capacity reduction to consider in planning routes to obtain a user-specified reliability level. The proposed methodology is demonstrated using a real-world intermodal network in the Gulf

Coast, Southeastern, and Mid-Atlantic regions of the U.S. It is found that the total system cost increases with the level of capacity uncertainty and with increased confidence levels for disruptions at links, nodes, and intermodal terminals.

1.5 LIST OF PAPERS AND STRUCTURE OF DISSERTATION

This dissertation includes four research papers, and these papers appear as separate chapters. They are:

1. Uddin, M., & Huynh, N. (2015). Freight traffic assignment methodology for large-scale road-rail intermodal networks. *Transportation Research Record, 2477*, 50–57.

2. Uddin, M., & Huynh, N. (2016). Routing model for multicommodity freight in an intermodal network under disruptions. *Transportation Research Record*, *2548*, 71–80.

3. Uddin, M., & Huynh, N. (2019). Reliable routing of road-rail intermodal freight under uncertainty. *Networks and Spatial Economics*. Advance online publication.

4. Uddin, M., Huynh, N., & Ahmed, F. (2019+). Assignment of freight traffic in a large-scale intermodal network under uncertainty. *Journal of Transportation Engineering, Part A: Systems* (under review).

The remaining chapters are organized as follows: Chapters 2 to 5 include the four research projects mentioned above. Lastly, Chapter 6 provides concluding remarks and future research direction.

CHAPTER 2

INTERMODAL FREIGHT ASSIGNMENT[1]

With the growth of intermodal transportation, there is a need by transportation planners and decision makers to forecast freight flows on the intermodal networks and to evaluate strategic network expansion options. Furthermore, well-informed infrastructure, economic, and environmental planning depends on effective freight forecasting (Chow et al., 2014) which is obtained from the freight assignment step. The multimodal nature of the freight movement presents an additional layer of complexity to the freight assignment problem. Additionally, freight demand and cost data are not as readily available. To this end, this chapter proposes an integrated freight assignment methodology that considers road, rail and intermodal shipments.

The assignment of freight over multimodal networks has been studied by many researchers in the past few decades. Crainic et al. (1984) developed a nonlinear optimization model to route freight train, schedule train services and allocate classification work between yards. Guelat et al. (1990) proposed a Gauss-Seidel-Linear approximation algorithm to assign multiproduct in a multimode network for strategic planning. Their algorithm was implemented in a strategic analysis tool named "strategic transportation analysis (STAN)" and solved a system-optimal (SO) problem with the objective of minimizing the total cost at arcs and node transfer. Their solution algorithm

considered intermodal transfer costs in the computation of shortest paths. Chow et al. (2014) used a variant of STAN for the freight assignment and calibrated their model to work for both user-equilibrium (UE) and SO conditions.

The freight network equilibrium model (FNEM) developed by Friesz et al. (1986) considered the combined role of shipper-carrier. Using the shipper and carrier sub-models FNEM provided the route choice decisions for both shippers and carriers on a multimodal freight network with nonlinear cost and delay function. By solving a variational inequality (VI) problem on the railway network Fernandez et al. (2004) developed a strategic railway freight assignment model. Agrawal and Ziliaskopoulos (2006) also used the VI approach for freight assignment to achieve market equilibrium where no shipper can reduce its cost by changing carrier. In their model, shippers were assumed to have UE behavior with the objective of minimizing cost without any consideration about other shippers in the market, whereas carriers followed a SO behavior with the objective of optimizing their system (i.e., complete operation).

Loureiro and Ralston (1996) proposed a multi-commodity multimodal network design model to use as a strategic planning tool; the model assumed that the goods are shipped at minimum total generalized cost and used path-based UE assignment algorithm to assign freight flows over the network. Kornhauser and Bodden (1983) analyzed highway and intermodal railway-highway freight network by routing freight over the network using a minimum cost path-finding algorithm and presented results as density map. Arnold et al. (2004) proposed a modeling framework for road-rail intermodal network, but the main purpose of their model was to optimally locate intermodal terminals by minimizing transportation cost of shipments. Mahmassani et al. (2007)

developed a dynamic freight network simulation-assignment model for the analysis of multiproduct intermodal freight transportation systems. The intermodal shortest path was calculated based on the link travel costs and node transfer delays. Zhang et al. (2008) validated the Mahmassani et al. model by applying it to a Pan-European rail network. Using a bi-level programming, where lower-level problem finds the multimodal multiclass user traffic assignment and upper-level problem determines the maximum benefit-cost ratio yielding network improvement actions, Yamada et al. (2009) developed a multimodal freight network model for strategic transportation planning. Chang (2008) formulated a route selection problem for international intermodal shipments considering multimodal multi-commodity flow. The model was formulated to consider multiple objectives, scheduled modes and demanded delivery times, and economies of scale. Hwang and Ouyang (2014) used the UE approach to assign freight shipments onto rail networks which were represented as directed graphs.

Based on the above review, to date, no model has been developed to comprehensively assign freight flows that are transported via multiple modes (road-only, rail-only, and road-rail intermodal) under equilibrium conditions. This study seeks to fill this gap in the literature by developing such a model. Specifically, given a set of freight demands between origins and destinations and designated modes (road-only, rail-only, and intermodal), the model seeks an equilibrium assignment that minimizes the total transportation cost (i.e., travel time) for the freight transport network. To solve the proposed model, a path-based algorithm, based on the gradient projection (GP) algorithm proposed by Jayakrishnan et al. (1994), is adopted. The GP algorithm is chosen because

it has been shown to converge faster than the conventional Frank-Wolfe algorithm (Frank and Wolfe, 1956) and outperform other path-based algorithms (Chen et al., 2002).

To model congestion effects in a network at the planning level, link performance functions are often used, which express the travel time on a link as a function of link flow. For highways, the standard Bureau of Public Road link performance function is commonly used. For rail, Borndörfer et al. (2013) suggested a link performance function for freight rail network. When applying these types of functions, it is necessary to calibrate the parameters to capture local and regional effects. In this study, the function proposed by Borndörfer et al. is adopted and calibrated to reflect characteristics of the U.S. rail infrastructure.

To validate the proposed model, the projected equilibrium freight flow pattern on the U.S. intermodal network is compared against the Freight Analysis Framework, version 3, (FAF3) network flow assignment pattern. FAF3 is the most comprehensive public source of freight data in the U.S. (Southworth et al., 2011). It should be noted that the FAF3 flow values are not absolute. Rather, the FAF3 flows are estimated using models that disaggregate interregional flows into flows between localities and then these flows are assigned to individual highways using average payloads per truck to produce truck counts. Thus, the FAF3 flow values could be different from actual truck counts.

2.1 MODELING AND ALGORITHMIC FRAMEWORK

This study takes a system's view and assumes that in the long run the activities carried out by shippers and carriers will lead to equilibrium where the cost of any shipment cannot be lowered by changing mode and/or route. The freight logistics

problem has two levels. The first and upper level involves decisions by shippers in selecting a carrier, and the second and lower level involves decisions by the carriers in minimizing the shipment times. The modeling framework proposed here (i.e., freight traffic assignment) is for the lower level. Therefore, it is assumed, the cost on all used paths via different modes (road-only, rail-only, and intermodal) is equal for each origin-destination (OD) demand pair and equal to or less than the cost on any unused path at equilibrium (Sheffi, 1985).

2.1.1 Notation

N set of nodes in the network

A set of links in the network

N_c set of freight zone centroid nodes in the network

N_t set of road nodes in the network

N_l set of rail nodes in the network

A_t set of road links in the network

A_l set of rail links in the network

A_f set of terminal links in the network

R set of origins in the network, $R \subseteq N$

S set of destinations in the network, $S \subseteq N$

r origin zone index, $r \in R$

s destination zone index, $s \in S$

x_a flow on link a, $a \in A$

$t_a(\omega)$ travel time on link a for a flow of ω

f_k^{rs} flow on path k connecting r and s

$f_{\bar{k}^{rs}}^{rs}$ flow on shortest path connecting r and s

q_t^{rs} freight truck demand from r to s

q_l^{rs} freight train demand from r to s

q_i^{rs} freight intermodal demand from r to s

K_t^{rs} set of paths with positive truck flow from r to s

K_l^{rs} set of paths with positive train flow from r to s

K_i^{rs} set of paths with positive intermodal flow from r to s

T set of available terminals for transfer of shipments

2.1.2 Formulation

Consider a network which is represented by a directed graph $G = (N, A)$, where N is the set of nodal points of the network ($N = N_c \cup N_t \cup N_l$), while A is the set of links joining them in the network ($A = A_t \cup A_l \cup A_f$). In the network, nodal points are made of three node sets: zone centroid represented by nodes (N_c), road intersections (N_t), and rail junctions (N_l). On the other hand, network links are formed by three sets: road segments (A_t), rail tracks (A_l), and terminal transfer links (A_f). Note that road-rail intermodal terminals are modeled as links and that flows are bi-directional on these links. Furthermore, their end nodes have different modes (one from the set N_t and the other from the set N_l). For truck traffic demand q_t^{rs} from origin $r \in R$ to destination $s \in S$ and

11

a set of paths that connect r to s for each OD pair K_t^{rs}, the independent variables are a

set of path flows f_k^{rs} that satisfy the demand $\left(\sum_{k \in K_t^{rs}} f_k^{rs} = q_t^{rs} \right)$. Similarly, the path flows

for train and intermodal on path-sets, K_l^{rs} and K_i^{rs}, satisfy their respective demands (q_l^{rs}

and q_i^{rs}) from r to s. Note that the path-set for intermodal consists of paths formed by

links from both road and rail segments of the network. Therefore, the total freight flow

on a road segment ($a \in A_t$) is the sum of the road-only flows and intermodal flows.

Similarly, the total freight flow on a rail segment ($a \in A_l$) is the sum of the rail-only and

intermodal flows. The user-equilibrium model for this problem is formulated as follows.

$$\text{Min } Z = \sum_{a \in A_t} \int_0^{x_a} t_a(\omega)\, d\omega + \sum_{a \in A_l} \int_0^{x_a} t_a(\omega)\, d\omega \tag{2.1}$$

Subject to

$$\sum_{k \in K_t^{rs}} f_k^{rs} = q_t^{rs}, \qquad \forall r \in R, s \in S \tag{2.2}$$

$$\sum_{k \in K_l^{rs}} f_k^{rs} = q_l^{rs}, \qquad \forall r \in R, s \in S \tag{2.3}$$

$$\sum_{k \in K_i^{rs}} f_k^{rs} = q_i^{rs}, \qquad \forall r \in R, s \in S \tag{2.4}$$

$$x_a = \sum_{r \in R} \sum_{s \in S} \sum_{k \in K_t^{rs}} f_k^{rs} \delta_{ka}^{rs} + \sum_{r \in R} \sum_{s \in S} \sum_{k \in K_i^{rs}} f_k^{rs} \delta_{ka}^{rs}, \quad \forall a \in A_t \tag{2.5}$$

$$x_a = \sum_{r \in R} \sum_{s \in S} \sum_{k \in K_l^{rs}} f_k^{rs} \delta_{ka}^{rs} + \sum_{r \in R} \sum_{s \in S} \sum_{k \in K_i^{rs}} f_k^{rs} \delta_{ka}^{rs}, \quad \forall a \in A_l \tag{2.6}$$

$$f_k^{rs} \geq 0, \quad \forall k \in K_t^{rs}, k \in K_l^{rs}, k \in K_i^{rs}, r \in R, s \in S \tag{2.7}$$

where, $\delta_{ka}^{rs} = \begin{cases} 1 & \text{if link } a \text{ is on path } k \text{ connecting } r \text{ and } s \\ 0 & \text{otherwise} \end{cases}$

The objective function (2.1) states that the total travel time for both segments (road and rail) associated with the flows between origins and destinations are to be minimized. Constraints (2.2) to (2.4) ensure that all freight demands are assigned to the network. Constraints (2.5) and (2.6) are definitional constraints that compute link flows. Lastly, constraint (2.7) ensures non-negative flows.

To model congestion effects in a network at the planning level, link performance functions are often used, which express the travel time on a link as a function of link flow. For highways, the standard Bureau of Public Road link performance function, named after the agency which developed it, is commonly used. For rail, a few functions have been proposed (Hwang and Ouyang, 2014; Krueger, 1999; Lai and Barkan, 2009). Borndörfer et al. (2013) suggested a link performance function for freight rail network. When applying these types of functions, it is necessary to calibrate the parameters to capture local and regional effects. In this study, the function proposed by Borndörfer et al. is adopted and calibrated to reflect characteristics of the U.S. rail infrastructure. The link performance functions have the following form:

$$t_a(x_a) = t_{o,t}\left(1 + 0.15\left(\frac{x_a}{C_a}\right)^4\right), \qquad \forall a \in A_t \tag{2.8}$$

$$t_a(x_a) = t_{o,l}\left(1 + \left(\frac{x_a}{C_a}\right)^\beta\right), \qquad \forall a \in A_l \tag{2.9}$$

where $t_{o,t}$ and $t_{o,l}$ are the free-flow travel time for road and rail links, respectively, and C_a is the capacity of the link. In equation (2.9), β represents the penalty rate and its value can be 2, 4, 7, 15 (Borndörfer et al., 2013). In this study β is calibrated to capture characteristics of the rail segment of the U.S. intermodal network. Calibration involved

changing the value of β such that the computed train delay resulted in realistic flow pattern. The functional form of equation (2.9) indicates that the travel time on rail links is more sensitive to flow when it is near capacity than that of road links.

Figure 2.1 illustrates the methodology used to calculate the intermodal shortest path. Figure 2.1*a* shows the typical intermodal freight transport elements that are used to ship goods from an origin to a destination; a typical shipment would go through two intermodal terminals. Figure 2.1*b* shows the corresponding network structure. The intermodal path is made up of the node sequence: $b \to c \to d \to e \to f \to g$. Thus, given b and g, the objective of the shortest path algorithm is to find nodes c, d, e, and f that result in the least travel time. Delays are incurred at intermodal terminals due to the transfer of modes and storage. This terminal delay is considered as terminal link delay $(t_a, \forall a \in A_f)$ in the path travel time calculation.
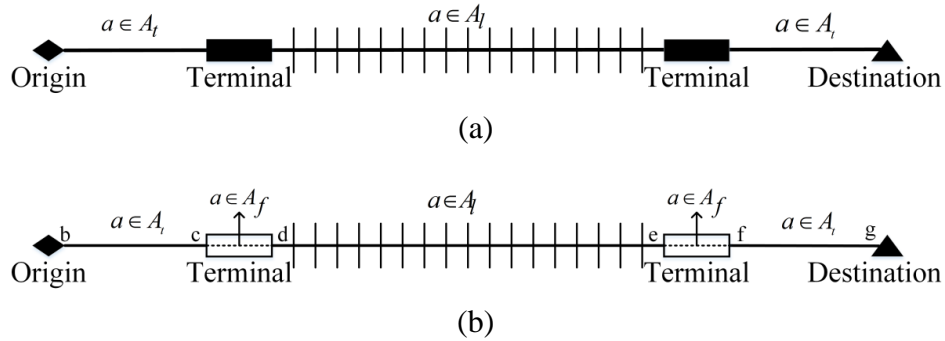
Figure 2.1 Shortest path calculation considering terminal: (a) basic intermodal structure and (b) modeled structure.

2.1.3 Solution Algorithm

A path-based algorithm (gradient projection) is used to solve the proposed user-equilibrium assignment problem. The adopted gradient projection algorithm is based on

14

the Goldstein-Levitin-Polyak gradient projection method formulated by Bertsekas (1976) and modified by Jayakrishnan et al. (1994) to solve the traffic assignment problem. In this study, this algorithm is further modified to address the assignment of freight demands that can be transported via three different modes: road-only, rail-only, and intermodal. Additionally, the algorithm is modified to consider intermodal terminals in the network. The iterative steps of the algorithm are as follows:

Step 0. Initialization.

Set $t_a = t_a(0), \forall a \in A$ and select terminals for all OD pairs. Assign OD demands q_t^{rs}, q_l^{rs}, and q_i^{rs} on the shortest path calculated based on $t_a, \forall a \in A_t$, $t_a, \forall a \in A_l$, and $t_a, \forall a \in A$, respectively and initialize the path-sets K_t^{rs}, K_l^{rs}, and K_i^{rs} with the corresponding shortest path for each OD pair (r,s). This yields path flows and link flows. Set iteration counter $n = 1$.

Step 1. For each OD pair (r,s):

Step 1.1. Update.

Set $t_a(n) = t_a(x_a(n)), \forall a \in A$. Update the first derivative lengths (i.e., path travel times at current flow): $d_{kt}^{rs}(n), \forall k \in K_t^{rs}$, $d_{kl}^{rs}(n), \forall k \in K_l^{rs}$, and $d_{ki}^{rs}(n), \forall k \in K_i^{rs}$.

Step 1.2. Direction finding.

Find the shortest path $\bar{k}_t^{rs}(n)$ based on $t_a(n), \forall a \in A_t$. If different from all the paths in K_t^{rs}, add it to K_t^{rs} and record $d_{\bar{k}_t^{rs}(n)}^{rs}$. If not, tag the shortest among the paths in K_t^{rs} as $\bar{k}_t^{rs}(n)$.

15

Repeat this procedure for K_l^{rs} and K_i^{rs} to find $d_{\bar{k}_l^{rs}(n)}^{rs}$ and $d_{\bar{k}_i^{rs}(n)}^{rs}$ based on

$t_a(n), \forall a \in A_l$ and $t_a(n), \forall a \in A$, respectively.

Step 1.3. Move.

Set the new path flows for K_t^{rs}.

$$f_k^{rs}(n+1) = \max\left\{0, f_k^{rs}(n) - \frac{\alpha(n)}{s_k^{rs}(n)}\left(d_{kt}^{rs}(n) - d_{\bar{k}_t^{rs}(n)}^{rs}\right)\right\}, \quad \forall k \in K_t^{rs}, k \neq \bar{k}_t^{rs}$$

where, $s_k^{rs}(n) = \sum_a \dfrac{\partial t_a^{rs}(n)}{\partial x_a^{rs}(n)}, \quad \forall k \in K_t^{rs}$

a denotes links that are on either k or $\bar{k}_t^{rs}$, but not on both. $\alpha(n)$ is the step-size.

Also, $f_{\bar{k}^{rs}}^{rs}(n+1) = q_t^{rs} - \sum f_k^{rs}(n+1), \qquad \forall k \in K_t^{rs}, k \neq \bar{k}_t^{rs}(n)$

Follow this procedure to find new path flows for K_l^{rs} and K_i^{rs}.

From path flows find the link flows $x_a(n+1)$.

Step 2. Convergence test.

If the convergence criterion is met, stop. Else, set $n = n+1$ and go to step 1.

For rail networks, the same infrastructure (i.e., rail tracks) is often shared by traffic flow in both directions. To model this feature, two separate directed links in opposite directions are used instead of one bi-directional link. These two links share the same properties such as length and capacity. Moreover, the link delay on any one link is dependent on the flow on it, as well as the flow on the opposite link (see Hwang and Ouyang (2014) for details). Due to the use of this modeling method, the link performance function shown in equation (2.9) needs to be modified. The modified version is shown in equation (2.10), where x_a is the link flow from node i to node j

16

and $x_{a'}$ is the flow from node j to node i. Equation (2.1) also needs to be modified and its modified version is shown in equation (2.11). The rest of the model is the same and the above solution algorithm remains applicable for solving the modified model.

$$t_a(x_a + x_{a'}) = t_{o,l}\left(1 + \left(\frac{x_a + x_{a'}}{C_a}\right)^{\beta}\right), \qquad \forall a \in A_l \tag{2.10}$$

$$Z = \sum_{a \in A_t}\int_0^{x_a} t_a(\omega)\,d\omega + \sum_{a \in A_l}\int_0^{x_a + x_{a'}} t_a(\omega)\,d\omega \tag{2.11}$$

The proposed model provides a general framework for addressing different types of freight transport networks and situations. While the highway mode generally allows truck to provide door-to-door service, there may be some situations where trucks are not allowed to traverse certain segments in the network. Similarly, certain rail track segments may be accessible or available to shippers. The proposed model can address this by restricting those links in shortest path calculation, and thus, those restricted links are not considered in the assignment process. The model can also address the situations when some intermodal terminals are not available for routing shipments between certain OD demand pairs. This can be done by excluding those terminals from the set (T) for an OD demand pair during terminal selection (i.e., initialization step of solution algorithm).

2.1.4 Special Case (Intermodal Demand Only)

The proposed model is also applicable for intermodal freight demand assignment, with a few modifications. Given all the network elements and demand (q_i^{rs}), the intermodal assignment problem is as follows:

$$\text{Min } Z = \sum_{a \in A_t}\int_0^{x_a} t_a(\omega)\,d\omega + \sum_{a \in A_l}\int_0^{x_a} t_a(\omega)\,d\omega \tag{2.12}$$

Subject to

$$\sum_{k \in K_i^{rs}} f_k^{rs} = q_i^{rs}, \quad \forall r \in R, s \in S \tag{2.13}$$

$$x_a = \sum_{r \in R} \sum_{s \in S} \sum_{k \in K_i^{rs}} f_k^{rs} \delta_{ka}^{rs}, \quad \forall a \in A \tag{2.14}$$

$$f_k^{rs} \geq 0, \quad \forall k \in K_i^{rs}, r \in R, s \in S \tag{2.15}$$

The solution algorithm described previously is also applicable for solving problem (2.12) to (2.15). However, path-set K_i^{rs} and shipment demand q_i^{rs} should be considered in the solution algorithm instead of three path-sets and three demands.

2.2 APPLICATION

To demonstrate the validity of the proposed methodology, the model is applied to the U.S. intermodal network created by Oak Ridge National Laboratory (Center for Transportation Analysis, 2014). Without loss of generality, the network is modified to retain only the primary elements of the network. The assignment problem is investigated from a strategic perspective. Thus, freight flows are assigned to the entire freight transport network without considering any restrictions on highway links, rail links, and intermodal terminals.

2.2.1 Network Description

The intermodal network considered is shown in Figure 2.2. Part (a) shows the detailed version, and part (b) shows the simplified version. The intermodal network comprises the U.S. interstates, Class I railroads and road-rail terminals. The squares represent freight zone centroids. The circles represent road-rail terminals. The black

18

lines represent interstates, and the gray lines represent Class I railroads. The simplified

network has a total of 1532 links and 301 nodes. The nodes include 120 centroids, 97

road intersections, and 84 rail junctions.
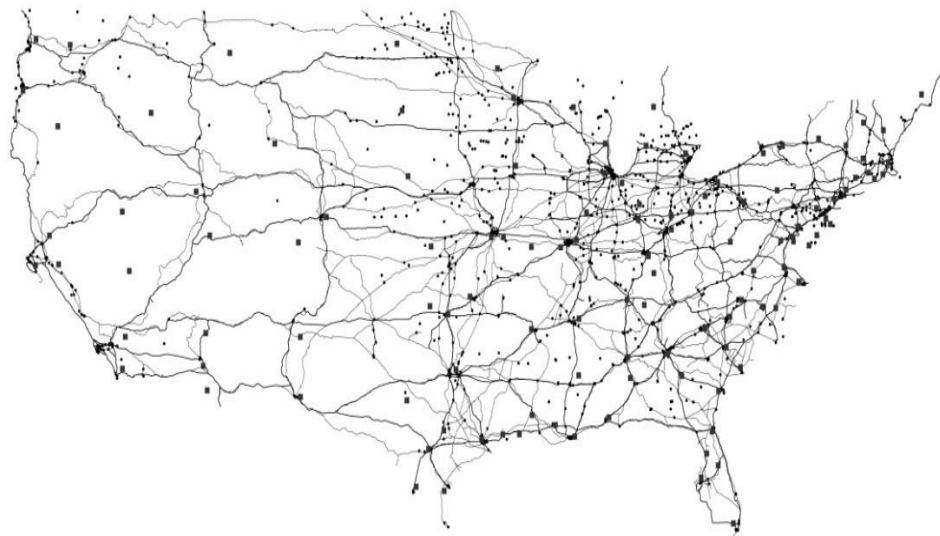
(a)
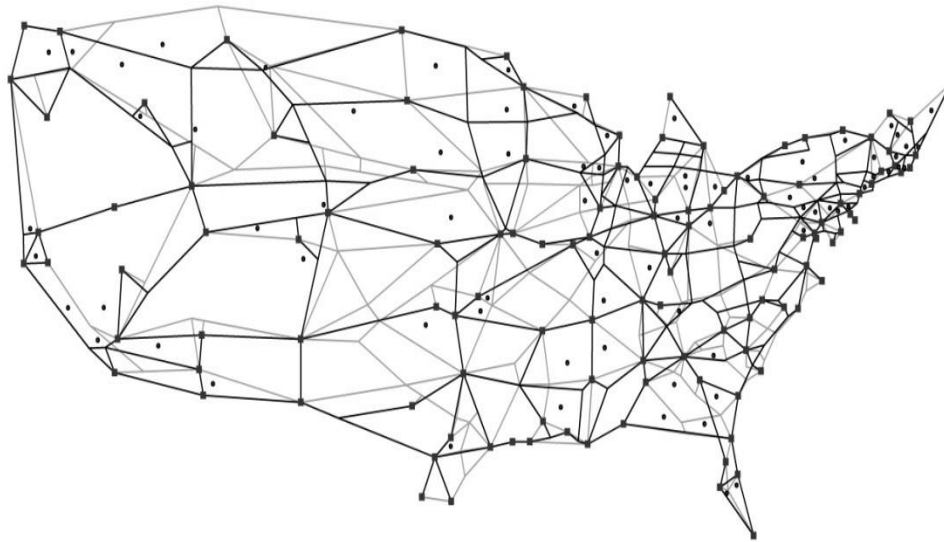
(b)

Figure 2.2 Road-rail transportation networks in the contiguous U.S.: (a) detailed network
and (b) simplified network.

Attributes of the network elements include link lengths, number of tracks, type of control for rail links, etc. The free-flow speed for the road links is calculated using the equation provided in the NCHRP Report 387 (Dowling et al., 1997) which requires speed limit as an input. For the rail links, the maximum speed for freight train is taken as 60 mph (Krueger, 1999). Free-flow travel times for links are calculated using free-flow speeds. Capacities for the rail links are obtained using the number of tracks and type of control for corresponding rail links (Cambridge Systematics, 2007). For rural interstates and urban interstates, a capacity of 21,000 vehicle/lane/day and 19,500 vehicle/lane/day is used, respectively (Standifer and Walton, 2000). Rail links are assumed to have full capacity, whereas road links are assumed to have reduced capacity due to congestion. In the network considered, contiguous U.S., the total number of freight zones is 120, and hence it is assumed that there are 14,400 possible OD demand pairs in the network. The freight demands for all OD pairs are obtained from the FAF3 database (Federal Highway Administration, 2013).

The FAF3 procedure to convert tonnage to truck counts (Oak Ridge National Laboratory, 2013) is used in this study and the key steps are summarized here: (i) compute distance between origin and destination centroid, (ii) using truck allocation factors based on five distance ranges allocate tonnage to five truck types, (iii) convert tonnage assigned to each truck type into their equivalent annual truck traffic values using the truck equivalency factors, which is based on 9 truck body types, (iv) find empty trips using empty truck factors and add empty trips to the loaded trips, (v) aggregate the total annual truck traffic for all body styles together for each truck types, and (vi) sum the traffic for all the truck types. The output of this conversion process is the overall annual

truck traffic between the origin and destination. This procedure is carried out for all the demands that are transported by trucks.

The procedure to convert tonnage to trainloads developed by Hwang (2014) is used in this study. The conversion steps are: (i) group FAF commodity types into 10 types based on similarities, (ii) convert tonnage into equivalent trainloads using average loading weight factors for each commodity group, and (iii) sum the trainloads for all commodity groups. This procedure is carried out for all the demands that are transported by rail.

FAF3 does not provide intermodal demand directly. Thus, to obtain this information the demand recorded as being transported by "multiple modes and mail" is used. To estimate the intermodal demand from this source, several filters are applied. The data are filtered to include only those commodities typically transported via intermodal (Cambridge Systematics, 2007) and only those shipments with a distance of 500 miles or greater (Slack, 1990). The average load for a container/trailer is used for conversion, and the average train length in terms of TOFC/COFC count (Cambridge Systematics, 2007) is used to determine the number of intermodal trains equivalent to trucks hauled. The conversion methodology is as follows: (i) sort commodities transported by intermodal trains, (ii) convert tonnage of those commodities into equivalent container/trailer using average loading capacity, (iii) sum all container/trailer counts, and (iv) convert container/trailer counts to equivalent trainloads using average train length information. In intermodal transportation, truck haulage takes place from origin to delivery terminal and then from receiving terminal to destination. Therefore, every intermodal truck trip generates an empty truck trip. Thus, the number of

21

container/trailer is doubled to obtain the intermodal truck flow. This procedure is carried out for all the demands that are transported via intermodal.

The conversion procedures were coded in Excel VBA to create freight OD trip tables for truck, rail, and intermodal in 120 x 120 x 3 matrix form. It is assumed that road and rail infrastructure remain open for operation 365 days in a year. Using the aforementioned data sources and procedures, it is determined that in a single day in the base year (2007), there are 618,190 shipments transported by trucks, 1,415 shipments transported by trains, and 12,474 shipments transported via intermodal.

2.2.2 Results and Discussions

The solution algorithm was coded in MATLAB, and the experiments were run on a desktop computer with an Intel Core i7 3.40 GHz processor and 8 GB of RAM. The terms in the objective function are normalized to yield consistent units. This was accomplished by dividing the first term by the sum of truck demand and intermodal truck demand and second term by the sum of train demand and intermodal train demand. The stopping criterion used is the value of relative gap (change in value of objective function with respect to the value in previous iteration). The algorithm converged after 10 iterations in 686.50 seconds with a relative gap of 10^{-4}. At convergence the value of the normalized objective function is 37.3594 hours. It should be noted that $\beta = 4$ is used here in the calculation of rail link delay.

The model was also solved using a classical algorithm (Frank-Wolfe). The Frank-Wolfe algorithm provides a normalized objective value of 37.3587 hours after 115 iterations and 2982.40 seconds of computational time. This result indicates that the

gradient projection algorithm is much more effective than the Frank-Wolfe algorithm in solving the proposed freight assignment model. This finding corroborates other studies which reported that the gradient projection algorithm is superior to the Frank-Wolfe algorithm (e.g., Jayakrishnan et al., 1994).

Among the four values tested for β, with $\beta = 2$ the flow on few links is very high, $\beta = 7$ the flow is reasonable, but the algorithm takes longer to converge, and $\beta = 15$ the flow results in very high travel time on some rail links. Therefore, for capturing freight train delay in the U.S. rail network, $\beta = 4$ is most suitable. Table 2.1 shows the percentage of link flow over capacity and link travel time of selected congested rail links, which were used to determine the best value for β. Note that, travel time is calculated based on the flow on corresponding link and flow on link opposite to it.

Table 2.1 Comparison of β Values

Link (Rail)	Percentage Increase in Flow over Capacity (Travel Time in Hour)			
Index	$\beta = 2$	$\beta = 4$	$\beta = 7$	$\beta = 15$
76	43.3 (10.1)	29 (7.9)	27 (6.6)	19.1 (39.9)
81	36 (9.6)	17 (9.5)	11.7 (8.4)	1.3 (11.5)
268	27.3 (2.6)	8.8 (2.2)	2.1 (1.9)	4.1 (2.5)
279	29.5 (6.6)	10.4 (6.1)	5.6 (6.2)	1 (7.2)
392	30.3 (11.2)	17.6 (8.8)	4.6 (5.2)	2.7 (15.5)

The resulting user-equilibrium flow for the road network is shown in Figure 2.3*a* and for the rail network is shown in Figure 2.3*b*. In Figure 2.3, the volume and spatial variation of freight traffic can be easily visualized by the thickness of the links.
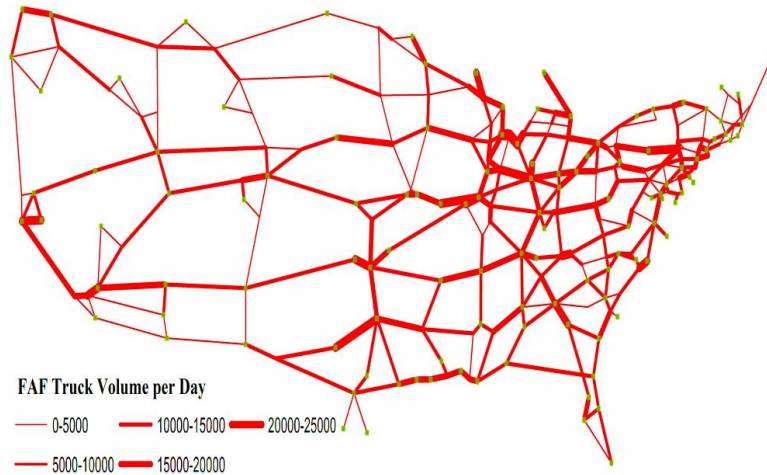
(a)

(b)

Figure 2.3 Freight traffic assignment results: (a) truck on road network and (b) train on rail network.

Figure 2.4*a* shows the FAF truck volume distribution on the U.S. national highway system for the year 2007. It shows truck flow patterns for trucks serving locations at least 50 miles apart and trucks not included in the "multiple modes and mail" (Federal Highway Administration, 2014). This truck flow pattern is very similar to the proposed model's projected user-equilibrium flow for the road network. Both maps indicate that there is high truck flow on interstates that traverse through California,

Washington, Texas, Arkansas, Tennessee, Georgia, Florida, Michigan, Illinois, Indiana, New York, New Jersey, and Connecticut. This similarity suggests that the proposed model is capable of forecasting actual truck flows.

Figure 2.4*b* shows the 2005 freight trains per day and 2007 passenger trains per day on primary rail freight corridors in the U.S. (Cambridge Systematics, 2007). Though the proposed model's projected flow is only for freight train, this train flow pattern can be compared against the projected flow due to the fact that freight train volume far outnumbers passenger train volume in the U.S. The map indicates that there is high train flow on rail tracks that traverse through Washington, Montana, North Dakota, Arizona, New Mexico, Texas, Missouri, Wyoming, Nebraska, Iowa, Illinois, Indiana, Pennsylvania, Ohio, Georgia, New York, and New Jersey. The depicted train flow pattern and volume in most of the states are very similar to the proposed model's projected flow pattern. However, there exist a few discrepancies. The reason may be due to the difference in the demand between 2005 and 2007 and difference in methodology adopted to forecast freight flow. Note that Figure 2.4*b* is derived using annual survey data, whereas Figure 2.3*b* is derived from the equilibrium assignment procedure.

The proposed model's projected ton-miles are also compared quantitatively against those reported in the Commodity Flow Survey (CFS) and the FAF3. The results are reported in Table 2.2. In 2007, for the highway mode, the CFS reported freight ton-miles (Margreta et al., 2009) is about 34% less than the FAF3 reported ton-miles. The difference in ton-miles between the proposed model and FAF3 and CFS is about 29% and 15%, respectively. Note that the FAF3 demand data was used as an input for the proposed model. Thus, the difference in ton-miles against FAF3 is reasonable because

the proposed model only considered the contiguous U.S., and that it may have underestimated the intermodal demand. For the rail mode, the proposed model's projected ton-miles is about 14% less than that of the FAF3 data. This is reasonable for the same reasons mentioned previously. Overall, for both truck and rail demand, the proposed model appears to produce reasonable ton-miles value despite having a few simplifications, including a simplified network.
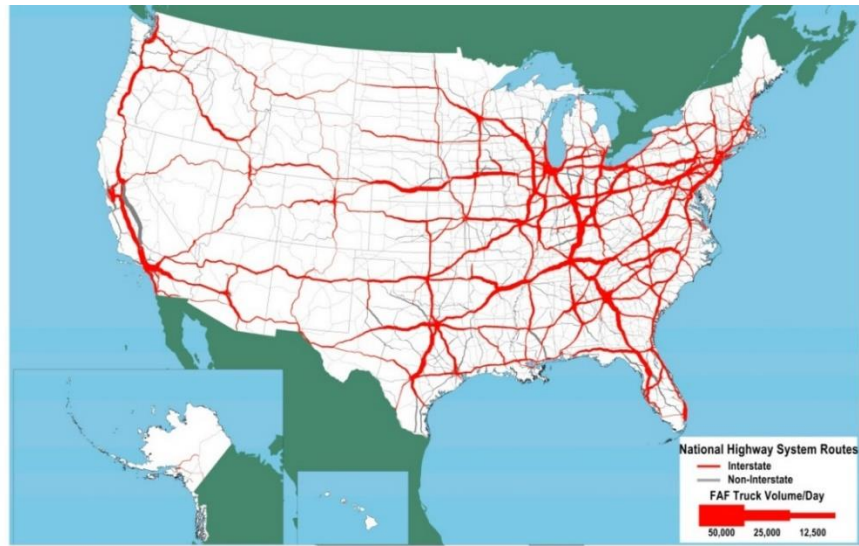
(a)
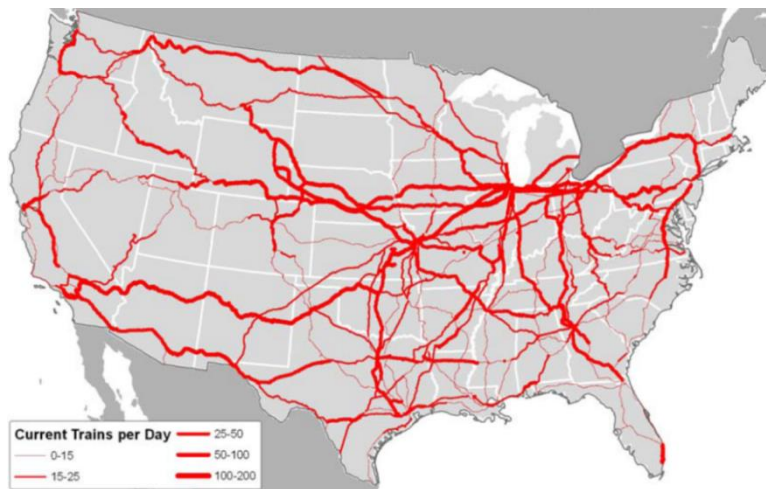
(b)

Figure 2.4 Freight traffic volume: (a) truck on U.S. highway system and (b) train on primary rail freight corridor.

Table 2.2 Freight Ton-Miles (Million) for Year 2007

Mode	FAF3	CFS	Proposed Model
Truck[a]	2,817,837	1,850,335	2,172,701
Rail[b]	1,991,182	1,755,154	1,703,039

[a]Includes truck and multiple modes and mail; [b]Includes rail and multiple modes and mail

2.3 CONCLUSION

This chapter proposes a methodology for freight traffic assignment in large-scale road-rail intermodal networks. The proposed framework considers the lower level of a bi-level freight logistics problem, where the carriers' goals are to deliver the goods in a minimal amount of time. Given a set of freight demands between origins and destinations and designated modes (road-only, rail-only, and intermodal), the model finds the user-equilibrium freight flow. To obtain the solution for the model, a path-based algorithm based on the gradient projection algorithm is adopted. The proposed model was tested using the U.S. intermodal network and the FAF3 2007 freight shipment data. It was found that 4 is the most appropriate value for the β parameter when applying the Borndörfer et al. link performance function on the U.S. intermodal network. The results of the analysis, volume and spatial variation of freight traffic, show that the model produces equilibrium flow pattern that was very similar to the FAF3 flow assignment. The ton-miles values obtained from the model were also very close to those values reported in FAF3 and CFS. An attractive feature of the proposed model is that it converges within a few iterations and in about 11 minutes for a very large network. The model was also solved for the same network using the Frank-Wolfe algorithm, and results indicate that the gradient projection algorithm is superior to the Frank-Wolfe algorithm in terms of convergence (i.e., fewer iterations) and computational time. The developed

model can be used by transportation planners and decision makers to forecast freight

flows and evaluate strategic network expansion options.

CHAPTER 3

INTERMODAL FREIGHT ASSIGNMENT UNDER UNCERTAINTY[1]

Efficient management of freight movements is essential to support domestic e-commerce and international trade. Freight activities are directly related to a country's Gross Domestic Product and economic viability. In recent years, the U.S. transportation system supports a growing volume of freight, and it is anticipated that this trend will continue in the coming years. For example, in 2015 the U.S. transportation system moved a daily average of about 49.3 million tons of freight valued at more than $52.5 billion. Freight tonnage is projected to increase at about 1.4% per year between 2015 and 2045 (Bureau of Transportation Statistics, 2017). To support the projected increase in freight volume, an efficient, reliable, and low-cost freight logistics system is necessary to keep the U.S. competitive in the global market.

Current freight forecasting methodologies assume that the freight transport network is always functioning and is never disrupted (e.g., Hwang and Ouyang, 2014; Uddin and Huynh, 2015). Hwang and Ouyang (2014) provided a framework for freight train traffic assignment in a network where the network links (i.e., rail tracks) are always available. Uddin and Huynh (2015) provided a methodology for road-rail freight traffic assignment in an intermodal network which considered that the network elements are never disrupted. The aforementioned assumptions were made by the authors to simplify

---

[1]This chapter has been adapted from "Uddin, M., Huynh, N., & Ahmed, F. (2019+). Assignment of freight traffic in a large-scale intermodal network under uncertainty. *Journal of Transportation Engineering, Part A: Systems* (under review)."

29

the scope of the studies and were appropriate for the problems addressed in those studies. Those studies did not consider the risks from weather-induced disruptions which have dramatically increased in recent years; several have occurred recently that severely affected the U.S. freight transport network. The Mississippi River flooding impacted a major freight route, I-40 in Arkansas in 2011. The tropical storm Irene caused damage to over 5,000 miles of highways and 34 bridges in Vermont in 2011. Hurricane Sandy caused billions of dollars in damage and severely flooded streets and tunnels in the New York and New Jersey region in 2011 (Federal Highway Administration, 2015). In 2017, the U.S. endured 16 separate weather-related disasters with losses exceeding $1 billion each, with a total cost of about $306 billion (National Oceanic and Atmospheric Administration, 2018). In 2018, flooding from Hurricane Florence caused closure of more than 200 roads in South Carolina and more than 600 roads in North Carolina, including several stretches of I-95, which is a major freight route along the Eastern seaboard (Barton, 2018). Given the growing occurrence of such disasters and their impact on the freight transport network (Adams et al., 2012), there is a need to develop freight forecasting methods that address network uncertainties caused by natural disasters.

To this end, this study proposes a stochastic model for the assignment of freight, considering road, rail, and intermodal shipments, on a road-rail intermodal network that is subject to uncertainty. Given the exact evaluation of the stochastic model is difficult, an algorithmic framework is proposed for solving the model. To account for uncertainties in a realistic manner (i.e., disasters), the U.S. natural disaster risk map (Alert Systems Group, 2018) is used. The disaster types considered are earthquake,

hurricane, tornado, and flood. For each disaster scenario, the model seeks an equilibrium assignment that minimizes the total transportation cost (i.e., travel time) for a given set of freight demands between origins and destinations and available modes (road-only, rail-only, and intermodal). A comparative analysis of different disaster scenarios is performed to assess their impacts on the resulting freight flows.

3.1 LITERATURE REVIEW

The problem of assigning freight flows to a single-mode or multi-mode network has been studied by many researchers in the past few decades. Crainic et al. (1984) developed a non-linear multi-commodity model to address the routing and scheduling of freight trains. The model was solved using a heuristic and was tested using data from the Canadian National Railroads. Guelat et al. (1990) developed a model to solve the traffic assignment problem for a multi-mode network with the objective of minimizing the total cost. The model was solved using the Gauss-Seidel linear approximation algorithm. Fernandez et al. (2004) formulated a model which considers the detailed operation of the freight rail system to predict the equilibrium flows. The model was formulated using the Variational Inequality (VI) approach and was solved using the diagonalization algorithm. Winebrake et al. (2008b) developed a geospatial model to be used in intermodal freight network. The model sought to find the least-cost routes between origins and destinations. Additionally, it considered the impact of freight assignment in terms of energy and emission attributes. Chang (2008) formulated a multi-mode multi-commodity flow model with time windows and concave costs. His model can route freight in an international intermodal network. Hwang and Ouyang (2014) developed a model to

predict freight flow in a rail network. Their model's objective was to find the user-equilibrium freight train flow by minimizing the total railroad link travel time. Uddin and Huynh (2015) developed a methodology to assign user-equilibrium freight truck and train flow considering road, rail, and road-rail intermodal demands. The authors demonstrated their model using the U.S. intermodal network and freight demands from the Freight Analysis Framework.

A few researchers have focused on capturing the interaction between freight shippers and carriers. One of the first shipper-carrier models was formulated by Friesz et al. (1986). Their model has two separate sub-models (shipper and carrier). The shipper sub-model selects the origin-destination (OD) pair, modes, transshipment locations, and carriers. These decisions are then used by the carrier sub-model to assign freight flow over the rail-water intermodal and rail-only network. Agrawal and Ziliaskopoulos (2006) also developed a shipper-carrier model where the shippers seek to minimize their cost by choosing carriers with the lowest shipping cost. The VI formulation was used to model the shippers' decision to choose carriers.

The multimodal network design problem has been explored from an investment perspective in some studies. Loureiro and Ralston (1996) developed a multi-commodity multi-mode network design model to determine the best set of investment options for the freight network. The model captured the competition among various modes by assuming that goods are shipped at minimum total generalized cost. Yamada et al. (2009) developed an investment freight planning model for a multi-mode network. A bi-level programming model was developed, where the upper level model determined the

equilibrium freight flows and the lower level model determined the network improvement actions.

Another approach used by researchers to determine freight assignment is network simulation. The simulation-assignment approach allows for the flexibilities to consider operational issues, such as delays at different nodes in the network, advanced traveler information system, and advanced traffic information. Mahmassani et al. (2007) developed a dynamic freight network simulation-assignment model to analyze multi-product freight flows. The link travel cost and transfer cost were included in the model to find the least-cost path using a sequence of different modes (i.e., truck, train, ferry) available in the intermodal network. Zhang et al. (2008) validated the above model by applying it to a Pan-European rail network.

The aforementioned studies assumed that the transport network is failed proof and always functioning. Some studies have relaxed this constraint by considering network uncertainty (i.e., disruption or disaster). Garg and Smith (2008) considered a multi-commodity network flow problem with link failure. The authors formulated an optimization model to determine a minimum-cost set of links for construction to address the disruption and to maintain feasible flow in the network. Peterson and Church (2008) addressed the routing of shipments when there is a loss of links in the freight rail transportation network. The authors developed a routing-based model for both capacitated and uncapacitated networks. Chen and Miller-Hooks (2012) developed a model to quantify network resilience for intermodal freight transport. A stochastic model was formulated to maximize the number of shipments between OD pairs. Huang et al. (2011) considered real-time disruption management for intermodal transport. Their

model aimed to predict the duration of the disruption. Miller-Hooks et al. (2012) formulated a model to determine the optimal level of preparedness and recovery actions to achieve the maximum level of resilience given a budget constraint. Gedik et al. (2014) presented a model that outlines a course of actions after disruptions. In their model, rail links were removed, and freight trains were re-routed in the available residual network. Uddin and Huynh (2016) proposed a stochastic model for the routing of multi-commodity freight in an intermodal network that is subject to disruptions. Uddin and Huynh (2019) extended their previous model to allow users to specify the reliability level and the model in turn provides a routing plan for the intermodal freight considering the reduced capacity of the network elements.

3.2 MODEL FORMULATION

The formulation assumes that a road-rail intermodal freight transportation network is represented by a directed graph $\mathcal{G} = (\mathcal{N}, \mathcal{A})$, where $\mathcal{N}$ is the set of nodal points of the network and $\mathcal{A}$ is the set of links joining them in the network. Set $\mathcal{N}$ consists of the set of freight zone centroid nodes $\mathcal{N}_c$, the set of road intersections $\mathcal{N}_t$, and the set of rail junctions $\mathcal{N}_l$, that is, $\mathcal{N} = \mathcal{N}_c \cup \mathcal{N}_t \cup \mathcal{N}_l$. Set $\mathcal{A}$ consists of the set of road segments $\mathcal{A}_t$, the set of rail tracks $\mathcal{A}_l$, and the set of terminal transfer links $\mathcal{A}_f$, that is, $\mathcal{A} = \mathcal{A}_t \cup \mathcal{A}_l \cup \mathcal{A}_f$. The road-rail intermodal terminals are modeled as network links. The flows are bi-directional on the terminal links. The end nodes of terminals have different nodes, that is, one from set $\mathcal{N}_t$ and the other from set $\mathcal{N}_l$. Origin and destination sets are represented by $\mathcal{R} \subseteq \mathcal{N}$ and $\mathcal{S} \subseteq \mathcal{N}$, respectively. Table 3.1 summarizes the notations used in the model.

Table 3.1 Notations

Notation	Description
$\mathcal{N}$	set of nodes in network
$\mathcal{A}$	set of links in network
$\mathcal{N}_c$	set of freight zone centroid nodes in network
$\mathcal{N}_t$	set of road intersections in network
$\mathcal{N}_l$	set of rail junctions in network
$\mathcal{A}_t$	set of road segments in network
$\mathcal{A}_l$	set of rail tracks in network
$\mathcal{A}_f$	set of terminal transfer links in network
$\mathcal{R}$	set of origins in network, $\mathcal{R} \subseteq \mathcal{N}$
$\mathcal{S}$	set of destinations in network, $\mathcal{S} \subseteq \mathcal{N}$
$\mathcal{T}$	set of available intermodal terminals for transfer of shipments
r	origin zone index, $r \in \mathcal{R}$
s	destination zone index, $s \in \mathcal{S}$
K_t^{rs}	set of paths with positive truck flow from r to s
K_l^{rs}	set of paths with positive train flow from r to s
K_i^{rs}	set of paths with positive intermodal flow from r to s
q_t^{rs}	freight truck demand from r to s
q_l^{rs}	freight train demand from r to s
q_i^{rs}	freight intermodal demand from r to s
Ξ	set of disruption-scenario samples
ξ	a disruption-scenario sample, $\xi \in \Xi$
$f_{k\xi}^{rs}$	flow on path k connecting r and s under disruption-scenario sample ξ
$x_{a\xi}$	flow on link $a \in \mathcal{A}$ under disruption-scenario sample ξ
$C_{a\xi}$	capacity of link $a \in \mathcal{A}$ under disruption-scenario sample ξ
$t_{a\xi}(\omega)$	travel time on link $a \in \mathcal{A}$ for flow of ω under disruption-scenario sample ξ

The capacity of each network link $a \in \mathcal{A}$ is disruption-scenario dependent, that is, capacities will be different depending on disruption-scenario sample $\xi \in \Xi$. A decision variable $x_{a\xi}$ is defined to represent the assigned freight flow on link $a \in \mathcal{A}$ under

disruption-scenario sample $\xi \in \Xi$. Typically, rail tracks are shared by train in both directions. For that reason, the link delay on any rail track is dependent on the flow on it as well as the flow in the opposite rail track. In the following model, for train flow, $x_{a\xi}$ represents the flow from node $i \in \mathcal{N}_l$ to node $j \in \mathcal{N}_l$, and $x_{a'\xi}$ represents the flow from node $j \in \mathcal{N}_l$ to node $i \in \mathcal{N}_l$.

For freight truck demand q_t^{rs} from origin $r \in \mathcal{R}$ to destination $s \in \mathcal{S}$ and a set of paths K_t^{rs} that connect r to s for each origin-destination (OD) pair, the path flow $f_{k\xi}^{rs}$ satisfies the demand under disruption-scenario sample $\xi \in \Xi$. Similarly, the path flows for freight train and intermodal on path sets K_l^{rs} and K_i^{rs} satisfy their respective demands (q_l^{rs} and q_i^{rs}) from r to s under disruption-scenario sample ξ. Since the intermodal path set consists of paths formed by links from both road segments and rail tracks, the total freight flow on a road segment ($a \in \mathcal{A}_t$) is the sum of the road-only flows and the intermodal flows. Similarly, the total freight flow on a rail track ($a \in \mathcal{A}_l$) is the sum of the rail-only flows and intermodal flows. The following stochastic model finds the equilibrium freight flows in a road-rail intermodal network.

$$\text{Min } \mathbb{E}_{\xi} \left[\sum_{a \in \mathcal{A}_t} \int_0^{x_{a\xi}} t_{a\xi}(\omega) \, d\omega + \sum_{a \in \mathcal{A}_l} \int_0^{x_{a\xi}+x_{a'\xi}} t_{a\xi}(\omega) \, d\omega \right] \tag{3.1}$$

Subject to

$$\sum_{k \in K_t^{rs}} f_{k\xi}^{rs} = q_t^{rs}, \qquad \forall \, r \in \mathcal{R}, s \in \mathcal{S}, \xi \in \Xi \tag{3.2}$$

$$\sum_{k \in K_l^{rs}} f_{k\xi}^{rs} = q_l^{rs}, \qquad \forall \, r \in \mathcal{R}, s \in \mathcal{S}, \xi \in \Xi \tag{3.3}$$

$$\sum_{k \in K_i^{rs}} f_{k\xi}^{rs} = q_i^{rs}, \qquad \forall \, r \in \mathcal{R}, s \in \mathcal{S}, \xi \in \Xi \tag{3.4}$$

$$x_{a\xi} = \sum_{r\in\mathcal{R}}\sum_{s\in\mathcal{S}}\sum_{k\in K_t^{rs}} f_{k\xi}^{rs}\delta_{ka}^{rs} + \sum_{r\in\mathcal{R}}\sum_{s\in\mathcal{S}}\sum_{k\in K_i^{rs}} f_{k\xi}^{rs}\delta_{ka}^{rs}, \qquad \forall\, a\in\mathcal{A}_t, \xi\in\Xi \tag{3.5}$$

$$x_{a\xi} = \sum_{r\in\mathcal{R}}\sum_{s\in\mathcal{S}}\sum_{k\in K_l^{rs}} f_{k\xi}^{rs}\delta_{ka}^{rs} + \sum_{r\in\mathcal{R}}\sum_{s\in\mathcal{S}}\sum_{k\in K_i^{rs}} f_{k\xi}^{rs}\delta_{ka}^{rs}, \qquad \forall\, a\in\mathcal{A}_l, \xi\in\Xi \tag{3.6}$$

$$f_{k\xi}^{rs} \geq 0, \qquad \forall\, k\in K_t^{rs}, k\in K_l^{rs}, k\in K_i^{rs}, r\in\mathcal{R}, s\in\mathcal{S}, \xi\in\Xi \tag{3.7}$$

where

$$\delta_{ka}^{rs} = \begin{cases} 1 & \text{if link } a \text{ is on path } k \text{ connecting } r \text{ and } s \\ 0 & \text{otherwise} \end{cases}$$

The objective function in equation (3.1) seeks to minimize the total expected travel time across different disruption scenario samples. Specifically, the total travel time includes the travel time on both road and rail segments. Constraints (3.2) through (3.4) ensure that all freight demands are assigned to the network. Constraints (3.5) and (3.6) compute the link flows on road and rail segments, respectively. Lastly, constraint (3.7) enforces all flow to be nonnegative.

To estimate the objective function value in equation (3.1), travel time on road and rail segments as a function of the flow are needed. For the road travel time, the Bureau of Public Roads link performance function is used. For rail travel time, the link performance function proposed by Uddin and Huynh (2015) is used. The link performance functions have the following form:

$$t_{a\xi}\left(x_{a\xi}\right) = t_{0,t}\left(1 + 0.15\left(\frac{x_{a\xi}}{C_{a\xi}}\right)^4\right), \qquad \forall\, a\in\mathcal{A}_t, \xi\in\Xi \tag{3.8}$$

$$t_{a\xi}\left(x_{a\xi} + x_{a'\xi}\right) = t_{0,l}\left(1 + \left(\frac{x_{a\xi} + x_{a'\xi}}{C_{a\xi}}\right)^4\right), \qquad \forall\, a\in\mathcal{A}_l, \xi\in\Xi \tag{3.9}$$

$t_{0,t}$ and $t_{0,l}$ are the free-flow travel time for road and rail links, respectively. $C_{a\xi}$ is the capacity of the link a under disruption-scenario sample ξ.

3.3 ALGORITHMIC STRATEGY

The proposed model (3.1) – (3.7) is a stochastic program, which is difficult to solve because of the need to evaluate the expectation in the objective function. One approach is to approximate the expected value through sample averaging (Santoso et al., 2005; Uddin and Huynh, 2016). This approach is known as sample average approximation (SAA). In this study, the SAA algorithm proposed by Santoso et al. (2005) is adopted. The objective function of the model (equation 3.1) can be rewritten as follows, without loss of generality, where y represents the decision variable.

$$\text{Min } \mathbb{E}_{\xi}\left[\mathcal{Q}(y,\xi) \right] \tag{3.10}$$

3.3.1 The SAA Algorithm

Step 1. Generate M independent disruption-scenario samples each of size N, i.e., $\xi_m^1,...,\xi_m^N$ for $m=1,...,M$. For each sample, solve the corresponding SAA problem.

$$\text{Min } \frac{1}{N}\sum_{n=1}^{N}\mathcal{Q}\left(y,\xi_m^n\right) \tag{3.11}$$

Let z_N^m and $\hat{y}_N^m$, $m=1,...,M$, be the corresponding optimal objective value and an optimal solution, respectively.

Step 2. Compute the following two values.

$$\bar{z}_{N,M} := \frac{1}{M}\sum_{m=1}^{M} z_N^m \tag{3.12}$$

$$\sigma^2_{\bar{z}_{N,M}} := \frac{1}{(M-1)M} \sum_{m=1}^{M} \left(z_N^m - \bar{z}_{N,M} \right)^2 \qquad (3.13)$$

The expected value of z_N is less than or equal to the optimal value z^* of the true problem (Santoso et al., 2005). Thus, $\bar{z}_{N,M}$ provides a lower statistical bound for the optimal value z^* of the true problem, and $\sigma^2_{\bar{z}_{N,M}}$ is an estimate of the variance of this estimator.

Step 3. Choose a feasible solution $\tilde{y}$ from the above-computed solutions $\hat{y}_N^m$, and generate another N' independent disruption-scenario sample, i.e., $\xi^1, ..., \xi^{N'}$. Then estimate true objective function value $\tilde{z}_{N'}(\tilde{y})$ and variance of this estimator as follows:

$$\tilde{z}_{N'}(\tilde{y}) := \frac{1}{N'} \sum_{n=1}^{N'} \mathcal{Q}\left(\tilde{y}, \xi^n\right) \qquad (3.14)$$

$$\sigma^2_{N'}(\tilde{y}) := \frac{1}{(N'-1)N'} \sum_{n=1}^{N'} \left[\mathcal{Q}\left(\tilde{y}, \xi^n\right) - \tilde{z}_{N'}(\tilde{y}) \right]^2 \qquad (3.15)$$

Typically, N' is much larger than the sample size N used in solving the SAA problems. $\tilde{z}_{N'}(\tilde{y})$ is an unbiased estimator of $z(\tilde{y})$. Also, $\tilde{z}_{N'}(\tilde{y})$ is an estimate of the upper bound on z^*.

Step 4. Compute an estimate of the optimality gap of the solution $\tilde{y}$ using the lower bound estimate and the objective function value estimate from Steps 2 and 3, respectively, using the equations below:

$$\text{gap}_{N,M,N'}(\tilde{y}) := \tilde{z}_{N'}(\tilde{y}) - \bar{z}_{N,M} \qquad (3.16)$$

$$\sigma^2_{\text{gap}} = \sigma^2_{N'}(\tilde{y}) + \sigma^2_{\bar{z}_{N,M}} \qquad (3.17)$$

3.3.2 Gradient Projection Algorithm

The SAA problem in equation (3.11) is the standard traffic assignment problem, which cannot be solved analytically. This study adopts the path-based algorithm (gradient projection) proposed by Uddin and Huynh (2015) to solve the traffic assignment problem. The gradient projection (GP) algorithm was first used by Jayakrishnan et al. (1994) to solve the traffic assignment problem. Uddin and Huynh (2015) further modified the GP algorithm to consider the situation where freight traffic demands could be transported via one of three modes (road-only, rail-only and intermodal). Their GP algorithm also considered intermodal terminals in the network. The adopted GP algorithm has the following iterative steps for a specific disruption-scenario sample ξ.

Step 0. Initialization

Set $t_{a\xi} = t_{a\xi}(0), \forall a \in \mathcal{A}$, and select terminals from the available terminals $\mathcal{T}$ for all OD pairs. Assign OD demand q_t^{rs}, q_l^{rs}, and q_i^{rs} on the shortest path calculated based on $t_{a\xi}, \forall a \in \mathcal{A}_t$, $t_{a\xi}, \forall a \in \mathcal{A}_l$, and $t_{a\xi}, \forall a \in \mathcal{A}$, respectively, and initialize the path sets K_t^{rs}, K_l^{rs}, and K_i^{rs} with the corresponding shortest path for each OD pair (r,s). This initialization yields path flows and link flows. Set iteration count to $p=1$.

Step 1. For each OD pair (r,s):

    Step 1.1. Update

    Set $t_{a\xi} = t_{a\xi}(x_{a\xi}(p)), \forall a \in \mathcal{A}$. Update the first derivative lengths, i.e., path travel

    times at current flow: $d_{kt}^{rs}(p), \forall k \in K_t^{rs}$, $d_{kl}^{rs}(p), \forall k \in K_l^{rs}$, and $d_{ki}^{rs}(p), \forall k \in K_i^{rs}$.

Step 1.2. Direction finding

Find the shortest path $\bar{k}_t^{rs}(p)$ based on $t_{a\xi}(p), \forall a \in \mathcal{A}_t$. If different from all the paths in K_t^{rs}, add it to K_t^{rs} and record $d_{\bar{k}_t^{rs}(p)}^{rs}$. If not, tag the shortest among the paths in K_t^{rs} as $\bar{k}_t^{rs}(p)$. Repeat this procedure for K_l^{rs} and K_i^{rs} to find $d_{\bar{k}_l^{rs}(p)}^{rs}$ and $d_{\bar{k}_i^{rs}(p)}^{rs}$ based on $t_{a\xi}, \forall a \in \mathcal{A}_l$ and $t_{a\xi}, \forall a \in \mathcal{A}$, respectively.

Step 1.3. Move

Set the new path flows for K_t^{rs}.

$$f_{k\xi}^{rs}(p+1) = \max\left\{0, f_{k\xi}^{rs}(p) - \frac{\alpha(p)}{s_{k\xi}^{rs}(p)}\left(d_{kt}^{rs}(p) - d_{\bar{k}_t^{rs}(p)}^{rs}\right)\right\}, \quad \forall k \in K_t^{rs}, k \neq \bar{k}_t^{rs}$$

where $s_{k\xi}^{rs}(p) = \sum_a \dfrac{\partial t_{a\xi}^{rs}(p)}{\partial x_{a\xi}^{rs}(p)}, \quad \forall k \in K_t^{rs}$

a denotes the links that are on either k or $\bar{k}_t^{rs}$, but not on both. $\alpha(p)$ is the step size; the value of this parameter is set as 1 (Jayakrishnan et al., 1994). Now,

$$f_{\bar{k}^{rs}\xi}^{rs}(p+1) = q_t^{rs} - \sum f_{k\xi}^{rs}(p+1), \quad \forall k \in K_t^{rs}, k \neq \bar{k}_t^{rs}(p)$$

Follow the above procedure to find new path flow for K_l^{rs} and K_i^{rs}. From path flows find the link flows $x_{a\xi}(p+1)$.

Step 2. Convergence test

If the convergence criterion is met, stop. Else set $p = p + 1$ and go to Step 1.

Figure 3.1 shows a flow chart that illustrates how the SAA and GP algorithms are used to solve the traffic assignment problem. The model solution procedure starts with the input of OD demands and intermodal network data. Then, a number of disruption-

41

scenario samples are generated following the procedure described in Step 1 of the SAA algorithm. Then, for a specific scenario sample, GP algorithm solves the assignment problem and outputs the network link flows. This is repeated until all the scenario samples have been considered. After that, the procedure continues to Step 2 to 4 of the SAA algorithm.
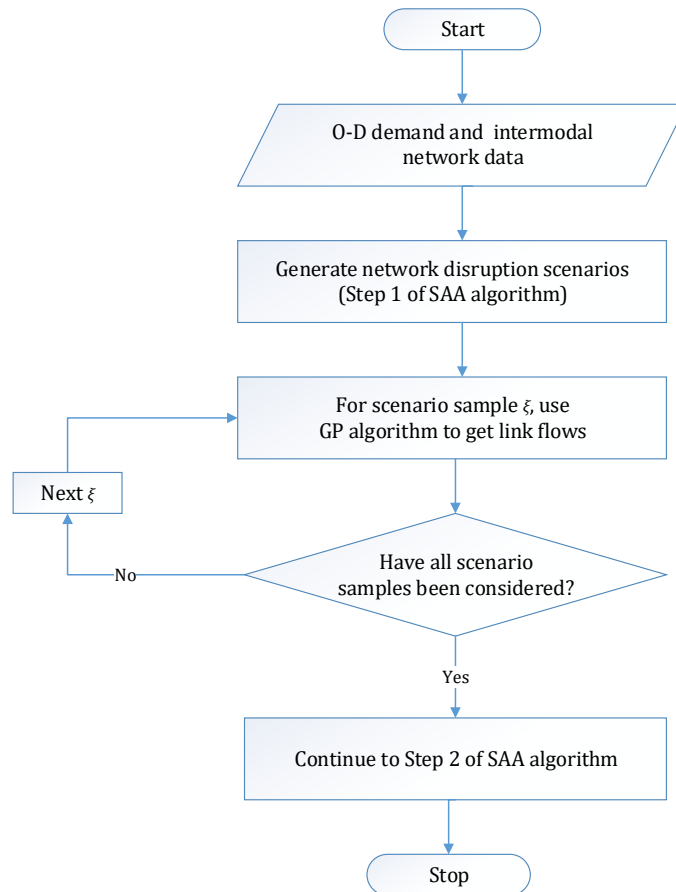

Figure 3.1 Algorithmic framework.

3.4 NUMERICAL EXPERIMENTS

The proposed algorithmic framework was coded in MATLAB R2018a. The experiments were run on a desktop computer with an Intel Core i7 3.40-GHz processor

and 24 GB of RAM. To validate the proposed model and algorithmic framework, the road-rail transportation network in the contiguous U.S. and five disaster scenarios were considered.

3.4.1 Network and Disaster Data

The U.S. road-rail intermodal network shown in Figure 3.2 was used (Uddin and Huynh, 2015). The network was simplified from the U.S. intermodal network created by Oak Ridge National Laboratory (Center for Transportation Analysis, 2014). The simplified network consists of only Interstates, Class I railroads, and road-rail terminals. In Figure 3.2, the squares represent Freight Analysis Zone (FAZ) centroids, the circles represent road-rail terminals, the black lines represent Interstates, and the grey lines represent Class I railroads. In all, the network has a total of 1,532 links and 301 nodes. The nodes include 120 FAZ centroids, 97 major road intersections, and 84 major rail junctions.

The Freight Analysis Framework (FAF) is the most comprehensive public source of freight data in the U.S. (Federal Highway Administration, 2013). Currently, FAF version 4 is available. However, in this chapter FAF version 3 was used given that the network used for experiments is based on FAF version 3 (Uddin and Huynh, 2015). Note that the proposed model and algorithmic framework can assign freight flows using the input from any version of FAF. The FAF version 3 has a total of 120 FAZ; hence, it is assumed that there are 14,400 possible Origin-Destination (OD) demand pairs in the network. One issue with the FAF demand is that it provides freight demands in terms of tonnage. Therefore, it is required to convert tonnage to truck or rail counts to be used as

input in the model. This study used the converted freight demands from Uddin and Huynh (2015); readers are referred to the work for the detailed procedure used for conversion. The freight OD trip tables for the truck, rail, and intermodal trips are in 120 x 120 x 3 matrix form. For a single day in the base year (2007), there are 618,190 truck shipments, 1,415 rail shipments, and 12,474 intermodal shipments.
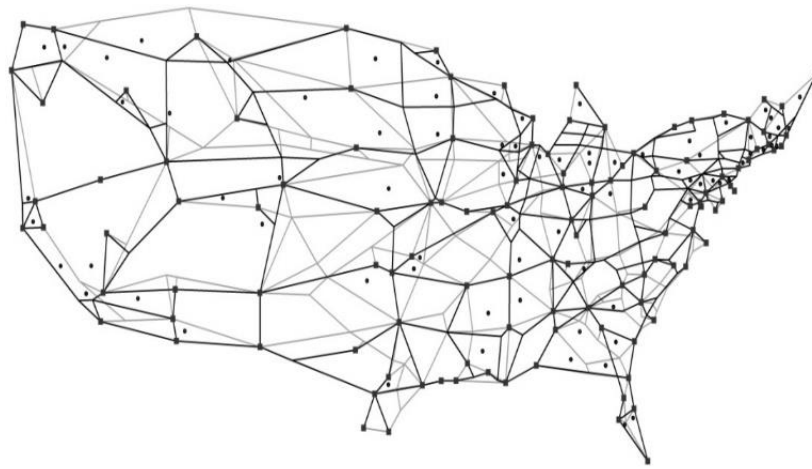
Figure 3.2 U.S. road-rail intermodal network.

To create disaster scenarios, the U.S. natural disaster risk map (Alert Systems Group, 2018) was used. The map is generated using the disaster risk data from the American Red Cross and the National Oceanic and Atmospheric Administration (Alert Systems Group, 2018). It shows the vulnerable areas under four natural disasters: earthquakes (both high and moderate risks), hurricanes, tornadoes, and floods. Based on this, five disaster scenarios were considered for the numerical experiments. The scenarios are earthquake (high risk), earthquake (high and moderate risk), hurricane, tornado, and flood.

In the experiments, the capacities of the links were assumed to have a uniform distribution, each with a specified range (Miller-Hooks et al., 2012; Uddin and Huynh,

2016). For each disaster scenario, at first link capacities were randomly drawn from their corresponding distributions. Then to replicate the impact of the disaster, the capacities of 50% of the links in the risk areas were further reduced; these links are randomly selected. The reduction in capacity could be as high as 100%, if the objective is to make a link impassable. Since the network employed for the experiments is simplified, there are fewer alternate paths between the OD pairs. For this reason, an 80% reduction in capacity was assumed to avoid a complete gridlock. Other studies have also used a similar approach for capacity reductions (e.g., Chen and Miller-Hooks, 2012; Miller-Hooks et al., 2012). The aim of these experiments is to understand at a very high level how the different natural disasters impact freight logistics, for which limited information is available in the literature. Once this information is better understood, future work can focus on examining specific cases such as comparing the cost of a hurricane in the Gulf Coast (e.g., Hurricane Harvey) versus one in the Southeastern region (e.g., Hurricane Florence) versus one in the Northeastern region (e.g., Hurricane Sandy).
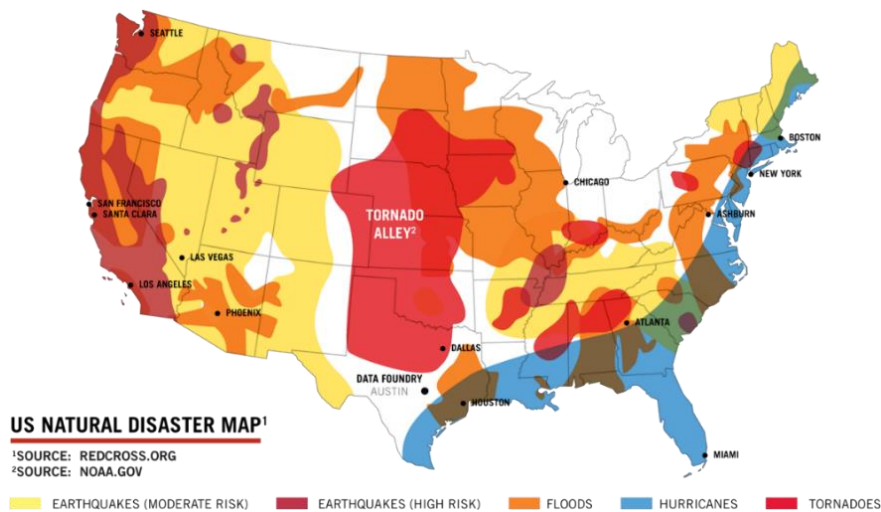

Figure 3.3 U.S. natural disaster risk map (Alert Systems Group, 2018).

45

3.4.2 Results and Discussion

To apply the SAA algorithm, the number of independent disruption-scenario samples (M) was set to 100, the sample size (N) was set to 1, and the number of large-size samples (N') was set to 1,000. For the GP algorithm, the value of the relative gap (i.e., convergence criterion) was set to 0.0001 (Boyce et al., 2004), which is the relative change in the value of the objective function from one iteration to the next. Note that the terms in the objective function were normalized to yield consistent units. Specifically, the first term was divided by the sum of truck demand and intermodal truck demand and the second term divided by the sum of rail demand and intermodal rail demand.

With the above values, the SAA method will produce several candidate freight flow patterns, but no more than 100 ($M = 100$). Among these candidate flow patterns, the optimal flow pattern is the one that yields the lowest optimality gap (equation 3.16) when each candidate flow pattern was applied to the 1,000 test scenarios ($N' = 1,000$).

Table 3.2 Cost Statistics for Solutions under Different Disasters

Total Cost (Hour/day)	Earthquake (High Risk)	Earthquake (High and Moderate Risk)	Hurricane	Tornado	Flood
Average	50.0401	76.2006	47.9100	149.9243	199.1450
Std. dev.	0.0579	0.1524	0.1294	0.0268	0.3699
Minimum	47.7146	70.0737	42.7106	148.8488	184.2753
Maximum	54.4278	87.7608	57.7205	151.9536	227.2015
gap	0.2001	0.4912	0.4162	0.0976	1.1830
σ_{gap}	0.1939	0.5147	0.4355	0.0900	1.2484

Table 3.2 summarizes the cost statistics for the five disaster scenarios. The CPU run times for the five disaster scenarios (high-risk earthquake, high and moderate risk earthquake, hurricane, tornado, and flood) were 595.9, 716.2, 669.2, 531.4, and 417.1

minutes, respectively. As shown, the impact of hurricane is least costly (mean total cost = 50 hours/day) and flood is most costly (mean total cost = 200 hours/day).

The resulting user-equilibrium flow for road and rail networks for different disaster scenarios are shown in Figures 3.4 through 3.8. The thickness of the links signifies the volume of assigned freight traffic. The result in Figure 3.4*a* indicates that there is high truck flow on Interstates that traverse Arizona, California, Florida, Georgia, Idaho, Illinois, Indiana, Michigan, New York, Ohio, and Wyoming under the high-risk earthquake scenario. The high truck flow on I-80 in Nevada and Utah is due to freight being diverted from I-5 in California when there is an earthquake. The result in Figure 3.4*b* indicates that there is high train flow on rail tracks that traverse Illinois, Indiana, Iowa, Minnesota, Montana, North Dakota, South Dakota, West Virginia, and Wisconsin under the high-risk earthquake scenario. Compared to the base case scenario (without any disaster), there is little difference in the train flow because the rail tracks in these states are not affected by the earthquake in California.

FAF Truck Volume per Day

— 0-5,000 — 10,001-15,000 — 20,001-25,000
— 5,001-10,000 — 15,001-20,000

Freight Train per Day

— 0-15 — 26-50 — 101-200
— 16-25 — 51-100

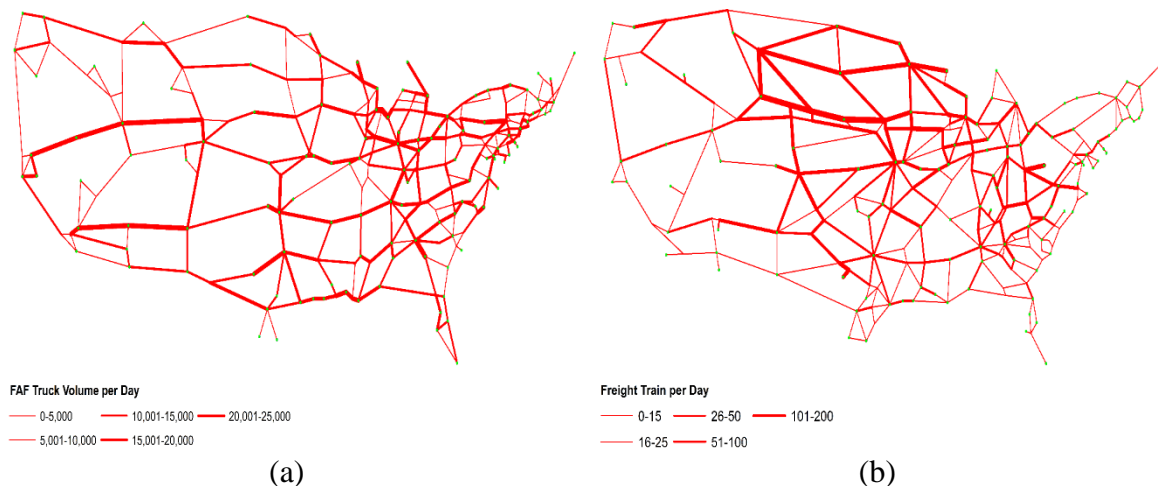(a)   (b)

Figure 3.4 Freight traffic assignment under earthquake (high risk): (a) road and (b) rail.

Figure 3.5 shows the assigned freight flow under the high and moderate risk earthquake scenario. The result in Figure 3.5*a* indicates that there is high truck flow on Interstates that traverse Georgia, Indiana, Kentucky, Pennsylvania, Tennessee, and Texas. Compared to the high-risk earthquake scenario, there is a more even distribution of truck flow in the Western states (such as California, Nevada, Arizona, and Utah). The result in Figure 3.5*b* indicates that there is high train flow on rail tracks that traverse Illinois, Iowa, Minnesota, Montana, North Dakota, South Dakota, West Virginia, and Wisconsin. This assigned rail flow is very similar to that of the high-risk earthquake scenario.

(a)   (b)

Figure 3.5 Freight traffic assignment under earthquake (high and moderate risk): (a) road and (b) rail.

Figure 3.6 shows the assigned freight traffic flow under the hurricane scenario. The result in Figure 3.6*a* indicates high truck flow on Interstates that traverse California, Illinois, Indiana, Missouri, Ohio, Tennessee, Texas, and Pennsylvania. Compared to the base case, trucks are diverted from the East and Gulf Coast to the North when there is a hurricane in these regions. The result in Figure 3.6*b* indicates high train flow on rail tracks that traverse Iowa, Minnesota, Nebraska, North Dakota, South Dakota, and

Wyoming. As is the case with truck flow, there is a higher concentration of rail flow in the Midwest regions.

FAF Truck Volume per Day
— 0-5,000   — 10,001-15,000   — 20,001-25,000
— 5,001-10,000   — 15,001-20,000

Freight Train per Day
— 0-15   — 26-50   — 101-200
— 16-25   — 51-100

(a)   (b)
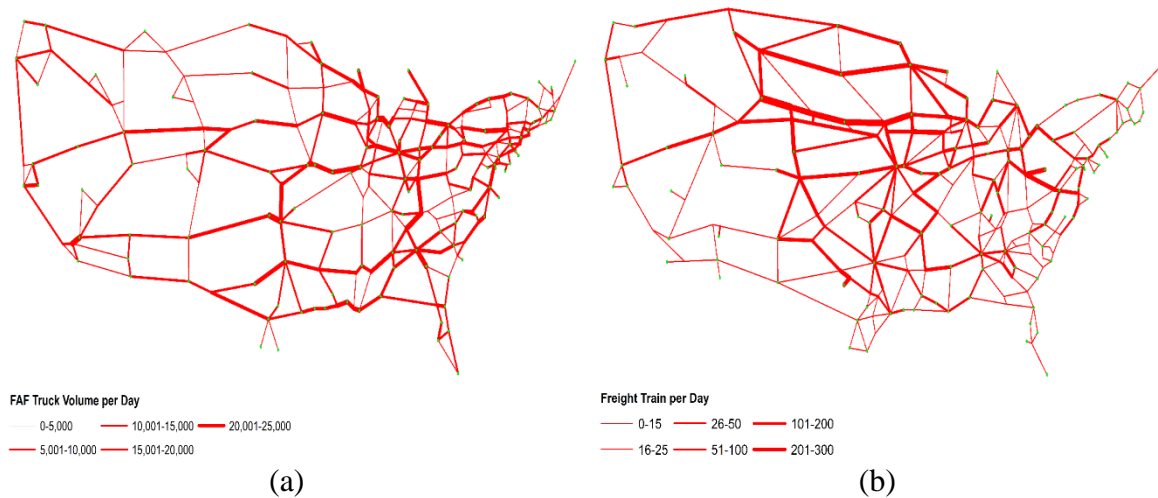
Figure 3.6 Freight traffic assignment under hurricane: (a) road and (b) rail.

Figure 3.7 shows the assigned freight traffic flow under the tornado scenario. The result in Figure 3.7*a* indicates that there is high truck flow on Interstates that traverse Illinois, Louisiana, Minnesota, Montana, North Dakota, Texas, and Wisconsin. Compared to the other three disaster scenarios (high-risk earthquake, high and moderate risk earthquake, and hurricane), the truck flow is very high on some Interstates (more than 20,000 FAF trucks per day); particularly, I-10 in Louisiana and Texas, and I-94 in Wisconsin, Minnesota, and North Dakota. This is due to the fact that trucks are avoiding the Interstates that traverse the tornado alley. The result in Figure 3.7*b* indicates that there is high train flow on rail tracks that traverse Arizona, Colorado, Iowa, Montana, New Mexico, North Dakota, Wisconsin, and Wyoming. As is the case with trucks, the trains are avoiding the rail tracks that traverse the tornado alley.

FAF Truck Volume per Day		
0-5,000	10,001-15,000	20,001-25,000
5,001-10,000	15,001-20,000	25,001-30,000

(a)

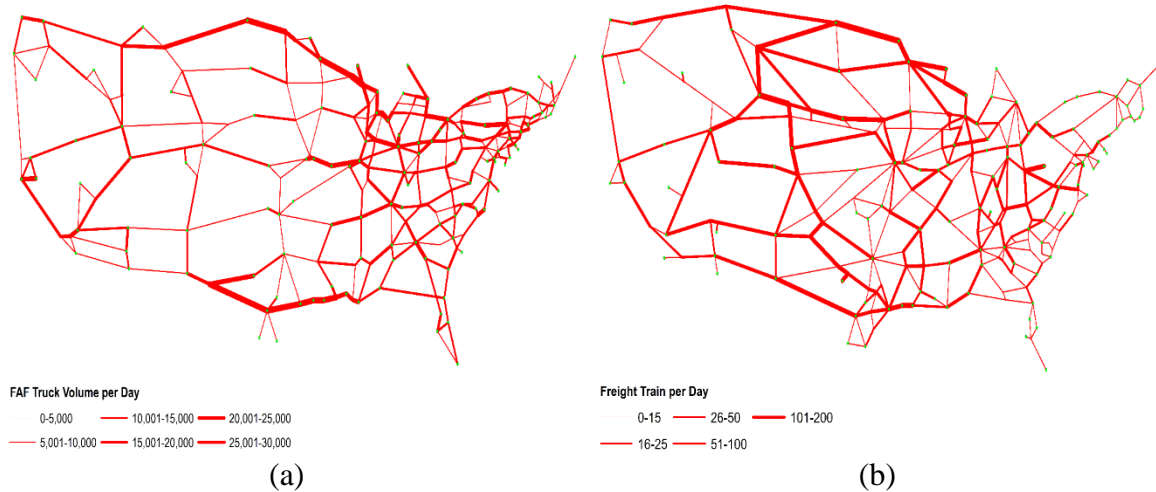| Freight Train per Day		
0-15	26-50	101-200
16-25	51-100	

(b)

Figure 3.7 Freight traffic assignment under tornado: (a) road and (b) rail.

Lastly, Figure 3.8 shows the assigned freight traffic flow under the flooding scenario. The result in Figure 3.8*a* indicates that there is high truck flow on Interstates that traverse Alabama, Arkansas, Indiana, New Mexico, New York, Oklahoma, Pennsylvania, Tennessee, and Texas. Similar to the tornado scenario, some of the Interstates have very high truck flow; particularly, I-40 in Arkansas and Oklahoma, and I-90 in New York. The reason that trucks are diverting from the Interstates that traverse the Midwestern states is because there is a higher percentage on links in these states that are affected by the flood. The result in Figure 3.8*b* indicates that some of the rail tracks have very high train flow (i.e., more than 200 trains per day); particularly, rail tracks in Montana and Wyoming. Furthermore, most of the Mountain states have high rail flow through their states under the flooding scenario. This is also because the trains are avoiding the use of rail tracks in the Midwest regions.

The proposed model's projected ton-miles under different disaster scenarios are compared quantitatively against those reported in FAF3 and Uddin and Huynh (2015). As evident from Table 3.3, for both highway and railway modes, the freight ton-miles are

higher than that of Uddin and Huynh (2015) because the authors did not consider any network uncertainty. The highway freight ton-miles is 8% higher for high-risk earthquake, 8% higher for high and moderate risk earthquake, 3% higher for hurricane, 8% higher for tornado, and 16% higher for flood compared to that of the deterministic case. The rail freight ton-miles is 2% higher for high-risk earthquake, 4% higher for high and moderate risk earthquake, 1% higher for hurricane, 10% higher for tornado, and 20% higher for flood compared to that of the deterministic case. Overall, when disasters are considered, freight ton-miles are always higher, which is expected because of the need to make detours. The impact of flooding is the highest because there are more states in the flood-risk areas, and they are scattered throughout the U.S.

(a)   (b)
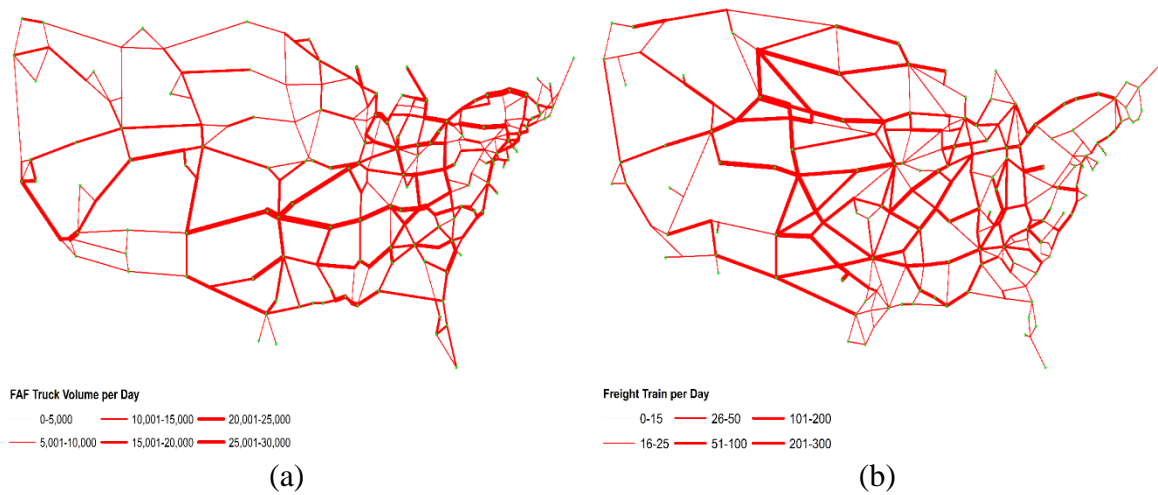
Figure 3.8 Freight traffic assignment under flood: (a) road and (b) rail.

Table 3.3 Million of Freight Ton-Miles for 2007 under Different Disasters

Mode of Transport	FAF3	Uddin and Huynh (2015)	Earthquake (High Risk)	Earthquake (High and Moderate Risk)	Hurricane	Tornado	Flood
Truck[†]	2,817,837	2,172,701	2,343,715	2,342,831	2,245,430	2,338,086	2,513,778
Rail[‡]	1,991,182	1,703,039	1,743,840	1,774,065	1,724,057	1,878,646	2,044,679

FAF3 = Freight Analysis Framework, Version 3. [†]Includes truck, and multiple modes and mail. [‡]Includes rail, and multiple modes and mail.

3.5 CONCLUSION

This paper developed a stochastic model to assign freight traffic in a large-scale road-rail intermodal network that is subject to network uncertainty (i.e., natural disaster or disruption). For a specific disaster scenario and given a set of freight demands between origins and destinations and designated modes (road-only, rail-only, and intermodal), the model finds the user-equilibrium freight flow. This paper also provided an algorithmic framework, based on the Sample Average Approximation and Gradient Projection algorithm, to solve the model. Five disaster scenarios were considered in the numerical experiments: high-risk earthquake, high and moderate risk earthquake, hurricane, tornado, and flood. The proposed model and algorithmic framework were tested using the U.S. road-rail intermodal network and the Freight Analysis Framework shipment data. The results indicated that when disasters are considered the freight ton-miles are higher than when no disaster is considered, which is expected. The resulting user-equilibrium flows clearly indicate the impact of disasters; that is, truck and rail flow are shifted away from the impacted areas. These results highlight the need to address highways and rail tracks in areas that are normally underutilized but heavily used by trucks and trains when there is a disaster. In terms of cost and freight ton-miles, the impact of flooding is the highest.

CHAPTER 4

INTERMODAL FREIGHT ROUTING UNDER DISRUPTIONS[1]

The freight transport network is an essential component of the economy as it supports supply chains by connecting spatially-separated origins and destinations of supply and demand. As such, it needs to be robust and resilient to support and enhance economic development. Due to the increase in international trade, freight flows have increased significantly, and this trend is expected to continue in the future (Tavasszy and De Jong, 2013). For example, a daily average of 54 million tons of freight moved through the U.S. transportation system in 2012. The projected freight flows will stress both public and private infrastructures as more elements of the network reach or exceed capacity, which in turn will affect network performances (Strocko et al., 2013).

The freight transport network is vulnerable to various disruptions. A disruptive event can be a natural disaster (e.g., earthquake, flooding, tornado, and hurricane) or a man-made disaster (e.g., accident, labor strike, and terrorism). A number of such disasters have occurred recently that severely impacted the freight transport network. The earthquake that occurred in 1994 on the Hayward Fault in San Francisco, CA caused more than 1,600 road closures and damaged most of the toll bridges and major highways (Okasaki, 2003). The collapse of the I-35W bridge in Minneapolis affected about 140,000 daily vehicle trips and the daily re-routing cost was $400,000 for the impacted

---

[1]This chapter has been adapted from "Uddin, M., & Huynh, N. (2016). Routing model for multicommodity freight in an intermodal network under disruptions. *Transportation Research Record*, *2548*, 71–80." Reprinted here following SAGE's Green Open Access policy.

users (Zhu and Levinson, 2012). Hurricane Sandy made landfall over the New York and New Jersey region in 2012 caused billions of dollars in damage and severely flooded streets and tunnels along the East Coast of the U.S. Due to the labor strike at the Port of Long Beach in 2012, the movement of $650 million worth of goods was halted each day (Federal Highway Administration, 2015). These events highlight that damage to the transportation network not only disrupt transportation services but also result in economic losses and sociological effects. Disruptions in freight movements have a number of ramifications: (1) receivers will not receive their goods on time, (2) carriers need to find alternative routes to transport the goods that are impeded by the disruption, and (3) shippers need to adjust their supply chains to account for the disruption. For these reasons, adequate redundancy in the freight transport network is needed to prevent significant service losses in the event of a disruption.

This study proposes a stochastic model for the routing of multicommodity freight on a road-rail intermodal network that is subject to various disruptions. The model can be used by carriers to determine the optimal road segments (highway links), rail segments (rail lines), and intermodal terminals to use under different types of disruptions. Since the exact evaluation of the stochastic model is difficult or impossible (Chang et al., 2007), the developed model is solved using the Sample Average Approximation algorithm proposed by Santoso et al. (2005).

4.1 LITERATURE REVIEW

The multimodal freight transportation planning problem has been studied by many researchers over the past few decades, and its study was accelerated during the last

decade (SteadieSeifi et al., 2014). One of the earlier studies was done by Crainic and Rousseau (1986), which presented a general modeling and algorithmic framework for the multicommodity, multimode freight service network to be used at the strategic and tactical planning level. The objective of their model is to minimize costs and delays, if a single authority controls the supply of transportation services and routing of goods through the service network. Their model considered capacitated network elements (i.e., roadways, rail lines, and terminals have finite capacities) and a penalty cost for excess assignment over capacity.

The majority of the studies that deal with intermodal freight shipments seek to minimize routing cost. Barnhart and Ratliff (1993) proposed a model for minimizing routing cost in a road-rail intermodal network. Their model was to help shippers in deciding routing options. It used shortest path and matching algorithmic procedures to achieve the objective. Boardman et al. (1997) developed a software-based decision support system (DSS) to assist shippers in making the best selection given a combination of modes. The crux of this DSS is the calculation of least-cost paths using a k-shortest path method, while requiring the transportation costs of all modes and transfer costs between modes as input. A similar approach was used by Song and Chen (2007) in their development of mode selection software. However, the modes considered by Song and Chen had pre-scheduled departure times. The authors concluded that the minimum cost delivery problem is equivalent to the shortest path problem if the release time at the origin and the due date at the destination are provided.

A number of studies have addressed the intermodal routing problem with time windows. Ziliaskopoulos and Wardell (2000) proposed an algorithm for finding the

optimal time-dependent intermodal path in a multimodal transportation network. Their algorithm considered mode and arc switching delays. Xiong and Wang (2014) developed a bi-level multi-objective model and genetic algorithmic framework for the routing problem with time windows in a multimodal network. Ayar and Yaman (2012) investigated an intermodal multicommodity routing problem where release times and due dates of commodities were pre-scheduled in a planning horizon.

All of the aforementioned studies assume that the freight transport network is always functioning and is never disrupted, which is not realistic. To account for natural or man-made disruptions, some researchers have studied the reliability, vulnerability, and resiliency of transportation networks. Snyder and Daskin (2005) presented a reliable uncapacitated location problem considering failure of facilities in the network. Their model finds reliable facility location by taking into account the expected transportation cost after failure, in addition to the minimum operational cost. Cui et al. (2010) extended this work to consider failures with site-dependent probabilities and re-routing of customers when there are failures. Peng et al. (2011) also considered disruptions of facility in reliable logistics network design. Their mixed integer program not only minimizes the nominal cost but also reduces disruption risks by employing the *p*-robustness criterion.

A resilient freight transport network is one that can recover from any disruption by preventing, absorbing, or mitigating its effects (SteadieSeifi et al., 2014). A decision model to address disruptive events in an intermodal freight transport network was proposed by Huang et al. (2011). Their model re-routes flows if the forecasted delay on a distressed link exceeds a pre-specified threshold. In a study performed by Chen and

Miller-Hooks (2012), a method to quantify resilience of an intermodal freight transport network was developed. They formulated a stochastic mixed integer program that aims to minimize unsatisfied demands during disruptions. Their model was solved using several exact algorithms; however, the application was limited to only small-scale networks due to high computational time requirements. Miller-Hooks et al. (2012) extended this work to maximize freight transport network resiliency by implementing preparedness and recovery activities within a given budget. A stochastic program was developed which maximizes freight flows in the network under disruptions. Similar to their previous study, the model was applied to the same small-scale networks.

A few studies have considered network vulnerability in the planning decision. Peterson and Church (2008) investigated rail network vulnerability by formulating both uncapacitated and capacitated routing-based model and applied their model to a statewide network. Garg and Smith (2008) presented a methodology for designing a survivable multicommodity flow network. Their model analyzes failure scenarios involving multiple arcs. Most recently, Gedik et al. (2014) assessed network vulnerability and re-routing of coal by rail when disruptions occur in the network.

This study fills a gap in the literature by addressing the multicommodity routing problem in an intermodal road-rail network that is subject to disruptions. This study is most closely related to the works performed by Chen and Miller-Hooks (2012) and Miller-Hooks et al. (2012) in that they focus on solving the road-rail intermodal freight routing problem with explicit consideration of network disruptions. However, there are several notable differences between our work and theirs: (1) our study considers the multicommodity aspect (different commodities may have different delivery requirements

and some commodities might need to be separated to facilitate early or delayed delivery); (2) our study proposes a new model that uses a link-based formulation; and (3) our model is applied to an actual large-scale intermodal freight network.

4.2 MODEL FORMULATION

The formulation assumes that a road-rail intermodal freight transportation network is represented by a directed graph $G = (N, A)$, where N is the set of nodes and A is the set of links. Set N consists of the set of major highway intersections H, the set of major rail junctions R, and the set of intermodal terminals S, i.e., $N = H \cup R \cup S$. Set A consists of the set of highway links A_h and the set of railway links A_r, i.e., $A = A_h \cup A_r$. Shipments can change mode at the intermodal terminal nodes S. Each highway link $(i, j) \in A_h$ and railway link $(i, j) \in A_r$ have unit transportation costs associated with them for each commodity $k \in K$ shipment. Each intermodal terminal $s \in S$ has also a unit transfer cost for each commodity $k \in K$ shipment. Another important cost parameter is the penalty cost of unsatisfied demand Ψ. The capacity of each highway link, railway link, and intermodal terminal are disruption-scenario dependent, i.e., capacities will be different at different disruption scenarios. Similarly, the travel time on highway and railway links and the transfer time at terminals are disruption-scenario dependent.

4.2.1 Sets/Indices

H set of major highway intersections

R set of major rail junctions

S set of candidate intermodal terminals

A_h set of highway links

A_r set of railway links

C set of OD pairs

K set of commodities

P^c set of paths p connecting OD pair c

Ω set of disruption scenarios

k commodity type, $k \in K$

i, j, s node, $i, j, s \in N$

c an OD pair, $c \in C$

ω a disruption scenario, $\omega \in \Omega$

4.2.2 Parameters

d_k^c original demand of commodity $k \in K$ between OD pair $c \in C$

Ψ unit penalty cost for unsatisfied demand

β_{ijk} unit cost of transporting commodity $k \in K$ by truck in link $(i, j) \in A_h$

$\tilde{\beta}_{ijk}$ unit cost of transporting commodity $k \in K$ by rail in link $(i, j) \in A_r$

β_{sk} unit cost of transferring commodity $k \in K$ in intermodal terminal $s \in S$

$Q_{ij}(\omega)$ capacity of highway link $(i, j) \in A_h$ under disruption ω

$\tilde{Q}_{ij}(\omega)$ capacity of railway link $(i, j) \in A_r$ under disruption ω

$Q_s(\omega)$ capacity of intermodal terminal $s \in S$ under disruption ω

$t_{ij}(\omega)$ travel time on highway link $(i, j) \in A_h$ under disruption ω

$\tilde{t}_{ij}(\omega)$ travel time on railway link $(i, j) \in A_r$ under disruption ω

$t_s(\omega)$ processing time in intermodal terminal $s \in S$ under disruption ω

T_k^c delivery time for commodity $k \in K$ between OD pair $c \in C$

Ξ sufficiently large number

ε sufficiently small number

4.2.3 Continuous Variables

$X_{ijk}^c(\omega)$ fraction of commodity $k \in K$ transported in highway link $(i, j) \in A_h$ between OD pair $c \in C$ under disruption ω

$\tilde{X}_{ijk}^c(\omega)$ fraction of commodity $k \in K$ transported in railway link $(i, j) \in A_r$ between OD pair $c \in C$ under disruption ω

$U_k^c(\omega)$ unsatisfied demand of commodity $k \in K$ between OD pair $c \in C$ under disruption ω

$F_{sk}^c(\omega)$ fraction of commodity $k \in K$ between OD pair $c \in C$ transferred at terminal $s \in S$ under disruption ω

4.2.4 Indicator Variables

$Y_{sk}^c(\omega)$ binary variable indicating whether or not intermodal terminal $s \in S$ is selected for commodity $k \in K$ between OD pair $c \in C$ under disruption ω

(= 1 if intermodal terminal s is selected for commodity k between OD pair c, = 0 otherwise)

$\delta_{ijk}^c(\omega)$ binary variable indicating whether or not there is any flow in highway link $(i, j) \in A_h$ for commodity $k \in K$ between OD pair $c \in C$ under disruption ω (= 1 if highway link (i, j) carries flow of commodity k between OD pair c, = 0 otherwise)

$\tilde{\delta}_{ijk}^c(\omega)$ binary variable indicating whether or not there is any flow in railway link $(i, j) \in A_r$ for commodity $k \in K$ between OD pair $c \in C$ under disruption ω (= 1 if railway link (i, j) carries flow of commodity k between OD pair c, = 0 otherwise)

4.2.5 Model Formulation

The stochastic multicommodity intermodal freight shipment routing (**SMIFR**) problem is formulated as follows.

$$\text{Min } \mathrm{E}_\omega \left[\sum_{k \in K} \sum_{c \in C} \left(\begin{array}{l} d_k^c \left(\displaystyle\sum_{(i,j) \in A_h} \beta_{ijk} X_{ijk}^c(\omega) + \sum_{(i,j) \in A_r} \tilde{\beta}_{ijk} \tilde{X}_{ijk}^c(\omega) + \sum_{s \in S} \beta_{sk} F_{sk}^c(\omega) \right) \\ + \Psi U_k^c(\omega) \end{array} \right) \right] \tag{4.1}$$

Subject to

$$\sum_{(i,m) \in A_h} X_{imk}^c(\omega) - \sum_{(m,i) \in A_h} X_{mik}^c(\omega) \begin{cases} \leq & +1 & \text{if } i = \text{ori}^c \\ \geq & -1 & \text{if } i = \text{des}^c, \ \forall i \in H, k \in K, c \in C, \omega \in \Omega \\ = & 0 & \text{otherwise} \end{cases} \tag{4.2}$$

$$\sum_{i \in \text{ori}^c} X_{imk}^c(\omega) - \sum_{j \in \text{des}^c} X_{mjk}^c(\omega) = 0, \ \forall k \in K, c \in C, \omega \in \Omega \tag{4.3}$$

61

$$X_{imk}^c(\omega) \le \delta_{imk}^c(\omega), \ \forall (i,m) \in A_h, k \in K, c \in C, \omega \in \Omega \tag{4.4}$$

$$X_{mik}^c(\omega) + \delta_{imk}^c(\omega) \le 1, \ \forall (m,i) \in A_h, k \in K, c \in C, \omega \in \Omega \tag{4.5}$$

$$\sum_{(i,m) \in A_h} X_{imk}^c(\omega) \sum_{(m,i) \in A_h} X_{mik}^c(\omega) = 0, \ \forall i \in ori^c, k \in K, c \in C, \omega \in \Omega \tag{4.6}$$

$$\sum_{(i,n) \in A_r} \tilde{X}_{ink}^c(\omega) - \sum_{(n,i) \in A_r} \tilde{X}_{nik}^c(\omega) = 0, \ \forall i \in R, k \in K, c \in C, \omega \in \Omega \tag{4.7}$$

$$\sum_{(s,m) \in A_h} X_{smk}^c(\omega) - \sum_{(m,s) \in A_h} X_{msk}^c(\omega) + \sum_{(s,n) \in A_r} \tilde{X}_{snk}^c(\omega) - \sum_{(n,s) \in A_r} \tilde{X}_{nsk}^c(\omega) = 0,$$
$$\forall s \in S, k \in K, c \in C, \omega \in \Omega \tag{4.8}$$

$$\left(\sum_{(s,n) \in A_r} \tilde{X}_{snk}^c(\omega) - \sum_{(n,s) \in A_r} \tilde{X}_{nsk}^c(\omega) \right) \left(1 - Y_{sk}^c(\omega) \right) = 0, \ \forall s \in S, k \in K, c \in C, \omega \in \Omega \tag{4.9}$$

$$F_{sk}^c(\omega) = \left| \sum_{(s,m) \in A_h} X_{smk}^c(\omega) - \sum_{(m,s) \in A_h} X_{msk}^c(\omega) \right|, \ \forall s \in S, k \in K, c \in C, \omega \in \Omega \tag{4.10}$$

$$\varepsilon Y_{sk}^c(\omega) \le F_{sk}^c(\omega) \le Y_{sk}^c(\omega), \ s \in S, k \in K, c \in C, \omega \in \Omega \tag{4.11}$$

$$\sum_{(i,j) \in (A_h \cap p)} \delta_{ijk}^c(\omega) t_{ij}(\omega) + \sum_{(i,j) \in (A_r \cap p)} \tilde{\delta}_{ijk}^c(\omega) \tilde{t}_{ij}(\omega) + \sum_{s \in (S \cap p)} Y_{sk}^c(\omega) t_s(\omega) \le T_k^c,$$
$$\forall p \in P^c, k \in K, c \in C, \omega \in \Omega \tag{4.12}$$

$$\varepsilon \delta_{ijk}^c(\omega) \le X_{ijk}^c(\omega) \le \delta_{ijk}^c(\omega), \ \forall (i,j) \in A_h, k \in K, c \in C, \omega \in \Omega \tag{4.13}$$

$$\varepsilon \tilde{\delta}_{ijk}^c(\omega) \le \tilde{X}_{ijk}^c(\omega) \le \tilde{\delta}_{ijk}^c(\omega), \ \forall (i,j) \in A_r, k \in K, c \in C, \omega \in \Omega \tag{4.14}$$

$$\sum_{k \in K} \sum_{c \in C} d_k^c X_{ijk}^c(\omega) \le Q_{ij}(\omega), \ \forall (i,j) \in A_h, \omega \in \Omega \tag{4.15}$$

$$\sum_{k \in K} \sum_{c \in C} d_k^c \tilde{X}_{ijk}^c(\omega) \le \tilde{Q}_{ij}(\omega), \ \forall (i,j) \in A_r, \omega \in \Omega \tag{4.16}$$

$$\sum_{k \in K} \sum_{c \in C} d_k^c F_{sk}^c(\omega) \le Q_s(\omega), \ \forall s \in S, \omega \in \Omega \tag{4.17}$$

$$d_k^c \left(1 - \sum_{i \in H} X_{ijk}^c(\omega)\right) = U_k^c(\omega), \quad \forall k \in K, c \in C, j = \mathrm{des}^c, \omega \in \Omega \tag{4.18}$$

$$0 \le X_{ijk}^c(\omega) \le 1, \quad \forall (i,j) \in A_h, k \in K, c \in C, \omega \in \Omega \tag{4.19}$$

$$0 \le \tilde{X}_{ijk}^c(\omega) \le 1, \quad \forall (i,j) \in A_r, k \in K, c \in C, \omega \in \Omega \tag{4.20}$$

$$0 \le F_{sk}^c(\omega) \le 1, \quad \forall s \in S, k \in K, c \in C, \omega \in \Omega \tag{4.21}$$

$$U_k^c(\omega) \in Z^+, \quad \forall k \in K, c \in C, \omega \in \Omega \tag{4.22}$$

$$Y_{sk}^c(\omega) \in \{0,1\}, \quad \forall s \in S, k \in K, c \in C, \omega \in \Omega \tag{4.23}$$

$$\delta_{ijk}^c(\omega) \in \{0,1\}, \quad \forall (i,j) \in A_h, k \in K, c \in C, \omega \in \Omega \tag{4.24}$$

$$\tilde{\delta}_{ijk}^c(\omega) \in \{0,1\}, \quad \forall (i,j) \in A_r, k \in K, c \in C, \omega \in \Omega \tag{4.25}$$

The objective function (4.1) seeks to minimize the total expected system cost across disruption scenarios. Specifically, the expected system cost includes the transportation cost on highway and railway links, the transfer cost at intermodal terminals, and the penalty cost for unsatisfied demands. Constraints (4.2) to (4.6) ensure flow conservation at highway nodes (H). The notations ori^c and des^c denote the origin and destination node, respectively, of an OD pair $c \in C$. Similarly, constraint (4.7) ensures flow conservation at railway nodes (R). Constraints (4.8) and (4.9) ensure flow conservation at intermodal terminals (S); constraint (4.8) maintains the conservation if a terminal is selected whereas constraint (4.9) maintains conservation if the terminal is not selected. The decision variables $F_{sk}^c(\omega), \forall s \in S, k \in K, c \in C, \omega \in \Omega$ are calculated in constraint (4.10). Constraint (4.11) establishes the relationship between decision variables $F_{sk}^c(\omega)$ and $Y_{sk}^c(\omega)$. Constraint (4.12) ensures that each commodity shipment is

delivered before the delivery deadline $T_k^c, \forall k \in K, c \in C$. The relationship between

decision variables $X_{ijk}^c(\omega)$ and $\delta_{ijk}^c(\omega)$ are expressed in constraint (4.13), and the

relationship between decision variables $\tilde{X}_{ijk}^c(\omega)$ and $\tilde{\delta}_{ijk}^c(\omega)$ are expressed in constraint

(4.14). Constraints (4.15) to (4.17) ensure that flows are less than or equal to the capacity

of highway links, railway links, and intermodal terminals, respectively. Constraint (4.18)

determines the unsatisfied demand $U_k^c(\omega), \forall k \in K, c \in C, \omega \in \Omega$. Lastly, constraints (4.19)

to (4.21) are the definitional constraints, constraint (4.22) is the integrality constraint, and

constraints (4.23) to (4.25) are the binary constraints.

4.2.6 Linear Formulation

The proposed model is not linear, since it has several non-linear constraints: (4.6),

(4.9), and (4.10). Non-linear models are generally very difficult to solve; thus, the non-

linear constraints are reformulated to make the model tractable. The equivalent linear

forms are:

$$\sum_{(i,m) \in A_h} X_{imk}^c(\omega) \geq \Xi \sum_{(m,i) \in A_h} X_{mik}^c(\omega), \ \forall i \in \mathrm{ori}^c, k \in K, c \in C, \omega \in \Omega \tag{4.26}$$

$$-\Xi Y_{sk}^c(\omega) \leq \sum_{(s,n) \in A_r} \tilde{X}_{snk}^c(\omega) - \sum_{(n,s) \in A_r} \tilde{X}_{nsk}^c(\omega) \leq \Xi Y_{sk}^c(\omega), \ \forall s \in S, k \in K, c \in C, \omega \in \Omega \tag{4.27}$$

$$-F_{sk}^c(\omega) \leq \sum_{(s,m) \in A_h} X_{smk}^c(\omega) - \sum_{(m,s) \in A_h} X_{msk}^c(\omega) \leq F_{sk}^c(\omega), \ \forall s \in S, k \in K, c \in C, \omega \in \Omega \tag{4.28}$$

Constraint (4.26) is equivalent to constraint (4.6), which prevents sub-tours.

Constraints (4.9) and (4.10) can be reformulated as constraints (4.27) and (4.28),

respectively. By replacing constraints (4.6), (4.9) and (4.10) with constraints (4.26), (4.27), and (4.28), the revised model is a stochastic mixed integer linear program.

4.3 ALGORITHMIC STRATEGY

A key difficulty in solving a stochastic program is in evaluating the expectation of the objective function. One approach for accomplishing this is to approximate the expected objective function value through sample averaging. This study adopts the Sample Average Approximation (SAA) algorithm proposed by Santoso et al. (2005). Without loss of generality, the objective function of the model can be rewritten as follows, where λ represents the decision variables.

$$\text{Min } E_{\omega}\left[\Theta(\lambda, \omega)\right] \tag{4.29}$$

4.3.1 The SAA Algorithm

Step 1. Generate M independent disruption-scenario samples each of size N, i.e., ($\omega_j^1, ..., \omega_j^N$) for $j = 1, ..., M$. For each sample, solve the corresponding SAA problem.

$$\text{Min } \frac{1}{N}\sum_{n=1}^{N}\Theta(\lambda, \omega_j^n) \tag{4.30}$$

Let f_N^j and $\hat{\lambda}_N^j$, $j = 1, ..., M$ be the corresponding optimal objective function value and an optimal solution of the model, respectively.

Step 2. Compute $\bar{f}_N$ and $\sigma_{\bar{f}_N}^2$ using the following equations.

$$\bar{f}_N := \frac{1}{M}\sum_{j=1}^{M}f_N^j \tag{4.31}$$

65

$$\sigma_{\bar{f}_N}^2 := \frac{1}{M(M-1)} \sum_{j=1}^{M} (f_N^j - \bar{f}_N)^2 \tag{4.32}$$

Here $\bar{f}_N$ provides a lower statistical bound for the optimal value f^* of the true problem, and $\sigma_{\bar{f}_N}^2$ is an estimate of the variance of the estimator.

Step 3. Choose a feasible solution $\tilde{\lambda}$ from the above computed solutions $\hat{\lambda}_N^j$, and generate another N' independent disruption-scenario samples, i.e., $\omega^1,...,\omega^{N'}$. Then estimate the true objective function value $\tilde{f}_{N'}(\tilde{\lambda})$ and variance of this estimator as following:

$$\tilde{f}_{N'}(\tilde{\lambda}) := \frac{1}{N'} \sum_{n=1}^{N'} \Theta(\tilde{\lambda}, \omega^n) \tag{4.33}$$

$$\sigma_{N'}^2(\tilde{\lambda}) := \frac{1}{N'(N'-1)} \sum_{n=1}^{N'} \left[\Theta(\tilde{\lambda}, \omega^n) - \tilde{f}_{N'}(\tilde{\lambda}) \right]^2 \tag{4.34}$$

In solving SAA problems, typically, N' is much larger than the sample size N.

Step 4. Compute the optimality gap of the solution and variance of the gap estimator.

$$\mathrm{gap}(\tilde{\lambda}) := \tilde{f}_{N'}(\tilde{\lambda}) - \bar{f}_N \tag{4.35}$$

$$\sigma_{\mathrm{gap}}^2 = \sigma_{N'}^2(\tilde{\lambda}) + \sigma_{\bar{f}_N}^2 \tag{4.36}$$

4.4 NUMERICAL EXPERIMENTS

To assess the applicability of the proposed model and solution algorithm, two sets of experiments are conducted. The first set involves a hypothetical small-sized network with 15 nodes and 5 OD pairs. The second set involves an actual large-scale freight transport network, consisting of major highways, Class I railroads, and TOFC/COFC

(Trailer on Flat Car/Container on Flat Car) intermodal terminals in the Gulf Coast, Southeastern and Mid-Atlantic regions of the U.S.

4.4.1 Network and Data Description

Figure 4.1 shows the hypothetical 15-node road-rail freight transport network. Nodes 5, 7, 9, and 12 represent intermodal terminals, and node 8 represents a railway junction where trains can change track/route. The rest of the nodes represent highway intersections. The solid lines represent highway links, and the dashed lines represent railway links. The capacity of the links Q_{ij} are assumed to have a uniform distribution (Miller-Hooks et al., 2012), each with a specified range $[l_{ij}, u_{ij}]$ where l_{ij} is the lower bound and u_{ij} is the upper bound. The capacities of the intermodal terminals are also assumed to have a uniform distribution with a specified range. The demand in terms of number of shipments and delivery deadlines for each commodity between different OD pairs is provided in Table 4.1.
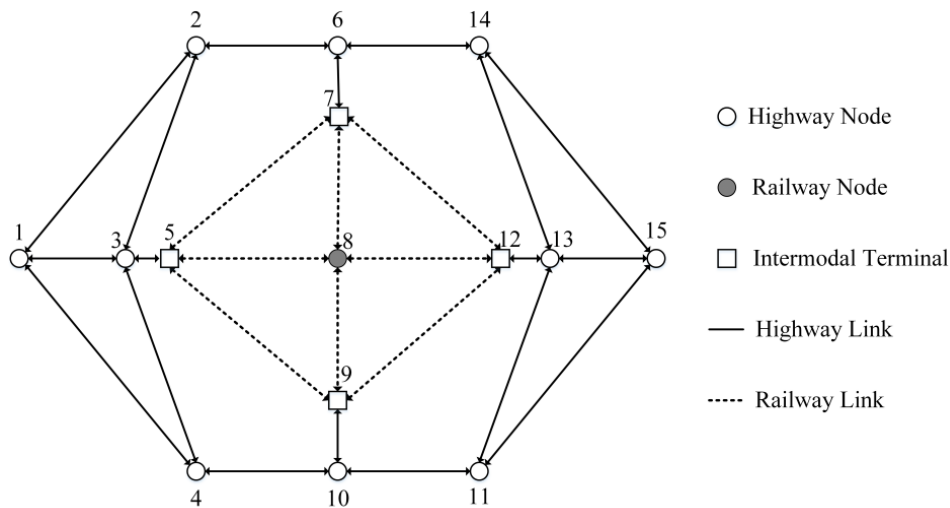

Figure 4.1 A hypothetical 15-node road-rail freight transport network.

67

Figure 4.2 shows the actual road-rail freight transport network used in the second set of experiments. As shown, it covers all of the states in the Gulf Coast, Southeastern and Mid-Atlantic regions of the U.S.: Texas, Oklahoma, Louisiana, Alabama, Mississippi, Arkansas, Georgia, Florida, South Carolina, North Carolina, Tennessee, Kentucky, Virginia, Maryland, West Virginia, and Delaware. In all, the network has a total of 682 links (U.S. interstates and major highways and Class I railroads) and 187 nodes, including 44 intermodal terminals. The Freight Analysis Zone (FAZ) centroids from the Freight Analysis Framework, version 3, (FAF3) database (Federal Highway Administration, 2013) are treated as actual origins and destinations of commodity shipments. There is a total of 48 centroids in the study region. OD pairs are constructed from these 48 FAZ centroids, and demands are obtained from the FAF3 database. The demand data are filtered to include only those commodities typically transported via intermodal (Cambridge Systematics, 2007), and demands are converted into the number of TOFC/COFC containers using an average load of 40,000 lbs per container. It is assumed that all commodities need to be delivered within 7 days.
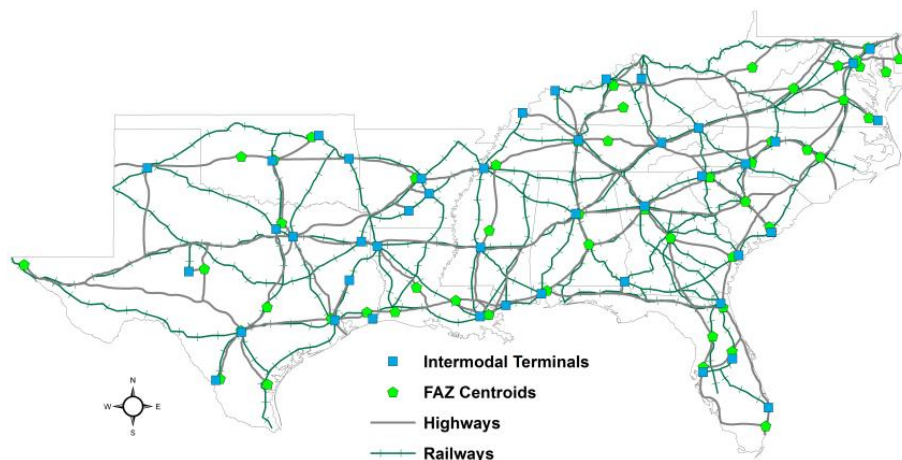

Figure 4.2 Large-scale U.S. road-rail intermodal network.

Table 4.1 Number of Shipments and Delivery Deadlines

OD Pair	Commodity Index	Number of Shipments	Delivery Deadline (hours)
1→15	1	40	84
	2	35	72
	3	22	60
	4	20	72
1→11	1	30	72
	2	35	72
	3	40	48
2→13	1	42	60
	2	30	48
	3	50	60
	4	55	48
15→4	1	35	72
	2	45	60
	3	50	72
	4	30	60
14→3	1	45	48
	2	30	60

The transport cost on highways and railways are estimated to be $1.67 per mile per shipment (Torrey and Murray, 2014) and $0.60 per mile per shipment (Cambridge Systematics, 1995), respectively. The transfer cost at intermodal terminals is estimated to be $70 per shipment (Winebrake et al., 2008a). The travel times on highway and railway links are calculated using free-flow speeds. The number of potential paths between an origin and destination could be large. For that reason, after getting all the available paths between a specific OD pair, only those paths that have lengths less than or equal to five times of the corresponding minimum path length are considered in the path set. This approach is deemed reasonable because the discarded paths would not have satisfied the delivery deadline constraint.

4.4.2 Disruption Types

Three types of disruptive-events are considered: (1) link disruption, (2) node disruption, and (3) intermodal terminal disruption. Link disruptions are modeled by randomly selecting several connected links and reducing their capacities by 50%. The travel times on the affected links are increased as a result of reduced capacities. Node disruptions are modeled by reducing the capacities of all links connected to the nodes by 80%. And, terminal disruptions are modeled by randomly selecting a number of terminals and reducing their capacities by 80%; thus, the transfer times at the impacted terminals will increase. It should be noted that affected links, nodes, or terminals are selected based on their vulnerability, and the severity of the disruption can be captured by the amount of capacity that is reduced. Recurring disruptions are not considered in the numerical experiments. For example, daily variation in travel times and network element capacities (Torkjazi et al., 2018). However, these types of disruptions that occur continually over time and involving different links can easily be modeled given the generality of the model formulation and solution algorithm.

4.4.3 Experimental Results

The proposed solution methodology was implemented in Python, and the IBM ILOG CPLEX 12.6 solver was used to solve the mixed integer program. Experiments are run on a personal computer with Intel Core i7 3.20 GHz processor and 8.0 GB of RAM.

To apply the SAA algorithm, the number of independent disruption-scenario samples (M) is set to 100, the sample size (N) is set to 1, and the number of large-size samples (N') is set to 1,000 for all three types of disruption. With these values, the SAA

method will produce a number of candidate routes per commodity per OD pair but no more than 100 ($M = 100$). Among these candidate routes, the optimal route is the one that yields the lowest optimality gap when each candidate route is applied to the 1,000 test scenarios ($N' = 1,000$).

Table 4.2 Experimental Results for Hypothetical Network

	Link Disruption	Node Disruption	Terminal Disruption
M	100	100	100
N	1,000	1,000	1,000
CPU Time (min)	17.5	178.4	0.9
Objective Function Value (avg)	$92,439.62	$93,152.09	$59,419.30
gap	$540.87	$390.09	$4.76
σ_{gap}	$17.69	$3.80	$0.37

Table 4.2 summarizes the input parameters and associated SAA results for the hypothetical network. The term "gap" denotes the optimality gap as defined in equation 4.35, and σ_{gap} denotes the standard deviation of the gap estimates as defined in equation 4.36. In the case of link disruption, the average objective function value is $92,439.62, with an optimality gap of $540.87 and estimator standard deviation of $17.69. The associated computation time is 17.5 minutes. Similar information is presented for the node and terminal disruption cases. Among the three types of disruption, the node disruption case results in the highest objective function value, which indicates that it has the most negative impact on freight logistics. Conversely, the terminal disruption case has the least impact. This result is counterintuitive because one would expect the terminal disruption to have the highest impact since it serves as a hub in the freight transport network. This is due to the network structure which allows commodities to be shipped via road more efficiently and less costly. In other words, terminals handle only a

small percentage of the shipments, and thus, their disruptions have minimal impact on the freight logistics.

Table 4.3 Optimal Routes for Hypothetical Network

OD Pair	Commodity Index	Optimal Routes		
		Link Disruption	Node Disruption	Terminal Disruption
1→15	1	1–3–5–8–12–13–15 (100%)	1–4–10–11–15 (100%)	1–3–5–8–12–13–15 (100%)
	2	1–3–2–6–14–15 (100%)	1–4–10–11–15 (100%)	1–4–10–11–15 (100%)
	3	1–3–2–6–14–13–15 (100%)	1–4–10–11–15 (100%)	1–4–10–11–15 (100%)
	4	1–3–2–6–14–15 (100%)	1–4–10–11–15 (100%)	1–4–10–11–15 (100%)
1→11	1	1–3–5–9–10–11 (100%)	1–4–10–11 (100%)	1–4–10–11 (100%)
	2	1–3–5–9–10–11 (100%)	1–4–10–11 (100%)	1–4–10–11 (100%)
	3	1–2–6–14–13–11 (5%)	1–4–10–11 (100%)	1–4–10–11 (100%)
		1–4–10–11 (95%)		
2→13	1	2–6–7–12–13 (98%)	2–1–4–10–11–13 (33%)	2–6–14–13 (100%)
		2–6–14–13 (2%)	2–6–14–13 (67%)	
	2	2–3–5–8–12–13 (100%)	2–3–5–8–12–13 (73%)	2–6–14–13 (100%)
	3	2–6–7–12–13 (100%)	2–3–5–8–12–13 (100%)	2–6–7–12–13 (100%)
	4	2–3–5–8–12–13 (84%)	2–1–4–10–11–13 (65%)	2–6–14–13 (100%)
		2–6–14–13 (16%)		
15→4	1	15–13–12–8–5–3–4 (100%)	15–11–10–4 (100%)	15–11–10–4 (100%)
	2	15–11–10–4 (100%)	15–11–10–4 (100%)	15–11–10–4 (100%)
	3	15–13–12–8–5–3–4 (100%)	15–11–10–4 (100%)	15–11–10–4 (100%)
	4	15–13–12–8–5–3–4 (100%)	15–11–10–4 (100%)	15–11–10–4 (100%)
14→3	1	14–6–7–5–3 (100%)	14–6–7–5–3 (100%)	14–6–2–3 (100%)
	2	14–6–2–3 (100%)	14–6–7–5–3 (100%)	14–6–2–3 (100%)

The corresponding optimal routes are presented in Table 4.3. Optimal routes are shown as a series of nodes in the direction of origin to destination. For example, the optimal route to ship commodity #1 between OD pair (1→15) in the event of link disruptions is: 1–3–5–8–12–13–15. Note that if a particular route does not have sufficient capacity to handle a particular shipment, then the remaining shipment is shipped via a second-best route. This is the case with commodity #3 between OD pair

(1→11). There are two optimal routes: 1–2–6–14–13–11 (5% use this route) and 1–4–10–11 (95% use this route). It should be noted that the model places no restriction on the number of potential routes between each OD. Thus, a shipment could have several routes if there is insufficient capacity on the least-cost routes.

It is observed that since the network has very few rail links, most of the shipments are shipped via highway links. This finding corresponds to actual freight flows where the majority of freights are shipped via road. Furthermore, when highway links are disrupted, then railway links and terminals are more likely to be used. Again, this is a logical and expected result. An interesting result that highlights the usefulness of the model can be seen in the case of a node disruption for commodity #4 between OD pair (2→13). There is one optimal route, but it only contains 65% of the shipment which means that the remaining 35% failed to reach its destination (i.e., unsatisfied demand). There are no unsatisfied demands under link and terminal disruption cases.

To understand the impact of disruptions on an actual road-rail intermodal network, several instances of each disruption type are considered. For link disruptions, four different instances are solved to investigate how the objective function value and computational time change with respect to the severity of the link disruption. The severity of the link disruption is modeled by the number of impacted links, which was set to 30, 60, 100, and 200 for the four instances. The results for link disruption are summarized in Table 4.4. The results indicate that increasing the number of OD pairs and commodities ($|K|$) will increase computational efforts. Furthermore, for a particular number of OD pairs, the objective function value increases with the number of impacted links. The computational time is unaffected by the severity level.

Table 4.4 Experimental Results for Actual Network

OD	$|K|$	Link Disruption			Node Disruption			Terminal Disruption		
		Impacted Link #	Obj. Func. ($, thousands)	CPU (min)	Impacted Node #	Obj. Func. ($, thousands)	CPU (min)	Impacted Terminal #	Obj. Func. ($, thousands)	CPU (min)
5	9	30	556.4	29.8	5	557.7	29.9	15	550.2	29.4
		60	562.6	29.9	10	566.0	29.3	30	560.6	29.5
		100	573.9	29.9	20	604.1	33.6	44	651.9	36.5
		200	650.5	29.9	40	640.9	115.1			
10	21	30	959.8	146.8	5	942.2	142.7	15	930.3	147.0
		60	965.9	146.8	10	966.9	141.7	30	959.7	143.5
		100	979.3	142.6	20	1,015.1	154.9	44	1,077.8	173.2
		200	1,085.1	146.2	40	1,061.4	720.2			
20	43	30	1,478.8	484.1	5	1,461.2	486.2	15	1,481.3	483.5
		60	1,484.9	487.8	10	1,505.8	479.6	30	1,534.3	493.7
		100	1,500.9	486.7	20	1,558.4	528.2	44	1,705.8	636.5
		200	1,625.2	485.5	40	1,609.5	1,204.9			
50	87	30	3,885.8	1,937.8	5	3,870.7	1,937.2	15	3,959.0	1,953.7
		60	3,895.9	1,930.4	10	3,983.3	1,945.6	30	4,137.3	2,036.3
		100	3,952.3	1,926.4	20	4,062.6	2,007.6	44	*	*
		200	4,173.1	1,956.0	40	*	*			

*Program terminated due to memory limitation

For node disruptions, the four instances considered have 5, 10, 20, and 40 nodes disrupted. As shown in Table 4.4, the objective function value and computational time increase with higher number of OD pairs and commodities. Unlike link disruption, the computational time is affected by the number of disrupted nodes. Specifically, there is a significant increase from 20 to 40 nodes for the 10 OD pairs case (154.9 minutes to 720.2 minutes).

For terminal disruptions, three instances are considered with 15, 30, and 44 terminals disrupted. The objective function value and computational time exhibit a similar trend with respect to disruption severity as the link and node disruption cases. Similar to the node disruption case, the computational time is affected by the number of disrupted terminals.

Collectively, the numerical results indicate that, under link and node disruptions, the majority of the commodity shipments are shipped via road-rail intermodal due to lower rail cost and due to the robust freight transport network. A similar finding is reported in a study done by Ishfaq (2013) who concluded that the layout of the U.S. road-rail intermodal network and location of intermodal terminals provide sufficient redundancies to handle disruptions. When intermodal terminals are disrupted, the model indicates that commodities will be shipped via road directly. This result is expected since highway network is redundant and robust, as well as cost-effective.

In the aforementioned experiments, the unit penalty cost is assumed to be $10,000. This value is chosen to be high to ensure that the unsatisfied demand is minimized. To test the sensitivity of this parameter, experiments are performed where the unit penalty cost is set to $2,500, $5,000, and $7,500. It is found that these three

values for penalty cost resulted in same amount of unsatisfied demand. The computation time is observed to increase as the penalty cost value decreases. It can be concluded that the solution is not sensitive to the unit penalty cost parameter, given that it is set to a sufficiently large value. To test the sensitivity of the delivery deadline parameter, an experiment is performed where the delivery deadline is set to 14 days. The solution, including objective function value and computation time, is found to be the same when the delivery time is 7 days. This result suggests that the majority of the shipments require less than 7 days to reach their destinations, and thus, extending the delivery deadline has no effect on the solution.

Figure 4.3*a* illustrates how the optimal route generated by the model for a particular commodity going from Greensboro, NC to Dallas, TX under node disruptions compares with an actual route that a carrier would use. The left part of Figure 4.3*a* shows the optimal route generated by the model (shown in red), and the right part shows the route that a freight carrier would use (Direct Freight Services, 2015). By inspection, it is clear that the two routes are very similar to each other. However, there is one notable difference, and that is the model indicates road-rail intermodal to be optimal whereas the freight carrier chooses road-only. This discrepancy can be attributed to the fact that the carrier does not consider the potential node disruptions in the network.

Figure 4.3*b* illustrates how the optimal route generated by the model for a particular commodity going from Miami, FL to Houston, TX under link disruptions. By inspection, it is clear that the carrier chooses the route based on minimum travel time. The model, on the other hand, recognizes the potential link disruptions in the network and thereby chooses an intermodal route that avoids using the U.S. interstates (I-10 and I-12)

through Louisiana. This is because historically this area is vulnerable to hurricanes, such as Rita and Katrina. This result illustrates the importance of considering network disruptions when selecting a route for multicommodity freight in an intermodal network.
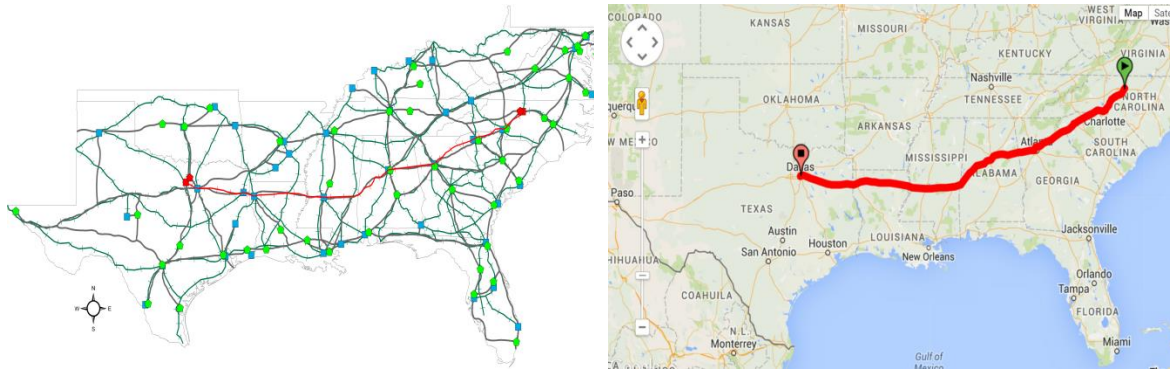
(a)
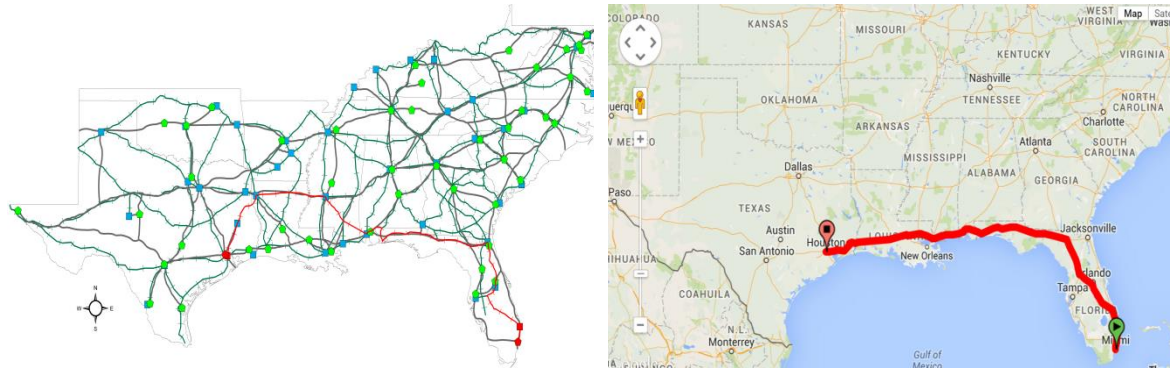
(b)

Figure 4.3 Optimal routes for selected OD pairs: (a) Greensboro – Dallas and (b) Miami – Houston.

4.5 CONCLUSION

This study developed a new stochastic mixed integer programming model to determine the optimal routes for delivering multicommodity freight in an intermodal freight network that is subject to disruptions (e.g., link, node, and terminal disruptions). To solve this model, the Sample Average Approximation (SAA) algorithm is adopted.

The model and solution algorithm was tested on a hypothetical 15-node network and an actual intermodal network in the Gulf Coast, Southeastern and Mid-Atlantic regions of the U.S.

The numerical experiments indicated that the model is capable of finding the optimal solutions for both small and large networks. The model runtime for a hypothetical 15-node network was reasonable (less than 3 hours for all instances). Naturally, the model runtime will increase as the network gets larger, as well as for the number of OD pairs and commodities. While the computational time was affected by the severity level of node and terminal disruptions, it was unaffected by link disruption severity. The model results indicated that under disruptions, goods in the study region should be shipped via road-rail intermodal due to lower rail cost and due to the built-in redundancy of the freight transport network. Furthermore, the model indicated that for a particular number of OD pairs, the total system cost will increase as the number of disrupted elements increases. The routes generated by the model are shown to be more robust than those typically used by freight carriers because they are often selected without consideration of potential network disruptions.

CHAPTER 5

RELIABLE ROUTING OF INTERMODAL FREIGHT UNDER

UNCERTAINTY[1]

Freight transportation involves various transportation modes, such as road, rail, air and water. The use of different transportation modes provides greater efficiency because it takes advantages of the strength of each transportation mode. Intermodal freight transportation uses two or more modes to transport goods without handling the goods themselves. Intermodal transportation offers an attractive alternative to unimodal transportation by highway in terms of cost for freight transported over long distances, and it reduces the carbon footprint of transport compared to the highway mode (Bureau of Transportation Statistics, 2015). In recent years, intermodal freight transport volume has grown significantly due to the aforementioned advantages.

Transportation infrastructures, particularly those supporting intermodal freight, are vulnerable to natural disasters (e.g., hurricane, earthquake, flooding) and man-made disasters (e.g., accidents, labor strike). These disruptions can drastically degrade the capacity of a transportation mode and consequently have adverse impacts on intermodal freight transport and freight supply chain (Miller-Hooks et al., 2012; Uddin and Huynh, 2016). For examples, Hurricane Katrina significantly damaged the transportation infrastructure in the Gulf Coast area (Godoy, 2007), and the West Coast port labor strike

severely disrupted the U.S. freight supply chain (D'Amico, 2002). Therefore, there is a need to develop a modeling framework that takes into account the reliability of the freight transport network when making strategic routing decisions. Network reliability means that the network can continue to deliver acceptable service when faced with disasters or disruptions that reduce capacity of network links, nodes, and intermodal terminals.

The majority of the studies that deal with intermodal freight shipments seek to minimize routing cost. Barnhart and Ratliff (1993) proposed a model for minimizing routing cost in a road-rail intermodal network. They developed procedures involving shortest paths and matching algorithm to help shippers in deciding routing options. Boardman et al. (1997) developed a software-based decision support system to assist shippers to select the best combination of transportation modes considering cost, service level, and the type of commodity. Xiong and Wang (2014) developed a bi-level multi-objective genetic algorithm for the routing of freight with time windows in a multimodal network. Ayar and Yaman (2012) investigated an intermodal multicommodity routing problem where release times and due dates of commodities were pre-scheduled in a planning horizon. Uddin and Huynh (2015) developed a methodology for freight traffic assignment in large-scale road-rail intermodal networks to be used by transportation planners to forecast intermodal freight flows. Rudi et al. (2016) proposed a capacitated multicommodity network flow model for the intermodal freight transportation problem that seeks to minimize transportation costs, carbon emissions, and in-transit holding costs. Their model was validated using industry data from an automotive supplier.

All of the aforementioned studies assume that the freight transport network is always functioning and is never disrupted. Daskin (1983) considered disruptions by

taking into account the facility unavailability in a maximum covering location problem. Snyder and Daskin (2005) presented a uncapacitated location problem considering failure of facilities in the network. Their reliability models find facility location by taking into account the expected transportation cost after failure, in addition to the minimum operational cost. Cui et al. (2010) extended this work to consider failures with site-dependent probabilities and re-routing of customers when there are failures. Peng et al. (2011) also considered disruptions at facilities in their work on design of reliable logistics network. In contrast, Cappanera and Scaparra (2011) sought to improve network reliability by optimally allocating protective resources in shortest path networks. Chen and Miller-Hooks (2012) developed a method to quantify resilience of an intermodal freight transport network. Miller-Hooks et al. (2012) extended this work to maximize freight transport network resiliency by implementing preparedness and recovery activities within a given budget. Huang and Pang (2014) evaluated resiliency of biofuel transport networks under possible natural disruptions. They formulated a multi-objective stochastic program to optimize the total system cost and total resilience cost. Marufuzzaman et al. (2014) proposed a reliable multimodal transportation network design model, where intermodal hubs are subject to site-dependent disruptions. This model employed a probabilistic framework. It was solved using the accelerated Benders decomposition algorithm and tested on a large-scale network. Uddin and Huynh (2016) proposed a stochastic mixed-integer model for the routing of multicommodity freight in an intermodal network under disruptions. Their study found that goods are better shipped via road-rail intermodal network during disruptions due to the built-in redundancy of the freight transport network.

A number of studies have considered network vulnerability in planning decision. Peterson and Church (2008) investigated rail network vulnerability by formulating both uncapacitated and capacitated routing-based model. Garg and Smith (2008) presented a methodology for designing a survivable multicommodity flow network, which analyzes failure scenarios involving multiple arcs. Rios et al. (2000) studied a similar problem, but their objective was to find the minimum-cost capacity-expansion options such that shipments can still be delivered to receivers through the network under disruptions. Gedik et al. (2014) proposed a capacitated mixed-integer interdiction programming model for coal transportation. They assessed network vulnerability and re-routing of coal by rail under network disruptions.

Another area of research that involves network uncertainty is disaster management, relief routing, response planning, and emergency and humanitarian logistics. Researchers have developed a wide variety of classical optimization programs to address these challenging problems. Haghani and Oh (1996) presented a disaster relief routing model for multicommodity freight in a multimodal network using the concept of time-space network. In the work by Ozdamar et al. (2004), commodity relief routing was studied as a hybrid of classical multicommodity network flow and vehicle routing problem. Given the uncertainty associated with network disruption, their model attempted to deliver commodities such that unsatisfied demand is minimized in a multimodal network. Barbarosoglu and Arda (2004) proposed a stochastic programming model for transporting multicommodity freight through a multimodal network during a natural disaster. Their model considered random arc capacity, where randomness is represented by a finite sample of scenarios. Chang et al. (2007) studied the rescue

resources location-routing problem in the event of a flooding disaster. Shen et al. (2009) investigated how to route vehicles in the event of a large-scale bioterrorism emergency. Their solution approach involves adjusting routes generated at the planning level to consider effects of disruptions. Rennemo et al. (2014) proposed a model comprising several stages to optimally locate relief distribution facilities.

Table 5.1 provides a summary of the key features addressed by prior studies related to the routing of freight. All of the prior studies where network uncertainty is considered make an explicit assumption about the probability density function (PDF) of the network link and/or node capacity. However, given that disruptive events are rare, there is often limited or no historical data available to determine the PDF of the network link or node capacity under a particular disruption scenario. A wrong assumption could have serious consequences of over design or under design. For example, assuming that a link capacity will follow the normal distribution in the event of a flash flood when in fact it follows a gamma distribution would lead to over design. This study contributes to the current body of knowledge by relaxing this explicit PDF assumption. A novel distribution-free approach is used to provide probabilistic guarantees on the resulting routes. This approach uses symmetric random variation, which is a popular method for solving robust optimization models (Bertsimas and Sim, 2004; Ng and Waller, 2012).

5.1 PROBLEM DESCRIPTION AND MODEL FORMULATION

The main objective of this study is to develop a reliable routing model for shipment of freight on a road-rail intermodal network that is subject to capacity uncertainty. The problem consists of determining the routes for commodity shipments

from their origins (shippers) to destinations (receivers). In this study, it is assumed that the origins and destinations are only accessible via highway links and that every intermodal route will involve at least two intermodal terminals. Additionally, it is assumed that the shipper and receiver facilities are either warehouses or distribution centers and that these facilities do not have rail connections. Figure 5.1 presents a typical road-rail freight transportation network where shipments can be transported via road-only or intermodal. The network consists of freight shippers, receivers, intermodal terminals, highway links, and rail lines.

Table 5.1 Summary of Prior Studies on the Routing of Freight

Study	Mode	Multi Commodity	Capacitated Link	Delivery Deadline	Uncertainty Consideration	Probability Distribution Assumption
Haghani and Oh (1996)	Multiple	✔	Multiple			
Barbarsoglu and Arda (2004)	Road, air	✔	Road, air		✔	✔
Garg and Smith (2008)	Road	✔	Road		✔	✔
Ayar and Yaman (2012)	Road, water	✔	Water	✔		
Chen and Miller-Hooks (2012)	Road, rail		Road, rail	✔	✔	✔
Miller-Hooks et al. (2012)	Road, rail		Road, rail	✔	✔	✔
Gedik et al. (2014)	Rail		Rail		✔	✔
Rudi et al. (2016)	Road, rail, water	✔	Road			
Uddin and Huynh (2016)	Road, rail	✔	Road, rail	✔	✔	✔
This current study	Road, rail	✔	Road, rail	✔	✔	

Following the notations from Uddin and Huynh (2016), it is assumed that a road-rail intermodal freight transportation network is represented by a directed graph $G = (N, A)$, where N is the set of nodes and A is the set of links. Set N consists of the set of major highway intersections H, the set of major rail junctions R, and the set of

intermodal terminals S. Set A consists of the set of highway links A_h and the set of railway links A_r. Shipments can change mode at the intermodal terminal nodes, S. Each highway link $(i,j) \in A_h$ and railway link $(i,j) \in A_r$ have unit transportation costs associated with them for each commodity $k \in K$ shipment. Each intermodal terminal $s \in S$ has also a unit transfer cost for each commodity $k \in K$ shipment. The definitions of sets, parameters, and decision variables are presented next, followed by the model formulation.
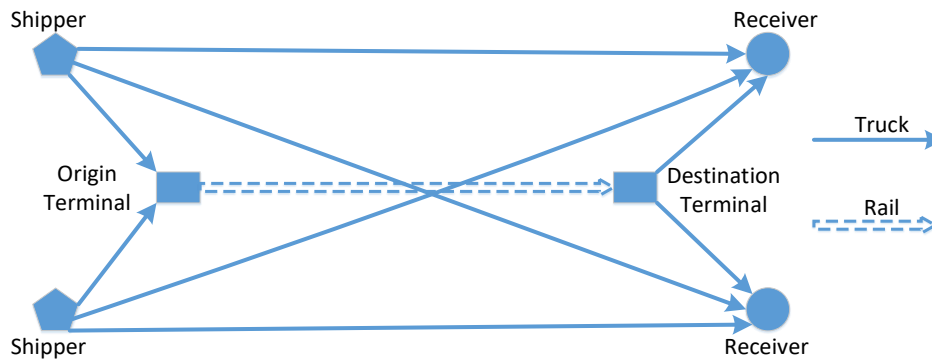
Figure 5.1 An example of road-rail freight transportation network.

5.1.1 Sets/Indices

H	set of major highway intersections
R	set of major rail junctions
S	set of intermodal terminals
A_h	set of highway links
A_r	set of railway links
C	set of origin-destination (OD) pairs
K	set of commodities
P^c	set of paths p connecting OD pair c
k	commodity type, $k \in K$
i,j,s	node, $i,j,s \in N$

c	an OD pair, $c \in C$
ori^c	origin node of an OD pair $c \in C$
des^c	destination node of an OD pair $c \in C$

5.1.2 Parameters

d_k^c	original demand of commodity $k \in K$ between OD pair $c \in C$ (expressed in number of intermodal containers)
Ψ	unit penalty cost for unsatisfied demand
β_{ijk}	unit cost of transporting commodity $k \in K$ by truck in link $(i, j) \in A_h$
$\tilde{\beta}_{ijk}$	unit cost of transporting commodity $k \in K$ by rail in link $(i, j) \in A_r$
β_{sk}	unit cost of transferring commodity $k \in K$ in intermodal terminal $s \in S$
Q_{ij}	capacity of highway link $(i, j) \in A_h$
$\tilde{Q}_{ij}$	capacity of railway link $(i, j) \in A_r$
Q_s	capacity of intermodal terminal $s \in S$
t_{ij}	travel time on highway link $(i, j) \in A_h$
$\tilde{t}_{ij}$	travel time on railway link $(i, j) \in A_r$
t_s	processing time in intermodal terminal $s \in S$
T_k^c	delivery time for commodity $k \in K$ between OD pair $c \in C$
M	sufficiently large number
ε	sufficiently small number

5.1.3 Decision Variables

X_{ijk}^c	fraction of commodity $k \in K$ transported in highway link $(i, j) \in A_h$ between OD pair $c \in C$
$\tilde{X}_{ijk}^c$	fraction of commodity $k \in K$ transported in railway link $(i, j) \in A_r$ between OD pair $c \in C$
U_k^c	unsatisfied demand of commodity $k \in K$ between OD pair $c \in C$

F_{sk}^c fraction of commodity $k \in K$ between OD pair $c \in C$ transferred at terminal $s \in S$

Y_{sk}^c binary variable indicating whether or not intermodal terminal $s \in S$ is selected for commodity $k \in K$ between OD pair $c \in C$ (= 1 if intermodal terminal s is selected for commodity k between OD pair c, = 0 otherwise)

δ_{ijk}^c binary variable indicating whether or not there is any flow in highway link $(i, j) \in A_h$ for commodity $k \in K$ between OD pair $c \in C$ (= 1 if highway link (i, j) carries flow of commodity k between OD pair c, = 0 otherwise)

$\tilde{\delta}_{ijk}^c$ binary variable indicating whether or not there is any flow in railway link $(i, j) \in A_r$ for commodity $k \in K$ between OD pair $c \in C$ (= 1 if railway link (i, j) carries flow of commodity k between OD pair c, = 0 otherwise)

The multicommodity intermodal freight shipment routing problem is formulated as follows.

$$\text{Min} \sum_{c \in C} \sum_{k \in K} \left(d_k^c \left(\sum_{(i,j) \in A_h} \beta_{ijk} X_{ijk}^c + \sum_{(i,j) \in A_r} \tilde{\beta}_{ijk} \tilde{X}_{ijk}^c + \sum_{s \in S} \beta_{sk} F_{sk}^c \right) + \Psi U_k^c \right) \tag{5.1}$$

Subject to

$$\sum_{(i,m) \in A_h} X_{imk}^c - \sum_{(m,i) \in A_h} X_{mik}^c \begin{cases} \leq & +1 & \text{if } i = \text{ori}^c \\ \geq & -1 & \text{if } i = \text{des}^c, \quad \forall i \in H, k \in K, c \in C \\ = & 0 & \text{otherwise} \end{cases} \tag{5.2}$$

$$\sum_{(i,m) \in A_h : i = \text{ori}^c} X_{imk}^c - \sum_{(m,j) \in A_h : j = \text{des}^c} X_{mjk}^c = 0, \ \forall k \in K, c \in C \tag{5.3}$$

$$X_{imk}^c \leq \delta_{imk}^c, \ \forall (i,m) \in A_h, k \in K, c \in C \tag{5.4}$$

$$X_{mik}^c + \delta_{imk}^c \leq 1, \ \forall (m,i) \in A_h, k \in K, c \in C \tag{5.5}$$

$$\sum_{(i,m) \in A_h} X_{imk}^c \geq M \sum_{(m,i) \in A_h} X_{mik}^c, \ \forall i \in \text{ori}^c, k \in K, c \in C \tag{5.6}$$

$$\sum_{(i,n)\in A_r}\tilde{X}_{ink}^c - \sum_{(n,i)\in A_r}\tilde{X}_{nik}^c = 0, \quad \forall i \in R, k \in K, c \in C \tag{5.7}$$

$$\sum_{(s,m)\in A_h}X_{smk}^c - \sum_{(m,s)\in A_h}X_{msk}^c + \sum_{(s,n)\in A_r}\tilde{X}_{snk}^c - \sum_{(n,s)\in A_r}\tilde{X}_{nsk}^c = 0, \quad \forall s \in S, k \in K, c \in C \tag{5.8}$$

$$-M\,Y_{sk}^c \leq \sum_{(s,n)\in A_r}\tilde{X}_{snk}^c - \sum_{(n,s)\in A_r}\tilde{X}_{nsk}^c \leq M\,Y_{sk}^c, \quad \forall s \in S, k \in K, c \in C \tag{5.9}$$

$$-F_{sk}^c \leq \sum_{(s,m)\in A_h}X_{smk}^c - \sum_{(m,s)\in A_h}X_{msk}^c \leq F_{sk}^c, \quad \forall s \in S, k \in K, c \in C \tag{5.10}$$

$$\sum_{(i,j)\in(A_h\cap p)}\delta_{ijk}^c t_{ij} + \sum_{(i,j)\in(A_r\cap p)}\tilde{\delta}_{ijk}^c \tilde{t}_{ij} + \sum_{s\in(S\cap p)}Y_{sk}^c t_s \leq T_k^c, \quad \forall p \in P^c, k \in K, c \in C \tag{5.11}$$

$$\sum_{c\in C}\sum_{k\in K}d_k^c X_{ijk}^c \leq Q_{ij}, \quad \forall (i,j)\in A_h \tag{5.12}$$

$$\sum_{c\in C}\sum_{k\in K}d_k^c \tilde{X}_{ijk}^c \leq \tilde{Q}_{ij}, \quad \forall (i,j)\in A_r \tag{5.13}$$

$$\sum_{c\in C}\sum_{k\in K}d_k^c F_{sk}^c \leq Q_s, \quad \forall s \in S \tag{5.14}$$

$$d_k^c\left(1-\sum_{i\in H}X_{ijk}^c\right)=U_k^c, \quad \forall k \in K, c \in C, j = \text{des}^c \tag{5.15}$$

$$\varepsilon\delta_{ijk}^c \leq X_{ijk}^c \leq \delta_{ijk}^c, \quad \forall (i,j)\in A_h, k \in K, c \in C \tag{5.16}$$

$$\varepsilon\tilde{\delta}_{ijk}^c \leq \tilde{X}_{ijk}^c \leq \tilde{\delta}_{ijk}^c, \quad \forall (i,j)\in A_r, k \in K, c \in C \tag{5.17}$$

$$\varepsilon Y_{sk}^c \leq F_{sk}^c \leq Y_{sk}^c, \quad \forall s \in S, k \in K, c \in C \tag{5.18}$$

$$X_{ijk}^c \in [0,1], \quad \forall (i,j)\in A_h, k \in K, c \in C \tag{5.19}$$

$$\tilde{X}_{ijk}^c \in [0,1], \quad \forall (i,j)\in A_r, k \in K, c \in C \tag{5.20}$$

$$F_{sk}^c \in [0,1], \quad \forall s \in S, k \in K, c \in C \tag{5.21}$$

$$U_k^c \in Z^+, \quad \forall k \in K, c \in C \tag{5.22}$$

$$\delta_{ijk}^c \in \{0,1\}, \quad \forall (i,j)\in A_h, k \in K, c \in C \tag{5.23}$$

$$\tilde{\delta}_{ijk}^{c} \in \{0,1\}, \quad \forall (i,j) \in A_r, k \in K, c \in C \tag{5.24}$$

$$Y_{sk}^{c} \in \{0,1\}, \quad \forall s \in S, k \in K, c \in C \tag{5.25}$$

The objective function (5.1) seeks to minimize the total system cost; specifically, the system cost includes the transportation cost on highway and railway links, the transfer cost at intermodal terminals, and the penalty cost for unsatisfied demands. Constraints (5.2) to (5.6) ensure flow conservation at highway nodes (*H*). Similarly, constraint (5.7) ensures flow conservation at railway nodes (*R*). Constraints (5.8) and (5.9) ensure flow conservation at intermodal terminals (*S*); constraint (5.8) maintains the conservation of flow if a terminal is selected whereas constraint (5.9) maintains the conservation of flow if the terminal is not selected. The decision variables F_c^{sk} are calculated in constraint (5.10). Constraint (5.11) ensures that commodity shipments are delivered before the delivery deadline. Constraints (5.12) to (5.14) ensure that flows are less than or equal to the capacity of highway links, railway links, and intermodal terminals, respectively. Constraint (5.15) determines the unsatisfied demand. Lastly, constraints (5.16) to (5.18) are the relational constraints, constraints (5.19) to (5.21) are the definitional constraints, constraint (5.22) is the integrality constraint, and constraints (5.23) to (5.25) are the binary constraints. For constraints (5.16) to (5.18), the left-hand side term could be 0 instead of the product of ε. However, the formulation as presented provides a computational advantage. In addition, unsatisfied demands are assumed to be integer since the original demands are in number of intermodal containers.

As mentioned earlier, a transportation network may experience service disruptions. Hence, the MIFR with deterministic link capacities are not always valid. To account for uncertainty in the network, random capacity of highway link is denoted as

$\hat{Q}_{ij}$, random capacity of railway link is denoted as $\hat{\tilde{Q}}_{ij}$, and random capacity of intermodal terminal is denoted as $\hat{Q}_s$. Using these definitions, equations (5.12), (5.13), and (5.14) have the following form.

$$\sum_{c \in C}\sum_{k \in K} d_k^c X_{ijk}^c \le \hat{Q}_{ij} \ , \ \sum_{c \in C}\sum_{k \in K} d_k^c \tilde{X}_{ijk}^c \le \hat{\tilde{Q}}_{ij} \ , \ \sum_{c \in C}\sum_{k \in K} d_k^c F_{sk}^c \le \hat{Q}_s \tag{5.26}$$

To incorporate the modified constraints above into the optimization model, chance constraint programming is employed which guarantees that the solution satisfies the constraints over a subset of the sample space. Assume the following for a highway link capacity $\hat{Q}_{ij}$.

$$\hat{Q}_{ij} = Q_{ij}\left(1 + \lambda_{ij}\hat{\xi}_{ij}\right) \tag{5.27}$$

where $\lambda_{ij} \ge 0$ is a measure of uncertainty and $\hat{\xi}_{ij}$ represents a symmetric random variable on the interval $[-1, 1]$; meaning that $\hat{\xi}_{ij}$ and $-\hat{\xi}_{ij}$ have identical distributions. It should be noted that λ_{ij} and $\hat{\xi}_{ij}$ is chosen in a way where $\hat{Q}_{ij} \ge 0$ always holds. Similarly, assume the following for the railway link and intermodal terminal capacities.

$$\hat{\tilde{Q}}_{ij} = \tilde{Q}_{ij}\left(1 + \tilde{\lambda}_{ij}\hat{\tilde{\xi}}_{ij}\right) \tag{5.28}$$

$$\hat{Q}_s = Q_s\left(1 + \lambda_s\hat{\xi}_s\right) \tag{5.29}$$

Let $E[Z]$ denotes the expected value of a random variable Z; then, $E\left[\hat{Q}_{ij}\right] = Q_{ij}$, $E\left[\hat{\tilde{Q}}_{ij}\right] = \tilde{Q}_{ij}$, and $E\left[\hat{Q}_s\right] = Q_s$. Hence, the model only requires the specification of mean values and the support of the random quantities instead of a specific probability distribution. Similar to chance constraint programming, this model has control over the

likelihood that the constraints in equation (5.26) are violated. The following additional constraints are introduced in the model.

$$\sum_{c \in C} \sum_{k \in K} d_k^c X_{ijk}^c \le Q_{ij} - \theta_{ij} \tag{5.30}$$

$$\sum_{c \in C} \sum_{k \in K} d_k^c \tilde{X}_{ijk}^c \le \tilde{Q}_{ij} - \tilde{\theta}_{ij} \tag{5.31}$$

$$\sum_{c \in C} \sum_{k \in K} d_k^c F_{sk}^c \le Q_s - \theta_s \tag{5.32}$$

where $\theta_{ij} \ge 0$, $\tilde{\theta}_{ij} \ge 0$, and $\theta_s \ge 0$. The following probability expression

$$\Pr\left\{ \sum_{c \in C} \sum_{k \in K} d_k^c X_{ijk}^c > \hat{Q}_{ij} \right\} \tag{5.33}$$

can be interpreted as the likelihood that the shipments based on the deterministic estimate of the highway link capacity exceed the realized capacity. To avoid this situation the probability in equation (5.33) needs to be acceptably small. Let us assume that X_{ijk}^c is a feasible solution of the model defined by equations (5.1) to (5.25), (5.30) to (5.32), then it follows:

$$\Pr\left\{ \sum_{c \in C} \sum_{k \in K} d_k^c X_{ijk}^c > \hat{Q}_{ij} \right\} = \Pr\left\{ \sum_{c \in C} \sum_{k \in K} d_k^c X_{ijk}^c > Q_{ij}\left(1 + \lambda_{ij}\hat{\xi}_{ij}\right) \right\} < \Pr\left\{ -Q_{ij}\lambda_{ij}\hat{\xi}_{ij} > \theta_{ij} \right\} \tag{5.34}$$

where the inequality follows from the following implication of events: since X_{ijk}^c is feasible, then the event $\left\{ \sum_{c \in C} \sum_{k \in K} d_k^c X_{ijk}^c > Q_{ij}\left(1 + \lambda_{ij}\hat{\xi}_{ij}\right) \right\}$ implies the event $\left\{ -Q_{ij}\lambda_{ij}\hat{\xi}_{ij} > \theta_{ij} \right\}$. If the probability distribution of $\hat{\xi}_{ij}$ is assumed to be known, the right-most probability in equation (5.34) can easily be bounded. This is similar to a chance constraint programming approach.

Using a distribution-free approach (i.e., there is no explicit assumption about probability distributions), without loss of generality, let us assume that $\eta > 0$. Then it follows:

$$\Pr\left\{-Q_{ij}\lambda_{ij}\hat{\xi}_{ij} > \theta_{ij}\right\} = \Pr\left\{\hat{\xi}_{ij} < \frac{\theta_{ij}}{-Q_{ij}\lambda_{ij}}\right\} = \Pr\left\{\hat{\xi}_{ij} > \frac{\theta_{ij}}{Q_{ij}\lambda_{ij}}\right\}$$
$$= \Pr\left\{\exp\left(\eta\hat{\xi}_{ij}\right) > \exp\left(\frac{\eta\theta_{ij}}{Q_{ij}\lambda_{ij}}\right)\right\}$$

(5.35)

Markov's inequality gives the following equation from the last part of the above.

$$\Pr\left\{\exp\left(\eta\hat{\xi}_{ij}\right) > \exp\left(\frac{\eta\theta_{ij}}{Q_{ij}\lambda_{ij}}\right)\right\} \le \exp\left(\frac{-\eta\theta_{ij}}{Q_{ij}\lambda_{ij}}\right) E\left[\exp\left(\eta\hat{\xi}_{ij}\right)\right]$$

(5.36)

Since $\hat{\xi}_{ij}$ is a symmetric random variable, we can express $E\left[\exp\left(\eta\xi_{ij}\right)\right]$ as follows:

$$E\left[\exp\left(\eta\xi_{ij}\right)\right] = \int_{-1}^{0}\exp(\eta y)\,dF(y) + \int_{0}^{1}\exp(\eta y)\,dF(y)$$

(5.37)

$$= \int_{0}^{1}\left[\exp(\eta y) + \exp(-\eta y)\right]dF(y)$$

(5.38)

$$\le \int_{0}^{1}\max_{0 \le y \le 1}\left[\exp(\eta y) + \exp(-\eta y)\right]dF(y)$$

(5.39)

$$\le \left[\exp(\eta) + \exp(-\eta)\right]\int_{0}^{1}dF(y)$$

(5.40)

$$= \left[\exp(\eta) + \exp(-\eta)\right]/2$$

(5.41)

Equation (5.38) holds due to the symmetry of $\hat{\xi}_{ij}$ and equation (5.39) holds since the integrand is replaced by its maximum value. Inequality (5.40) is obtained by using the fact that integrand in equation (5.38) is maximized at $y = 1$. Again, using the symmetry equation (5.41) is obtained. Taylor series expansions of $\exp(\eta)$ and $\exp(-\eta)$ give us the following.

92

$$\left[\exp(\eta) + \exp(-\eta)\right]/2 \le \exp(\eta^2/2) \tag{5.42}$$

Now, since $\eta > 0$ is arbitrary, the tightest possible bound can be obtained by minimizing over η. Therefore, using the above, equation (5.36) can be written as follows:

$$\Pr\left\{\exp\left(\eta\hat{\xi}_{ij}\right) > \exp\left(\frac{\eta\theta_{ij}}{Q_{ij}\lambda_{ij}}\right)\right\} \le \min_{\eta > 0} \exp\left(\frac{-\eta\theta_{ij}}{Q_{ij}\lambda_{ij}}\right)\exp\left(\eta^2/2\right) \tag{5.43}$$

To obtain equation (5.43) from the equation (5.36), it is assumed that random variations are symmetric, which is a common approach for solving robust optimization models (Bertsimas and Sim, 2004; Ng and Waller, 2012). The right-hand side of the equation (5.43) is strictly convex; hence, the unique optimal solution can be obtained by taking the derivative and setting it equal to zero. The optimal solution is:

$$\eta^* = \frac{\theta_{ij}}{Q_{ij}\lambda_{ij}} \tag{5.44}$$

Substituting the above value into equation (5.43), the following can be obtained.

$$\Pr\left\{\exp\left(\eta\hat{\xi}_{ij}\right) > \exp\left(\frac{\eta\theta_{ij}}{Q_{ij}\lambda_{ij}}\right)\right\} \le \exp\left(\frac{-\theta_{ij}^2}{2\left(Q_{ij}\lambda_{ij}\right)^2}\right) \tag{5.45}$$

The above discussion is summarized in the following proposition.

Proposition 5.1.1 *If $\hat{\xi}_{ij}$ is a symmetric random variable with support* [-1, 1] *and*

$$\theta_{ij} = \sqrt{-2\log\left(q_{ij}\right)} Q_{ij}\lambda_{ij}, \text{ where } 0 < q_{ij} \le 1, \text{ then}$$

$$\Pr\left\{\sum_{c \in C}\sum_{k \in K} d_k^c X_{ijk}^c > \hat{Q}_{ij}\right\} \le q_{ij}$$

Likewise, by imposing the constraints (5.31) and (5.32), the following two propositions can be shown.

Proposition 5.1.2 *If* $\hat{\tilde{\xi}}_{ij}$ *is a symmetric random variable with support* [-1, 1] *and*

$$\tilde{\theta}_{ij} = \sqrt{-2\log(\tilde{q}_{ij})}\, \tilde{Q}_{ij}\tilde{\lambda}_{ij}, \text{ where } 0 < \tilde{q}_{ij} \leq 1, \text{ then}$$

$$\Pr\left\{\sum_{c \in C}\sum_{k \in K} d_k^c \tilde{X}_{ijk}^c > \hat{\tilde{Q}}_{ij}\right\} \leq \tilde{q}_{ij}$$

Proposition 5.1.3 *If* $\hat{\xi}_s$ *is a symmetric random variable with support* [-1, 1] *and*

$$\theta_s = \sqrt{-2\log(q_s)}\, Q_s\lambda_s, \text{ where } 0 < q_s \leq 1, \text{ then}$$

$$\Pr\left\{\sum_{c \in C}\sum_{k \in K} d_k^c F_{sk}^c > \hat{Q}_s\right\} \leq q_s$$

5.2 NUMERICAL EXPERIMENTS

To demonstrate the applicability of the proposed modeling framework, an actual road-rail freight transport network shown in Figure 5.2 was used. It covers all of the states in the Gulf Coast, Southeastern and Mid-Atlantic regions of the U.S. The network has a total of 682 links (U.S. interstates and major highways and Class I railroads) and 187 nodes, including 44 intermodal terminals. The Freight Analysis Zone (FAZ) centroids from the Freight Analysis Framework version 3 (FAF3) database (Federal Highway Administration, 2013) were treated as actual origins and destinations of commodity shipments. There is a total of 48 centroids in the study region. Origin-Destination (OD) pairs were constructed from these 48 FAZ centroids, and demands are obtained from the FAF3 database. The demand data were filtered to include only those commodities typically transported via intermodal (Cambridge Systematics, 2007), and demands were converted into containers using an average load of 40,000 lbs per container. It was assumed that all commodities need to be delivered within 7 days. The

transport cost on highways and railways were estimated to be \$1.67 per mile per shipment (Torrey and Murray, 2014) and \$0.60 per mile per shipment (Cambridge Systematics, 1995), respectively. The transfer cost at intermodal terminals was estimated to be \$70 per shipment (Winebrake et al., 2008a). Using free-flow speeds, the travel times on highway and railway links were calculated.
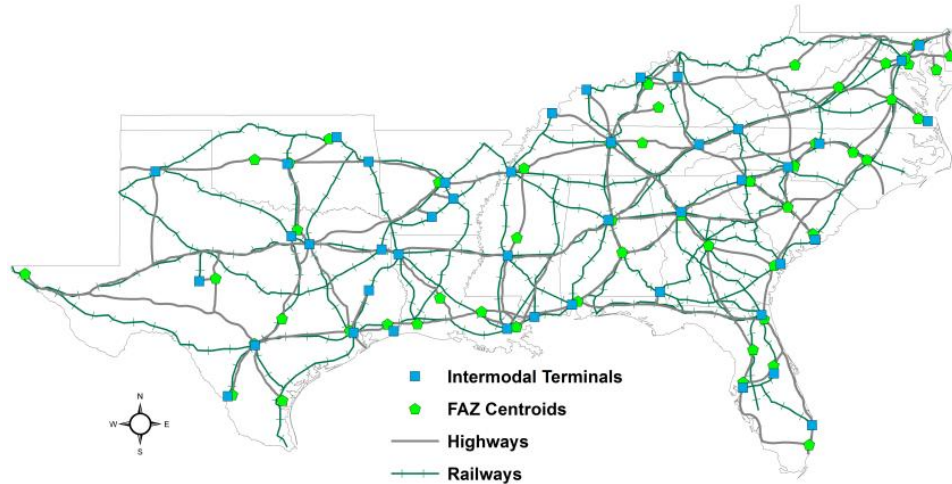
Figure 5.2 Large-scale U.S. road-rail intermodal network.

To simulate network uncertainty, three types of disruptive events were considered in this study: (1) link disruption, (2) node disruption, and (3) intermodal terminal disruption. Note that affected links, nodes, or terminals are selected based on their vulnerability. A factorial experimental design (FED) was used to examine the effect of confidence level and capacity uncertainty parameters in the proposed model on total system cost (i.e., objective function value). In case of FED, "factors" and "levels" are utilized; "factors" are the variables that are chosen to be studied and "levels" are the predefined discrete values of the factors. The combination of all levels of factors are considered and based on the resulting total system cost the effect of each combination of factors and levels is studied. Table 5.2 provides a summary of the FED. Three "factors"

were considered: (1) number of disrupted elements, (2) confidence level $\left(q_{ij},\tilde{q}_{ij},q_s\right)$, and

(3) capacity uncertainty $\left(\lambda_{ij},\tilde{\lambda}_{ij},\lambda_s\right)$. For an experiment with a particular number of OD

pairs and commodities, the combination of factors and levels result in a total of 112

instances for link disruptions, 112 instances for node disruptions, and 84 instances for

intermodal terminal disruptions.

Table 5.2 Summary of Factorial Experimental Design

Factors	Levels		
	Link disruption	Node disruption	Terminal disruption
Number of disrupted elements	(1) 30, (2) 60, (3) 100, and (4) 200	(1) 5, (2) 10, (3) 20, and (4) 40	(1) 15, (2) 30, and (3) 44
Confidence level $\left(q_{ij},\tilde{q}_{ij},q_s\right)$	(1) 0.05, (2) 0.1, (3) 0.15, and (4) 0.2	(1) 0.05, (2) 0.1, (3) 0.15, and (4) 0.2	(1) 0.05, (2) 0.1, (3) 0.15, and (4) 0.2
Capacity uncertainty $\left(\lambda_{ij},\tilde{\lambda}_{ij},\lambda_s\right)$	(1) 0, (2) 0.05, (3) 0.1, (4) 0.15, (5) 0.2, (6) 0.25, and (7) 0.3	(1) 0, (2) 0.05, (3) 0.1, (4) 0.15, (5) 0.2, (6) 0.25, and (7) 0.3	(1) 0, (2) 0.05, (3) 0.1, (4) 0.15, (5) 0.2, (6) 0.25, and (7) 0.3

The proposed modeling framework was implemented in Python, and the IBM

ILOG CPLEX 12.6 solver was used to solve the mixed-integer program. Experiments

were run on a personal computer with Intel Core i7 3.20 GHz processor and 24.0 GB of

RAM. For a given level of confidence and uncertainty level, using propositions 5.1.1 to

5.1.3, the amount of capacity reductions (θ) can be obtained. Figures 5.3 to 5.6 present

the experimental results for the real-world network for varying OD pairs and

commodities.

Figure 5.3 depicts the resulting objective function values for 5 OD pairs (9

commodities) of shipments: (a) is for 30 disrupted links, (b) is for 60 disrupted links, (c)

is for 100 disrupted links, (d) is for 200 disrupted links, (e) is for 5 disrupted nodes, (f) is

for 10 disrupted nodes, (g) is for 20 disrupted nodes, (h) is for 40 disrupted nodes, (i) is for 15 disrupted intermodal terminals, (j) is for 30 terminals, and (k) is for 44 terminals. It can be seen that the objective function value increases with the level of uncertainty. Furthermore, increased confidence level leads to an increase in the objective function value. As expected, the objective function value increases as the number of affected links increases. A similar trend is observed for node and intermodal terminal disruptions. The objective function value was highest when all of the intermodal terminals were disrupted. This finding is logical because when all of the intermodal terminals are disrupted, commodities can only be shipped via road.

Figure 5.4 shows the variations of objective function values under different levels of capacity uncertainty and confidence levels for 10 OD pairs and 21 commodities. Figure 5.5 shows variations for 20 OD pairs and 43 commodities, and Figure 5.6 shows variations for 50 OD pairs and 87 commodities. The objective function values follow the same pattern observed in the 5 OD pairs scenario.

Collectively, the results indicate that under link and node disruption scenarios, most shipments are shipped via road-rail intermodal when a lower confidence level is considered. This can be attributed to the lower rail cost. When a higher confidence level is required under link and node disruptions, shipments are transported by road directly. This is can be attributed to the fact that a truck can always find an alternative route on the highway network when the intermodal network is disrupted. Freight shippers could use the above findings to make shipping decisions when the intermodal network is disrupted by some events. In summary, the managerial implications of the findings are that if freight shippers want a higher reliability for the delivery of its shipment under disruptions

97
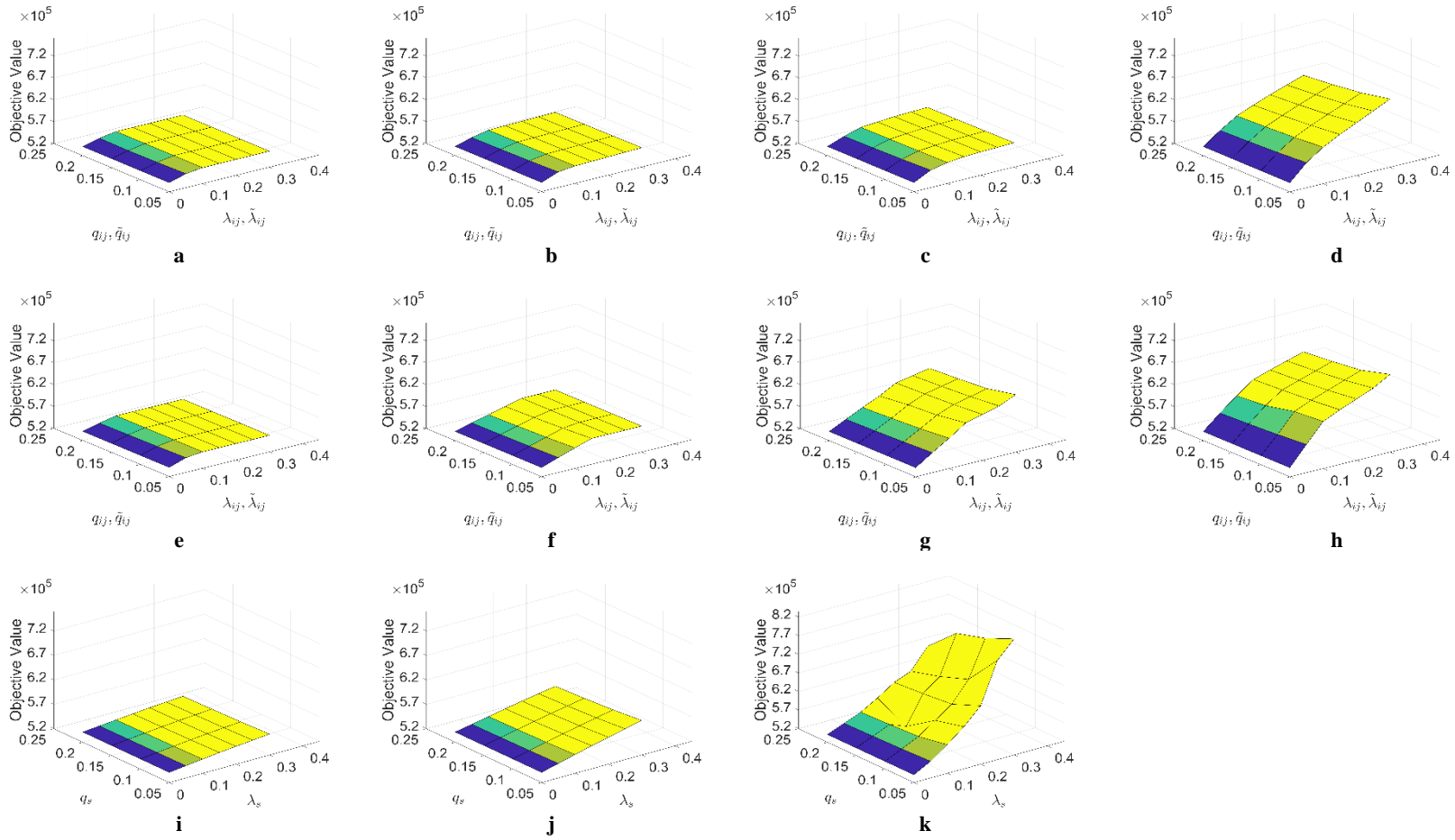
Figure 5.3 Objective function values under different levels of capacity uncertainty and confidence levels for 5 OD pairs (9 commodities): (a) 30 links, (b) 60 links, (c) 100 links, (d) 200 links, (e) 5 nodes, (f) 10 nodes, (g) 20 nodes, (h) 40 nodes, (i) 15 terminals, (j) 30 terminals, and (k) 44 terminals.
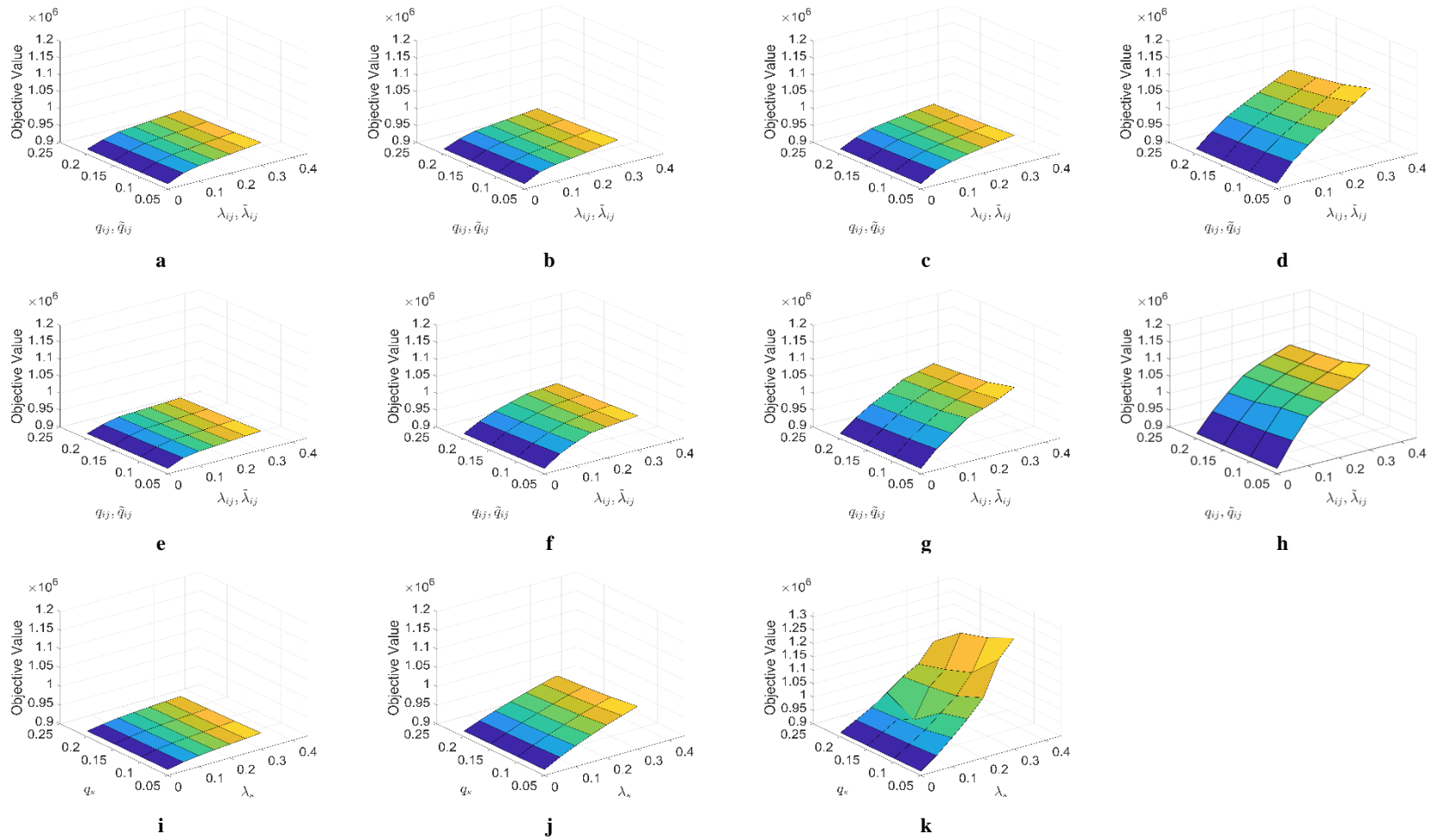
Figure 5.4 Objective function values under different levels of capacity uncertainty and confidence levels for 10 OD pairs (21 commodities): (a) 30 links, (b) 60 links, (c) 100 links, (d) 200 links, (e) 5 nodes, (f) 10 nodes, (g) 20 nodes, (h) 40 nodes, (i) 15 terminals, (j) 30 terminals, and (k) 44 terminals.
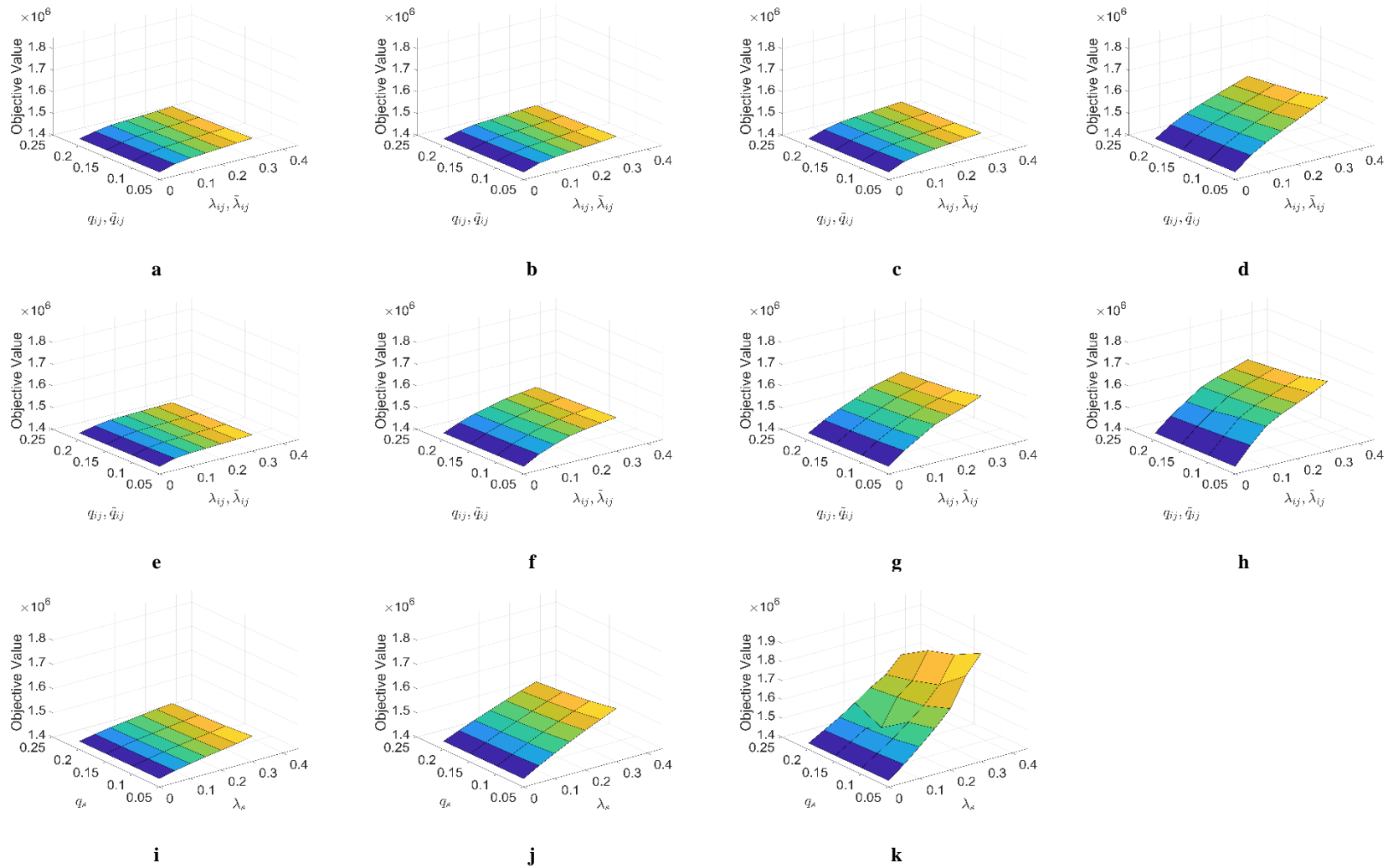
Figure 5.5 Objective function values under different levels of capacity uncertainty and confidence levels for 20 OD pairs (43 commodities): (a) 30 links, (b) 60 links, (c) 100 links, (d) 200 links, (e) 5 nodes, (f) 10 nodes, (g) 20 nodes, (h) 40 nodes, (i) 15 terminals, (j) 30 terminals, and (k) 44 terminals.
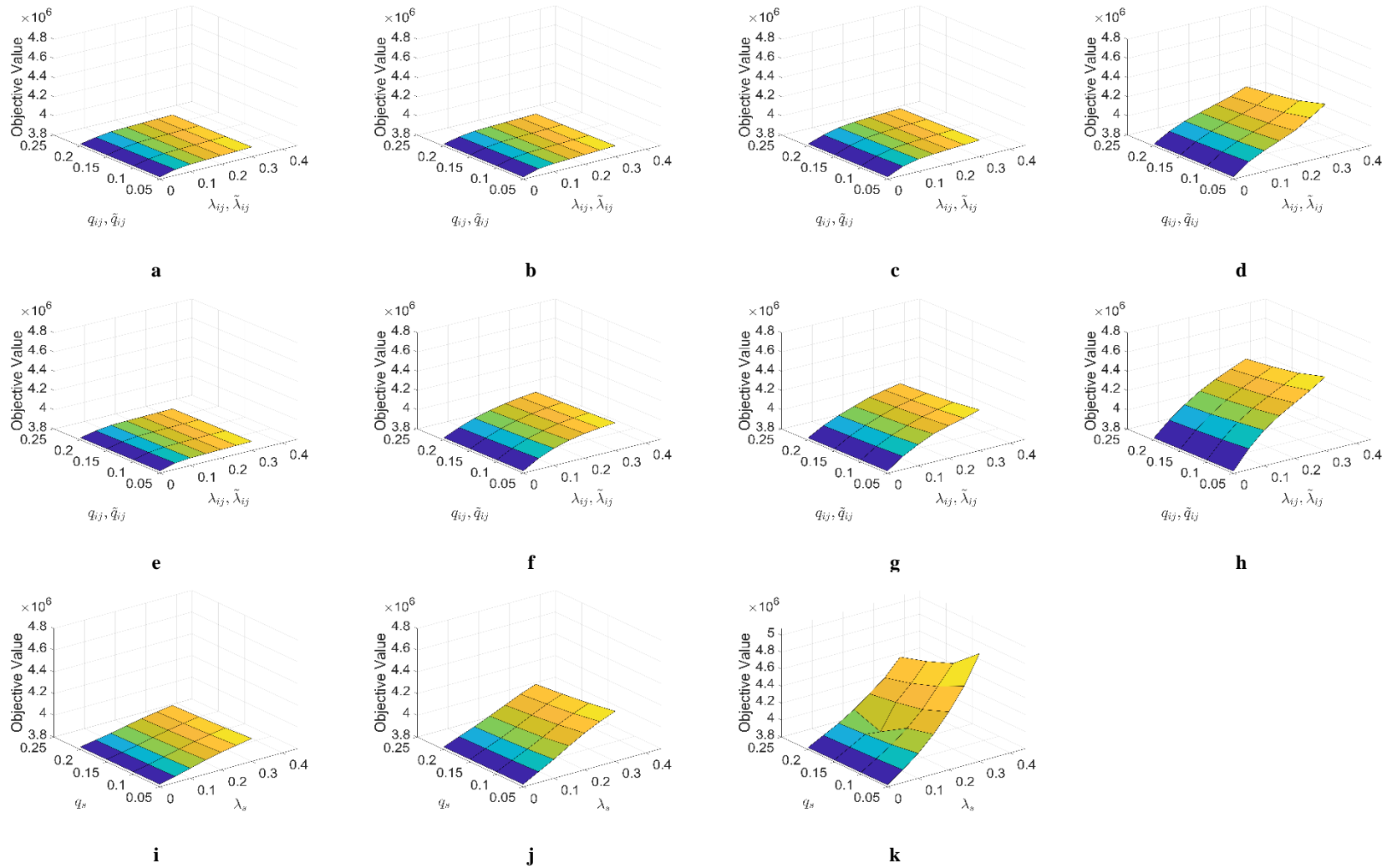
Figure 5.6 Objective function values under different levels of capacity uncertainty and confidence levels for 50 OD pairs (87 commodities): (a) 30 links, (b) 60 links, (c) 100 links, (d) 200 links, (e) 5 nodes, (f) 10 nodes, (g) 20 nodes, (h) 40 nodes, (i) 15 terminals, (j) 30 terminals, and (k) 44 terminals.

they should ship via truck only. On the other hand, if reliability is not a concern, they should ship via road-rail intermodal due to lower cost.

After analyzing the experimental results, it is possible to quantify and compare vulnerability of different elements in road-rail intermodal freight transport networks. The observations are summarized in two propositions. Before presenting the propositions, an index called *importance* is introduced. It is assumed that a link is disrupted when its travel time ($\hat{t}_{ij}$) is greater than the typical travel time (t_{ij}). In particular, the term $\hat{t}_{ij}$ denotes the link travel time (with uncertainty) under the disruption scenario, and the term t_{ij} denotes the link travel time (without uncertainty) under the normal scenario. The importance of a link $(i, j) \in A$ with respect to the entire network is defined as follows. The term $d_k^c X_{ijk}^c$ is a weight for each commodity $k \in K$ and OD pair $c \in C$ combination.

$$L_{ij}^{net} = \frac{\sum_{c \in C}\sum_{k \in K} d_k^c X_{ijk}^c \left(\hat{t}_{ij} - t_{ij}\right)}{\sum_{c \in C}\sum_{k \in K} d_k^c X_{ijk}^c t_{ij}}, \qquad (i, j) \in A \tag{5.46}$$

In this study, vulnerability is defined in terms of reduced serviceability. It is possible to measure the reduced serviceability (i.e., vulnerability) by computing the increase in generalized cost of travel (i.e., travel time) for commodity shipments (Jenelius et al., 2006). To measure and compare the vulnerability of transportation network elements, a number of measures have been developed. These include *criticality* (Jenelius et al., 2006), *importance* (Jenelius et al., 2006; Rupi et al., 2015), and *exposure* (Jenelius et al., 2006). The importance is defined above as the consequences of a network element in the road-rail intermodal network being disrupted. It is computed by accounting for the increase in travel time for each network element which in turn affects the performance of

the network. For this reason, importance can be used to measure and compare the vulnerability of a network element. Furthermore, this index can be used to compare vulnerability across different types of network elements.

For a node disruption, all links connected to that node are affected. If set J includes all the nodes connected to a specific node i', i.e., $J = \{j \mid (i', j) \in A, i' \neq j\}$, then the importance of node i' with respect to the entire network is defined as follows:

$$N_{i'}^{net} = \sum_{j \in J} L_{i'j}^{net} \qquad (5.47)$$

The following two propositions apply to intermodal freight transport networks.

Proposition 5.2 *Impact of a node disruption is always greater than that of a link disruption if and only if both elements are affected by the same disruptive event.*

Proof. Suppose that impact of a network element disruption can be quantified by the importance measures defined above. Thus, the network element that has a higher importance value will have a greater impact on an intermodal freight transport network during a disruptive event. During a disruption, if the relative increase in link travel time ($\hat{t}_{ij}/t_{ij}$) is the same for all links inside the affected region or area, then by definition, $|J| \geq 2$, and hence, the following always holds for any node i ($i = i'$ or $i \neq i'$).

$$N_{i'}^{net} > L_{ij}^{net}, \quad \forall (i, j) \in A \qquad (5.48)$$

Proposition 5.3 *Impact of an intermodal terminal disruption is always greater than that of a node disruption if and only if both elements are affected by the same disruptive event.*

Proof. The importance of a terminal with respect to the entire network is defined as follows:

$$N_t^{net} = \sum_{j' \in J'} L_{tj'}^{net} + L_{td}^{net} \tag{5.49}$$

The set J' includes all the nodes connected to the terminal t except for the dummy node d, i.e., $J' = J \setminus \{d\}$; to model a disruptive event, a dummy node and a dummy link is inserted between the terminal node and one of the network links connected to it. The travel time on the dummy link (t_d) is very large in the event of a disruption. Hence, the importance of any network node i is always less than the importance of the terminal that it is connected to. Mathematically, this relationship can be expressed as follows.

$$N_t^{net} > N_i^{net}, \; i \neq t \tag{5.50}$$

Corollary 5.1 *Impact of an intermodal terminal disruption is always greater than that of a link disruption if and only if both elements are affected by the same disruptive event.*

Proof. From Proposition 3, for any node i' and intermodal terminal t, we have the following.

$$N_t^{net} > N_{i'}^{net} \tag{5.51}$$

From Proposition 2, for any node i' and link $(i, j) \in A$, we have the following.

$$N_{i'}^{net} > L_{ij}^{net} \tag{5.52}$$

Hence, the following must always hold for any intermodal terminal t and link $(i, j) \in A$.

$$N_t^{net} > L_{ij}^{net} \tag{5.53}$$

5.3 SUMMARY AND CONCLUSION

This chapter proposed a new reliable modeling framework to determine the optimal routes for delivering multicommodity freight in an intermodal freight network that is subject to uncertainty. The finding from the proposed model is quite simple and intuitive: to ensure reliability, the model suggests that route planning be done by assuming the network elements have lower capacity than they actually have. To date, no formal framework has been developed to analytically determine the amount of capacity reduction needed to obtain a desired reliability level. This study addressed this important gap by proposing a novel distribution-free approach. The framework is distribution-free in the sense that it only requires the specification of the mean values and the uncertainty intervals. The developed model was tested on an actual intermodal network in the Gulf Coast, Southeastern and Mid-Atlantic regions of the U.S. It is found that the total system cost increases with the level of capacity uncertainty and with increased confidence levels for disruptions at links, nodes, and intermodal terminals.

CHAPTER 6

CONCLUSION AND FUTURE RESEARCH

Four research studies are presented in this dissertation that address practical problems for road-rail intermodal freight transportation. The solutions to these problems will make intermodal freight transport more efficient and cost-effective.

In Chapter 2, a methodology is presented for freight traffic assignment in large-scale road-rail intermodal networks. Given a set of freight demands between origins and destinations and designated modes (road-only, rail-only, and intermodal), the model finds the user-equilibrium freight flow. The proposed model was tested using the U.S. intermodal network and the Freight Analysis Framework, version 3 (FAF3), 2007 freight shipment data. The results of the analysis, volume and spatial variation of freight traffic, show that the model produces equilibrium flow pattern that was very similar to the FAF3 flow assignment.

In Chapter 3, a stochastic model is developed to assign freight traffic in a large-scale road-rail intermodal network that is subject to network uncertainty. For a specific disaster scenario and given a set of freight demands between origins and destinations and designated modes (road-only, rail-only, and intermodal), the model finds the user-equilibrium freight flow. Four disasters were considered in the numerical experiments: earthquake, hurricane, tornado, and flood. The proposed model and algorithmic framework were tested using the U.S. road-rail intermodal network and the FAF3 shipment data. The results indicated that when disasters are considered the freight ton-

miles are higher than when no disaster is considered. The resulting user-equilibrium flows clearly indicate the impact of disasters; that is, truck and rail flow are shifted away from the impacted areas.

In Chapter 4, a stochastic mixed integer programming model is developed to determine the optimal routes for delivering multicommodity freight in an intermodal freight network that is subject to disruptions (e.g., link, node, and terminal disruptions). The model results indicated that under disruptions, goods in the study region should be shipped via road-rail intermodal due to lower rail cost and due to the built-in redundancy of the freight transport network. Furthermore, the model indicated that for a particular number of OD pairs, the total system cost will increase as the number of disrupted elements increases. The routes generated by the model are shown to be more robust than those typically used by freight carriers because they are often selected without consideration of potential network disruptions.

In Chapter 5, a reliable modeling framework is proposed to determine the optimal routes for delivering multicommodity freight in an intermodal freight network that is subject to uncertainty. The framework is distribution-free in the sense that it only requires the specification of the mean values and the uncertainty intervals. The developed model was tested on an actual intermodal network in the Gulf Coast, Southeastern and Mid-Atlantic regions of the U.S. It is found that the total system cost increases with the level of capacity uncertainty and with increased confidence levels for disruptions at links, nodes, and intermodal terminals.

The environmental impact of road-rail intermodal freight could be assessed in the future. Freight transportation activities are responsible for a large share of air pollution

and greenhouse gas emissions in the U.S. Various freight transportation modes (such as road, rail, intermodal, etc.) have significantly different impacts on air quality and environmental sustainability. For that reason, using the publicly available data (e.g., Freight Analysis Framework) and advanced econometric model, the environmental impact of intermodal freight could be investigated based on various factors, such as value and distance of shipment, commodity types, and oil price.

REFERENCES

Adams, T. M., Bekkem, K. R., & Toledo-Durán, E. J. (2012). Freight resilience measures. *Journal of Transportation Engineering*, *138*(11), 1403–1409. https://doi.org/10.1061/(ASCE)TE.1943-5436.0000415

Agrawal, B. B., & Ziliaskopoulos, A. (2006). Shipper–carrier dynamic freight assignment model using a variational inequality approach. *Transportation Research Record: Journal of the Transportation Research Board*, *1966*, 60–70. https://doi.org/10.1177/0361198106196600108

Alert Systems Group. (2018). *Informative maps*. Retrieved from alertsystemsgroup.com/earthquake-early-warning/ informative-maps

Arnold, P., Peeters, D., & Thomas, I. (2004). Modelling a rail/road intermodal transportation system. *Transportation Research Part E: Logistics and Transportation Review*, *40*(3), 255–270. https://doi.org/10.1016/j.tre.2003.08.005

Ayar, B., & Yaman, H. (2012). An intermodal multicommodity routing problem with scheduled services. *Computational Optimization and Applications*, *53*(1), 131–153. https://doi.org/10.1007/s10589-011-9409-z

Barbarosoglu, G., & Arda, Y. (2004). A two-stage stochastic programming framework for transportation planning in disaster response. *Journal of the Operational Research Society*, *55*(1), 43–53. https://doi.org/10.1057/palgrave.jors.2601652

Barnhart, C., & Ratliff, H. D. (1993). Modeling intermodal routing. *Journal of Business Logistics*, *14*(1), 205–223.

Barton, T. (2018). *Nearly 200 SC roads, including stretch of I-95, closed as flooding worsens*. The State, Sept. 20. Retrieve from www.thestate.com/news/state/south-carolina/article218717275.html

Bertsekas, D. P. (1976). On the Goldstein-Levitin-Polyak gradient projection method. *IEEE Transactions on Automatic Control*, *21*(2), 174–184. https://doi.org/10.1109/TAC.1976.1101194

Bertsimas, D., & Sim, M. (2004). The price of robustness. *Operations Research*, *52*(1), 35–53. https://doi.org/10.1287/opre.1030.0065

Boardman, B. S., Malstrom, E. M., Butler, D. P., & Cole, M. H. (1997). Computer assisted routing of intermodal shipments. *Computers & Industrial Engineering*, *33*(1–2), 311–314. https://doi.org/10.1016/S0360-8352(97)00100-9

Borndörfer, R., Fügenschuh, A., Klug, T., Schang, T., Schlechte, T., & Schülldorf, H. (2013). *The freight train routing problem*. Retrieved from www.opus4.kobv.de/opus4-zib/frontdoor/index/index/docId/1899

Boyce, D., Ralevic-Dekic, B., & Bar-Gera, H. (2004). Convergence of traffic assignments: how much is enough? *Journal of Transportation Engineering*, *130*(1), 49–55. https://doi.org/10.1061/(ASCE)0733-947X(2004)130:1(49)

Brown, T. R., & Hatch, A. B. (2002). *The value of rail intermodal to the U.S. economy*. Retrieved from http://intermodal.transportation.org/Documents/brown.pdf

Bureau of Transportation Statistics, U.S. Department of Transportation. (2015). *Freight facts and figures 2015*. Retrieved from https://www.bts.gov/sites/bts.dot.gov/files/legacy/FFF_complete.pdf

Bureau of Transportation Statistics, U.S. Department of Transportation. (2017). *Freight*

　　facts and figures 2017. Retrieved from https://www.bts.gov/sites/bts.dot.gov/files/

　　docs/FFF_2017_Full_June2018revision.pdf

Bureau of Transportation Statistics, U.S. Department of Transportation. (2018). *U.S.*

　　freight on the move: highlights from the 2012 commodity flow survey preliminary

　　data. Retrieved from

　　https://www.bts.gov/sites/bts.dot.gov/files/legacy/CFS_Complete.pdf

Cambridge Systematics, Inc. (1995). *Characteristics and changes in freight*

　　transportation demand: a guidebook for planners and policy analysts. Retrieved

　　from https://ntl.bts.gov/lib/4000/4300/4318/ccf.html

Cambridge Systematics, Inc. (2007). *National rail freight infrastructure capacity and*

　　investment study. Retrieved from

　　https://expresslanes.codot.gov/programs/transitandrail/resource-materials-

　　new/AARStudy.pdf

Cappanera, P., & Scaparra, M. P. (2011). Optimal allocation of protective resources in

　　shortest-path networks. *Transportation Science*, *45*(1), 64–80.

　　https://doi.org/10.1287/trsc.1100.0340

Center for Transportation Analysis, Oak Ridge National Laboratory. (2014). *Intermodal*

　　transportation network. Retrieved from

　　www.cta.ornl.gov/transnet/Intermodal_Network.html

Chang, M.-S., Tseng, Y.-L., & Chen, J.-W. (2007). A scenario planning approach for the

　　flood emergency logistics preparation problem under uncertainty. *Transportation*

Research Part E: Logistics and Transportation Review, *43*(6), 737–754.

https://doi.org/10.1016/j.tre.2006.10.013

Chang, T.-S. (2008). Best routes selection in international intermodal networks. *Computers & Operations Research*, *35*(9), 2877–91. https://doi.org/10.1016/j.cor.2006.12.025

Chen, A., Lee, D.-H., & Jayakrishnan, R. (2002). Computational study of state-of-the-art path-based traffic assignment algorithms. *Mathematics and Computers in Simulation*, *59*(6), 509–518. https://doi.org/10.1016/S0378-4754(01)00437-2

Chen, L., & Miller-Hooks, E. (2012). Resilience: an indicator of recovery capability in intermodal freight transport. *Transportation Science*, *46*(1), 109–123. https://doi.org/10.1287/trsc.1110.0376

Chow, J. Y. J., Ritchie, S. G., & Jeong, K. (2014). Nonlinear inverse optimization for parameter estimation of commodity-vehicle-decoupled freight assignment. *Transportation Research Part E: Logistics and Transportation Review*, *67*, 71–91. https://doi.org/10.1016/j.tre.2014.04.004

Crainic, T. G., Ferland, J.-A., & Rousseau, J.-M. (1984). A tactical planning model for rail freight transportation. *Transportation Science*, *18*(2), 165–184. https://doi.org/10.1287/trsc.18.2.165

Crainic, T. G., & Rousseau, J. M. (1986). Multicommodity, multimode freight transportation: a general modeling and algorithmic framework for the service network design problem. *Transportation Research Part B: Methodological*, 20(3), 225–242. https://doi.org/10.1016/0191-2615(86)90019-6

Cui, T., Ouyang, Y., & Shen, Z.-J. (2010). Reliable facility location design under the risk of disruptions. *Operations Research*, *58*(4), 998–1011. https://doi.org/10.1287/opre.1090.0801

D'Amico, E. (2002). West coast port lockout creates problems for chemical shippers. *Chemical Week*, *164*(40), 10.

Daskin, M. S. (1983). A maximum expected covering location model: formulation, properties and heuristics solution. *Transportation Science*, *17*(1), 48–70. https://doi.org/10.1287/trsc.17.1.48

Direct Freight Services. (2015). *Calculate mileage*. Retrieved from www.directfreight.com/home/route

Dowling, R., Kittelson, W., Zegeer, J., & Skabardonis, A. (1997). *Planning techniques to estimate speeds and service volumes for planning applications*. Retrieved from http://onlinepubs.trb.org/Onlinepubs/nchrp/nchrp_rpt_387.pdf

Federal Highway Administration, U.S. Department of Transportation. (2013). *Freight analysis framework*. https://ops.fhwa.dot.gov/freight/freight_analysis/faf/

Federal Highway Administration, U.S. Department of Transportation. (2014). *National highway freight network map*. Retrieved from https://ops.fhwa.dot.gov/freight/infrastructure/nfn/maps/nhfn_map.htm

Federal Highway Administration, U.S. Department of Transportation. (2015). *Freight disruptions: impacts on freight movement from natural and man-made events*. Retrieved from https://ops.fhwa.dot.gov/freight/freight_analysis/fd/index.htm

Fernandez, J. E, De Cea, J., & Giesen, R. (2004). A strategic model of freight operations

for rail transportation systems. *Transportation Planning and Technology*, *27*(4),

231–260. https://doi.org/10.1080/0308106042000228743

Frank, M., & Wolfe, P. (1956). An algorithm for quadratic programming. *Naval

Research Logistics Quarterly*, 3(1-2), 95–110.

https://doi.org/10.1002/nav.3800030109

Friesz, T. L., Gottfried, J. A., & Morlok, E. K. (1986). A sequential shipper–carrier

network model for predicting freight flows. *Transportation Science*, *20*(2), 80–91.

https://doi.org/10.1287/trsc.20.2.80

Garg, M., & Smith, J. C. (2008). Models and algorithms for the design of survivable

multicommodity flow networks with general failure scenarios. *Omega*, *36*(6),

1057–1071. https://doi.org/10.1016/j.omega.2006.05.006

Gedik, R., Medal, H., Rainwater, C., Pohl, E. A., & Mason, S. J. (2014). Vulnerability

assessment and re-routing of freight trains under disruptions: a coal supply chain

network application. *Transportation Research Part E: Logistics and

Transportation Review*, *71*, 45–57. https://doi.org/10.1016/j.tre.2014.06.017

Godoy, L. A. (2007). Performance of storage tanks in oil facilities damaged by hurricanes

Katrina and Rita. *Journal of Performance of Constructed Facilities*, *21*(6), 441–

449. https://doi.org/10.1061/(ASCE)0887-3828(2007)21:6(441)

Guelat, J., Florian, M., & Crainic, T. G. (1990). A multimode multiproduct network

assignment model for strategic planning of freight flows. *Transportation Science*,

24(1), 25–39. https://doi.org/10.1287/trsc.24.1.25

Haghani, A., & Oh, S.-C., (1996). Formulation and solution of a multi-commodity, multi-modal network flow model for disaster relief operations. *Transportation Research Part A: Policy and Practice*, *30*(3), 231–250. https://doi.org/10.1016/0965-8564(95)00020-8

Hall, R. W. (Eds.). (2003). *Handbook of transportation science* (2nd ed.). Springer US.

Huang, M., Hu, X., & Zhang, L. (2011). A decision method for disruption management problems in intermodal freight transport. In J. Watada, G. Phillips-Wren, L. C. Jain, and R. J. Howlett (Eds.) *Intelligent Decision Technologies*. Springer, Berlin Heidelberg.

Huang, Y., & Pang, W. (2014). Optimization of resilient biofuel infrastructure systems under natural hazards. *Journal of Energy Engineering*, *140*(2), 1–11. https://doi.org/10.1061/(ASCE)EY.1943-7897.0000138

Huynh, N., Uddin, M., & Minh, C. (2017). Data analytics for intermodal freight transportation applications. In M. Chowdhury, A. Apon, & K. Dey (Eds.), *Data Analytics for Intelligent Transportation Systems* (pp. 241–262). Cambridge, MA: Elsevier. https://doi.org/10.1016/B978-0-12-809715-1.00010-9

Hwang, T. (2014). *Freight demand modeling and logistics planning for assessment of freight systems' environmental impacts* (Doctoral dissertation). Retrieved from http://hdl.handle.net/2142/49430

Hwang, T., & Ouyang, Y. (2014). Assignment of freight shipment demand in congested rail networks. *Transportation Research Record: Journal of the Transportation Research Board*, *2448*, 37-44. https://doi.org/10.3141/2448-05

Ishfaq, R. (2013). Intermodal shipments as recourse in logistics disruptions. *Journal of the Operational Research Society*, 64, 229–240. https://doi.org/10.1057/jors.2012.40

Jayakrishnan, R., Tsai, W., Prashker, J., & Rajadhyaksha, J. (1994). Faster path-based algorithm for traffic assignment. *Transportation Research Record: Journal of the Transportation Research Board*, *1443*, 75–83.

Jenelius, E., Petersen, T., & Mattsson, L.-G. (2006). Importance and exposure in road network vulnerability analysis. *Transportation Research Part A: Policy and Practice*, *40*(7), 537–560. https://doi.org/10.1016/j.tra.2005.11.003

Kornhauser, A. L., & Bodden, M. (1983). Network analysis of highway and intermodal rail-highway freight traffic. *Transportation Research Record: Journal of the Transportation Research Board*, *920*, 61–68.

Krueger, H. (1999). Parametric modeling in rail capacity planning. *Winter Simulation Conference Proceedings*, *2*, 1194–1200. https://doi.org/10.1109/WSC.1999.816840

Lai, Y.-C., & Barkan, C. (2009). Enhanced parametric railway capacity evaluation tool. *Transportation Research Record: Journal of the Transportation Research Board*, *2117*, 33–40. https://doi.org/10.3141/2117-05

Loureiro, C. F. G., & Ralston, B. (1996). Investment selection model for multicommodity multimodal transportation networks. *Transportation Research Record: Journal of the Transportation Research Board*, *1522*, 38–46. https://doi.org/10.3141/1522-05

Mahmassani, H. S., Zhang, K., Dong, J., Lu, C.-C., Arcot, V., & Miller-Hooks, E. (2007). Dynamic network simulation-assignment platform for multiproduct intermodal freight transportation analysis. *Transportation Research Record: Journal of the Transportation Research Board*, *2032*, 9–16. https://doi.org/10.3141/2032-02

Marufuzzaman, M., Eksioglu, S. D., Li, X., & Wang, J. (2014). Analyzing the impact of intermodal-related risk to the design and management of biofuel supply chain. *Transportation Research Part E: Logistics and Transportation Review*, 69, 122–145. https://doi.org/10.1016/j.tre.2014.06.008

Margreta, M., Ford, C., & Dipo, M. A. (2009). *U.S. freight on the move: highlights from the 2007 commodity flow survey preliminary data*. Retrieved from https://www.bts.gov/sites/bts.dot.gov/files/legacy/publications/special_reports_and_issue_briefs/special_report/2009_09_30/pdf/entire.pdf

Miller-Hooks, E., Zhang, X., & Faturechi, R. (2012). Measuring and maximizing resilience of freight transportation networks. *Computers & Operations Research*, *39*(7), 1633–1643. https://doi.org/10.1016/j.cor.2011.09.017

National Oceanic and Atmospheric Administration, National Centers for Environmental Information. (2018). *Billion-dollar weather and climate disasters: summary stats*. Retrieved from www.ncdc.noaa.gov/billions/summary-stats

Ng, M., & Waller, S. T. (2012). A dynamic route choice model considering uncertain capacities. *Computer-Aided Civil and Infrastructure Engineering*, *27*(4), 231–243. https://doi.org/10.1111/j.1467-8667.2011.00724.x

Oak Ridge National Laboratory. (2013). *FAF3 freight traffic analysis*. Retrieved from www.faf.ornl.gov/fafweb/Data/Freight_Traffic_Analysis/faf_fta.pdf

Okasaki, N. W. (2003). Improving transportation response and security following a
disaster. *ITE Journal*, 73(8), 30–32.

Ozdamar, L., Ekinci, E., & Kucukyazici, B. (2004). Emergency logistics planning in
natural disasters. *Annals of Operations Research*, *129*(1–4), 217–245.
https://doi.org/10.1023/B:ANOR.0000030690.27939.39

Peng, P., Snyder, L. V., Lim, A., & Liu, Z. (2011). Reliable logistics networks design
with facility disruptions. *Transportation Research Part B: Methodological*, *45*(8),
1190–1211. https://doi.org/10.1016/j.trb.2011.05.022

Peterson, S. K., & Church, R. L. (2008). A framework for modeling rail transport
vulnerability. *Growth and Change*, *39*(4), 617–641. https://doi.org/10.1111/
j.1468-2257.2008.00449.x

Rahman, M., Uddin, M., & Gassman, S. (2017). Pavement performance evaluation
models for South Carolina. *KSCE Journal of Civil Engineering*, *21*(7), 2695–
2706. https://doi.org/10.1007/s12205-017-0544-7

Rahman, M., & Gassman, S. (2018). Data collection experience for preliminary
calibration of the AASHTO pavement design guide for flexible pavements in
South Carolina. *International Journal of Pavement Research and Technology*,
11(5), 445-457. https://doi.org/10.1016/j.ijprt.2017.11.009

Research and Innovative Technology Administration, Bureau of Transportation Statistics,
U.S. Department of Transportation. (2010). *Freight transportation: global
highlights*. Retrieved from
https://www.bts.dot.gov/sites/bts.dot.gov/files/legacy/publications/freight_transpo
rtation/pdf/entire.pdf

Rennemo, S. J., Ro, K. F., Hvattum, L. M., & Tirado, G. (2014). A three-stage stochastic facility routing model for disaster response planning. *Transportation Research Part E: Logistics and Transportation Review*, *62*, 116–135. https://doi.org/10.1016/j.tre.2013.12.006

Rios, M., Marianov, V., & Gutierrez, M. (2000). Survivable capacitated network design problem: new formulation and Lagrangian relaxation. *Journal of the Operational Research Society*, 51(5), 574–582. https://doi.org/10.1057/palgrave.jors.2600913

Rudi, A., Frohling, M., Zimmer, K., & Schultmann, F. (2016). Freight transportation planning considering carbon emissions and in-transit holding costs: a capacitated multi-commodity network flow model. *EURO Journal on Transportation and Logistics*, *5*(2), 123–160. https://doi.org/10.1007/s13676-014-0062-4

Rupi, F., Bernardi, S., Rossi, G., & Danesi, A. (2015). The evaluation of road network vulnerability in mountainous areas: a case study. *Networks and Spatial Economics*, *15*(2), 397–411. https://doi.org/10.1007/s11067-014-9260-8

Santoso, T., Ahmed, S., Goetschalckx, M., & Shapiro, A. (2005). A stochastic programming approach for supply chain network design under uncertainty. *European Journal of Operational Research*, 167, 96–115. https://doi.org/10.1016/j.ejor.2004.01.046

Shen, Z., Dessouky, M. M., & Ordóñez, F. (2009). A two-stage vehicle routing model for large-scale bioterrorism emergencies. *Networks*, *54*(4), 255–269. https://doi.org/10.1002/net.20337

Sheffi, Y. (1985). *Urban transportation networks: equilibrium analysis with mathematical programming methods*. New Jersey: Prentice-Hall, Inc.

Slack, B. (1990). Intermodal transportation in North America and the development of

    inland load centers. *The Professional Geographer*, *42*(1), 72–83.

    https://doi.org/10.1111/j.0033-0124.1990.00072.x

Snyder, L. V., & Daskin, M. S. (2005). Reliability models for facility location: the

    expected failure cost case. *Transportation Science*, *39*(3), 400–416.

    https://doi.org/10.1287/trsc.1040.0107

Song, H., & Chen, G. (2007). *Minimum cost delivery problem in intermodal*

    transportation networks. Presented at IEEE International Conference on Industrial

    Engineering and Engineering Management, Singapore.

Southworth, F., Davidson, D., Hwang, H., Peterson, B. E., & Chin, S. (2011). *The freight*

    analysis framework version 3 (FAF3): a description of the FAF3 regional

    database and how it is constructed. Retrieved from

    http://faf.ornl.gov/faf3/Data/FAF3ODDoc611.pdf

Standifer, G., & Walton, C. M. (2000). *Development of a GIS model for intermodal*

    freight. Southwest Region University Transportation Center Research Report.

    Retrieved from http://citeseerx.ist.psu.edu/viewdoc/download?doi=10.1.1.196.371

    &rep=rep1&type=pdf

SteadieSeifi, M., Dellaert, N. P., Nuijten, W., Van Woensel, T., & Raoufi, R. (2014).

    Multimodal freight transportation planning: a literature review. *European Journal*

    of Operational Research, 233, 1–15. https://doi.org/10.1016/j.ejor.2013.06.055

Strocko, E., Sprung, M., Nguyen, L., Rick, C., & Sedor, J. (2013). *Freight facts and*

    figures 2013. Retrieved from https://ops.fhwa.dot.gov/freight/freight_analysis/

    nat_freight_stats/docs/13factsfigures/pdfs/fff2013_highres.pdf

Tavasszy, L., & De Jong, G. (2014). *Modelling Freight Transport*. Elsevier.

Torkjazi, M., Mirjafari, P., & Poorzahedy, H. (2018). Reliability-based network flow estimation with day-to-day variation: a model validation on real large-scale urban networks. *Journal of Intelligent Transportation Systems*, *22*(2), 121–143. https://doi.org/10.1080/15472450.2017.1413555

Torrey, W., & Murray, D. (2014). *An analysis of the operational costs of trucking: a 2014 update*. Retrieved from http://www.atri-online.org/wp-content/uploads/2014/09/ATRI-Operational-Costs-of-Trucking-2014-FINAL.pdf.

Uddin, M., & Huynh, N. (2015). Freight traffic assignment methodology for large-scale road-rail intermodal networks. *Transportation Research Record: Journal of the Transportation Research Board*, *2477*, 50–57. https://doi.org/10.3141/2477-06

Uddin, M., & Huynh, N. (2016). Routing model for multicommodity freight in an intermodal network under disruptions. *Transportation Research Record: Journal of the Transportation Research Board*, *2548*, 71–80. https://doi.org/10.3141/2548-09

Uddin, M., & Huynh, N. (2017). Truck-involved crashes injury severity analysis for different lighting conditions on rural and urban roadways. *Accident Analysis & Prevention*, *108*, 44–55. https://doi.org/10.1016/j.aap.2017.08.009

Uddin, M., & Huynh, N. (2018). Factors influencing injury severity of crashes involving HAZMAT trucks. *International Journal of Transportation Science and Technology*, *7*(1), 1-9. https://doi.org/10.1016/j.ijtst.2017.06.004

Uddin, M., & Ahmed, F. (2018). Pedestrian injury severity analysis in motor vehicle crashes in Ohio. *Safety*, *4*(2), 20. https://dx.doi.org/10.3390/safety4020020

Uddin, M., & Huynh, N. (2019). Reliable routing of road-rail intermodal freight under

uncertainty. *Networks and Spatial Economics*. Advance online publication.

https://doi.org/10.1007/s11067-018-9438-6

Uddin, M., Huynh, N., & Ahmed, F. (2019). *Assignment of freight traffic in a large-scale*

intermodal network under uncertainty. Presented at Transportation Research

Board 98th Annual Meeting, Washington, D.C.

Winebrake, J., Corbett, J., Hawker, J., & Korfmacher, K. (2008a). *Intermodal freight*

transport in the great lakes: development and application of a great lakes

geographic intermodal freight transport model. Retrieved from

www.glmri.org/downloads/winebrake08a.pdf

Winebrake, J., Corbett, J., Falzarano, A., Hawker, J., Korfmacher, K., Ketha, S., &

Zilora, S. (2008b). Assessing energy, environmental, and economic tradeoffs in

intermodal freight transportation. *Journal of the Air & Waste Management*

Association, *58*(8), 1004–1013. https://doi.org/10.3155/1047-3289.58.8.1004

Xiong, G., & Wang, Y. (2014). Best routes selection in multimodal networks using multi-

objective genetic algorithm. *Journal of Combinatorial Optimization*, *28*(3), 655–

673. https://doi.org/10.1007/s10878-012-9574-8

Yamada, T., Russ, B. F., Castro, J., & Taniguchi, E. (2009). Designing multimodal

freight transport networks: a heuristic approach and applications. *Transportation*

Science, *43*(2), 129–143. https://doi.org/10.1287/trsc.1080.0250

Zhang, K., Nair, R., Mahmassani, H. S., Miller-Hooks, E. D., Arcot, V. C., Kuo, A.,

Dong, J., & Lu, C. (2008). Application and validation of dynamic freight

simulation-assignment model to large-scale intermodal rail network: pan-

European case. *Transportation Research Record: Journal of the Transportation Research Board*, *2066*, 9–20. https://doi.org/10.3141/2066-02

Zhu, S., & Levinson, D. M. (2012). Disruptions to transportation networks: a review. In D. Levinson, H. Liu, and M. Bell (Eds.), *Network Reliability in Practice*, New York: Springer.

Ziliaskopoulos, A., & Wardell, W. (2000). An intermodal optimum path algorithm for multimodal networks with dynamic arc travel times and switching delays. *European Journal of Operational Research*, 125, 486–502. https://doi.org/10.1016/S0377-2217(99)00388-4

APPENDIX A

COPYRIGHT PERMISSIONS TO REPRINT

The following archiving and sharing policy applies for the articles "Uddin, M., & Huynh, N. (2015). Freight traffic assignment methodology for large-scale road-rail intermodal networks. *Transportation Research Record*, 2477, 50–57" and "Uddin, M., & Huynh, N. (2016). Routing model for multicommodity freight in an intermodal network under disruptions. *Transportation Research Record*, 2548, 71–80." Chapter 2 of this dissertation has been adapted from the first article and Chapter 4 from the second article.

Common Requests under Green Open Access Policy

	I WANT TO	CLEARED PERMISSION	REQUIRES PERMISSION
On a website	Upload my Contribution to my institution repository or department website (see Posting to an Institutional Repository)	Accepted Version[2]	
	Upload my Contribution to a non-commercial platform (including a database or repository NOT affiliated with my institution) *12 months after publication*	Accepted Version[2]	
	Upload my Contribution to a non-commercial platform (including a database or repository NOT affiliated with my institution) *without an embargo period*	Original Submission[1]	
In Education	Include my Contribution in my dissertation or thesis, which may be posted in an Institutional Repository or database	Final, Published Version[3]	
	Supply my Contribution to my students or use the Contribution for my own teaching purposes	Final, Published Version[3]	

The following permission to reprint applies for the article "Uddin, M., & Huynh, N. (2019). Reliable routing of road-rail intermodal freight under uncertainty. *Networks and Spatial Economics*. Advance online publication." Chapter 5 has been adapted from the above article.

Springer Nature Terms and Conditions for RightsLink Permissions

Springer Nature Customer Service Centre GmbH (the Licensor) hereby grants you a non-exclusive, world-wide licence to reproduce the material and for the purpose and requirements specified in the attached copy of your order form, and for no other use, subject to the conditions below:

1. The Licensor warrants that it has, to the best of its knowledge, the rights to license reuse of this material. However, you should ensure that the material you are requesting is original to the Licensor and does not carry the copyright of another entity (as credited in the published version).

   If the credit line on any part of the material you have requested indicates that it was reprinted or adapted with permission from another source, then you should also seek permission from that source to reuse the material.

2. Where **print only** permission has been granted for a fee, separate permission must be obtained for any additional electronic re-use.

3. Permission granted **free of charge** for material in print is also usually granted for any electronic version of that work, provided that the material is incidental to your work as a whole and that the electronic version is essentially equivalent to, or substitutes for, the print version.

4. A licence for 'post on a website' is valid for 12 months from the licence date. This licence does not cover use of full text articles on websites.

5. Where **'reuse in a dissertation/thesis'** has been selected the following terms apply: Print rights of the final author's accepted manuscript (for clarity, NOT the published version) for up to 100 copies, electronic rights for use only on a personal website or institutional repository as defined by the Sherpa guideline (www.sherpa.ac.uk/romeo/).

6. Permission granted for books and journals is granted for the lifetime of the first edition and does not apply to second and subsequent editions (except where the first edition permission was granted free of charge or for signatories to the STM Permissions Guidelines http://www.stm-assoc.org/copyright-legal-affairs/permissions/permissions-guidelines/), and does not apply for editions in other languages unless additional translation rights have been granted separately in the licence.

7. Rights for additional components such as custom editions and derivatives require additional permission and may be subject to an additional fee. Please apply to Journalpermissions@springernature.com/bookpermissions@springernature.com for these rights.

8. The Licensor's permission must be acknowledged next to the licensed material in print. In electronic form, this acknowledgement must be visible at the same time as the figures/tables/illustrations or abstract, and must be hyperlinked to the journal/book's homepage. Our required acknowledgement format is in the Appendix below.

9. Use of the material for incidental promotional use, minor editing privileges (this does not include cropping, adapting, omitting material or any other changes that affect the meaning, intention or moral rights of the author) and copies for the disabled are permitted under this licence.

10. Minor adaptations of single figures (changes of format, colour and style) do not require the Licensor's approval. However, the adaptation should be credited as shown in Appendix below.